5-2018

Estimating Likelihood of Severe Damage due to Earthquakes in Reinforced Concrete Frame Buildings in Afghanistan

Sekandar Zadran
Purdue University

ESTIMATING LIKELIHOOD OF SEVERE DAMAGE DUE TO EARTHQUAKES IN REINFORCED CONCRETE FRAME BUILDINGS IN AFGHANISTAN

by

Sekandar Zadran

A Thesis

Submitted to the Faculty of Purdue University

In Partial Fulfillment of the Requirements for the degree of

Master of Science in Civil Engineering

Lyles School of Civil Engineering

West Lafayette, Indiana

May 2018

THE PURDUE UNIVERSITY GRADUATE SCHOOL
STATEMENT OF COMMITTEE APPROVAL

Dr. Ayhan Irfanoglu, Chair

Department of Structural Engineering

Dr. Arun Prakash

Department of Structural Engineering

Dr. Santiago Pujol

Department of Structural Engineering

Approved by:

Dr. Dulcy M. Abraham

Head of the Graduate Program

Dedicated to my parents and wife

ACKNOWLEDGMENTS

Firstly, I would like to express my sincere gratitude to my advisor Professor Ayhan Irfanoglu for the continuous support of my MSCE study and related research, for his patience, motivation, and knowledge. His guidance not only enabled me in doing my research but also was a great help in writing of this thesis. I could not have imagined having a better advisor and mentor for my MSCE study. I will remain grateful and appreciative of all the support I have received from him along the way.

Besides my advisor, I would like to thank the other members of my thesis committee, Professor Santiago Pujol and Professor Arun Prakash, not only for their insightful comments and encouragement, but also for the questions during my defense which will help me widen my future research work.

I would also like to thank the US Department of State for providing me the financial opportunity to purse my graduate studies through Fulbright program. My Master's education, including this research, would not have been possible without my Fulbright Fellowship.

I am also thankful to Jenny Ricksy, Molly Stetler and all others in the Lyles School of Civil Engineering for their help and support. Also, my Afghan friends here at Purdue and back home have been of great help and support along this journey.

Last but not the least, I would like to thank my family: my parents and my siblings for supporting me spiritually throughout my time at Purdue and my life in general.

Most importantly, none of this could have happened without the support of my wife, Wahedi. Her love and encouragement have meant everything to me.

TABLE OF CONTENTS

LIST OF TABLES

APPENDIX - B Tables:

LIST OF FIGURES

APPENDIX A Figures:

APPENDIX C Figures:

ABSTRACT

Zadran Sekandar, MSCE. Purdue University, May 2018. Estimating Likelihood of Severe Damage due to Earthquakes in Reinforced Concrete Frame Buildings in Afghanistan.
Major Professor: Ayhan Irfanoglu

Afghanistan has a history of devastating earthquakes claiming many lives and causing extensive damage. It is important to identify buildings vulnerable to ground shaking in an efficient manner and to upgrade or rebuild them to avoid losses during earthquakes in the future. In June 2017, 51 reinforced concrete (RC) school buildings with solid masonry infill walls and no structural walls were surveyed in Kabul, Afghanistan. Besides photographic documentation and location information, building dimensions including column dimensions and masonry wall dimensions, as well as wall orientation information, and number of stories above ground were recorded. To rank these buildings in vulnerability and to identify which ones, if any, would need to be upgraded to avoid high likelihood of severe damage at different levels of ground shaking, a method based on the Priority Index (Hassan and Sozen, 1997) was used. Ratios of total cross-sectional areas of ground story columns and masonry walls to total floor area above ground formed two of the key parameters. Peak ground acceleration (PGA) was used as the parameter to indicate the level of ground shaking. Column-to-total floor area and masonry wall-to-total floor area ratios were divided by PGA to differentiate between different levels of shaking intensity. The method is calibrated and a threshold relationship is established to distinguish whether a building is more likely to sustain severe damage ("more vulnerable") or less likely to do so ("less vulnerable") using data from buildings surveyed following the 2016 Meinong, Taiwan earthquake. In particular, observations and measurements from survey of 50 RC frame buildings with no structural walls but with solid brick infill walls and located near ground motion recording stations were used. Peak ground acceleration recorded by the nearest ground motion recording station (within 5 km of a building) is used to scale the column and infill wall ratio based indices. Various combinations of the indices were studied to find a threshold description. Threshold expression choice was based on 1) the success rate in identifying buildings that sustained severe damage as "more vulnerable" while 2) minimizing the likelihood of identifying buildings that did not sustain severe damage as "more vulnerable." The primary objective in establishing this threshold is to minimize loss of life

while the secondary objective is to be effective and feasible to implement. Threshold expression found for buildings surveyed in Taiwan was then used to identify school buildings in Kabul that are more vulnerable to severe damage at different seismic hazard levels expressed in terms of PGA. The buildings were ranked in vulnerability using the Priority Index (Hassan and Sozen, 1997).

CHAPTER 1. SEISMICITY OF AFGHANISTAN

1.1 Introduction

Afghanistan is located in a region with high seismic activity (USGS, 2007) where the Indian tectonic plate is moving northwards towards the Eurasian plate at a rate of 3 to 4 cm/year (USGS, 2007) (Figure 1.1). This collision, which formed the highest mountains of the World, has been causing slips over major faults often resulting in catastrophic earthquakes. A recent catastrophic earthquake example is the Mw7.6 2005 earthquake in Kashmir of Pakistan which claimed around 80,000 lives and left 4 million people homeless (USGS, 2007). Every year Afghanistan is hit by moderate earthquakes and on average, every 10 to 20 years, the country experiences a strong earthquake resulting in high number of mortality and extensive damage (Table 1.1).

In the eastern part of Afghanistan shallow earthquakes are reported indicating the northward movement of the crust and mantle under Pakistan and India relative to the westward motion of Eurasian (USGS, 2007). Eastern part of the country has major young strike-slip faults which align almost parallel to the plate boundary of Chaman and Darvaz faults in the northeastern part of Afghanistan (Figure 1.2). Chaman fault system dominates the seismic hazard in eastern Afghanistan. The southeastern part of the country has faults distributed along a belt of length of hundreds of kilometers wide. (USGS, 2007).

In the northern part of the country there is evidence of high level earthquake activity since 1900, especially in regions near Mazer-e-Sharif. According to Ambraseys and Bilham (USGS, 2007), these earthquakes indicate a junction between Eurasian and Sistan block in the south-west of the country. It is suggested that it may have correlation with seismic activities originating from major north-south oriented fault zones in neighboring Iran. The Seismotectonic Map of Afghanistan prepared by USGS in 2005 provides information on the presence of an intensively active region of earthquakes with focal depth larger than 70 km in northeastearn part of Afghanistan. These are known as the Hindukush seismological activities, (USGS, 2007) which include earthquakes having Mw 7 or higher. While these earthquakes originate at depths larger than 70 km, which suggest that the likelihood of severe shaking on ground surface is less compared to those of shallow events. There have been earthquakes in northeastern Afghanistan that claimed many lives and caused severe damage. There are some reports on the seismic activities of the southern part of Afghanistan due to the subduction of Arabian plate (USGS, 2006). These activities can be categorized as the intermediate-depth shakings from 70 km to 300 km. Tables 1.1 and 1.2 list of some of the major earthquakes which took place within or in the vicinity of Afghanistan.

1.2 Afghanistan Earthquake Catalog

After the establishment of the new administration in 2001 in Afghanistan, the USGS developed an earthquake catalog for Afghanistan in order to assess the seismicity of Afghanistan (USGS, 2006). This catalog is also a useful tool to provide important information for the rehabilitation and reconstruction of civil infrastructure throughout the country. This catalog was provided based on the information from previously 26 existing catalogs. Because these 26 catalogs had different epicenter and magnitude information for some individual events, the preferred epicenters and magnitudes were selected (USGS, 2006).

The catalog extends beyond the borders of the country, because there are some seismic regions and faults which are not only limited to Afghanistan. Furthermore, large earthquakes which are taking place in the vicinity of Afghanistan boundaries could cause severe damage within Afghanistan. All earthquake events with a magnitude greater than 4.0 and occurred between 1964 and 2004 are included in this catalog. Additionally, earthquakes with magnitude of 5.5 or greater and happened between years 1900 are 1963 are included. This catalog also includes the earthquake shocks from years before 1900. The catalog is divided into three parts, Summary Catalog, Master Catalog and Macro seismic Effects. The focus here is on the Summary Catalog.

1.2.1 Summary Catalog of Afghanistan Earthquake (U.S. Geological Survey Open-File Report 2006–1185)

Information on 12728 earthquakes taken place from 2nd millennium BCE till 2004 CE are included. For each earthquake, epicenter and focal depth are listed. Information on the earthquakes for the four millennia listed by catalog is very poor in most cases because of the incomplete evidence and documentations, and has been taken based on the distribution of damage reported. Despite the incomplete information, the list provides important information on the seismicity of Afghanistan. The information listed for the past couple of decade is more accurate and complete. Based on the information from the recent installed earthquake monitoring stations in Afghanistan and surrounding regions, the catalog is considered to be complete for earthquakes with magnitude 5.0 and greater.

Because of the poor seismic information from the past times, it was difficult both for USGS and the Afghan government to prepare a broad seismic hazard map and collect data for various parts of Afghanistan. To address this issue, a new seismic center was recreated at the Kabul University in cooperation with USGS in 2006 after two decades of war in the country. This station transfers real-time seismic information to USGS. Based on the transmitted information, the location, size and depth of the earthquakes can be determined.

1.3 Earthquakes in the History of Afghanistan

There is some evidence of earthquakes in Afghanistan from the years before 2000 BCE, but most of these records are either incomplete or informal. Ambraseys and Bilham (USGS, 2007) used various methods, based on narrative accounts, to estimate the intensity and location of these earthquakes. Most of these earthquakes are considered to be from an era prior to instrumentation. Some reassessments were carried out for those earthquakes happened during the early instrumental era. Nearly 500 events were reevaluated and new values of magnitudes were computed for them. After the new catalog was introduced, Ambraseys and Bilham (USGS, 2007) were able to evaluate all records during the past 1200 years. This study was based on the modern ideas of plate tectonic and seismic hazard analysis. They also prepared detailed information on some earthquakes which can be seen in Table 1.2. This table does not include the entire list events took place during the past 1200 years, because there might be other devastative earthquakes which might have claimed many more lives and caused severe damages.

One of the conclusions is that the northeastern part of Afghanistan is one of those rare regions in the World where strong earthquakes take place within a depth of 200 km and more.

1.4 Earthquake Faults in Afghanistan

There is very limited information available to provide fault slip rate and the return time of large earthquakes for each of the existing faults in Afghanistan. Based on some initial studies, there are some faults known to be active. Based on observed surface rupture, evidence shows large earthquakes happened in the region. For the most part, the evaluation and assessment of faults are based on the studies carried out by Wheeler and Ruleman during 2005 and 2007 (USGS, 2007). The faults deemed to be active are listed Table 1.3.

Figure 1.2 illustrates the fault locations. Abbreviations of fault names in Afghanistan are as follows (modified from Wheeler and others, 2005).

Some properties of these faults including surface expressions and dimensions are similar to those for the Denali (Alaska), North-Anatolian (Turkey) and San Andreas Fault (California) systems. These faults can potentially generate earthquakes with a moment-magnitude of 7.0 to 8.0. Considering the history of devastating earthquakes in Afghanistan, there is a need to understand the seismicity level and the possible earthquake hazards in different parts of the country. Based on the provided earthquake hazard map by USGS in 2007, there is very high possibility of strong shaking in the coming fifty years in the north-eastern part of Afghanistan and along the Chaman fault.

1.4.1 Chaman Fault

This fault is said to have a length of more than 1000 km, surrounding the region from Hindukush in the northeastern part of the country towards the southwest through the eastern parts of Afghanistan and extends across the western parts of Pakistan. Evidence shows that there have been several devastating earthquakes in this fault which have caused surface rupture. For instance, the 1505 earthquake that took place near Kabul city had an estimated intensity of Ms 7.3, which produced a surface rupture of length 40 to 60 kilometers. There were several meters of vertical offset associated with this earthquake.

The Paghman fault which is a part of the Chaman faults is located 20 km west of the Kabul city. Based on the existing information, an earthquake associated with this fault took place in 1892 which produced 60 to 75 centimeters of left-lateral movement and caused the west side of the fault to be dropped by 20 to 30 centimeters. There was another earthquake with a moment magnitude of 6.4 took place in 1975 which caused a surface rupture of 5 kilometers length.

Some aerial photographs and geomorphology studies show that the Chaman fault system has an estimated slip rate of 0.2 to 2.0 cm/year. Others suggest that this amount will be quite higher on the southern end of the fault (USGS, 2007). In spite of the incomplete information on the slip rate, the Chaman fault poses a high risk in terms of seismic hazard and devastation an associated earthquake could result in. More geological studies are needed to provide better understanding on the measurement of the slip rate associated with this fault.

1.4.2 Hari Rud Fault

This fault is known to have a length of nearly 730 kilometers which intersects with the Chaman fault in the north of Kabul, and extends westward towards the border of Iran. This fault is said to have an exceptional geomorphic setting (USGS, 2007). There is debate about whether the Hari Rud Fault is an active one or not (USGS, 2007). The estimated slip rate with respect to this fault is somewhere between 0.2 to 0.3 cm/year.

1.4.3 Central Badakhshan Fault

There is not enough information on the slip rate of the central Badakhshan fault. Based on some assumptions that the slip rate is preserved at the intersection of Chaman and Hari Rud fault, a slip rate of 1.2 cm/year is assigned for the Badakshan fault (USGS, 2007).

1.4.4 Darvaz Fault

This fault, with a length of 380 kilometers, is oriented parallel to Central Badakhshan fault. It extends from northeastern Afghanistan northward to Tajikistan. The median associated slip rate used for this fault is 0.7 cm/year.

CHAPTER 2. SCHOOL BUILDINGS IN KABUL, AFGHANISTAN

2.1 Introduction

Fifty-one school buildings were surveyed during June 2017 in Kabul, the capital of Afghanistan. The data gathered for each building during this survey are the architectural dimensions of the building, column dimensions, infill wall dimensions and orientation, geographical location, and photographs of the front, back and side views. These buildings all have reinforced concrete moment-resisting frames with solid brick masonry infill walls. None of the buildings has any reinforced concrete structural walls. The school buildings range from one to three story above ground. The data were collected in cooperation with the Afghanistan Ministry of Education. Later, based on the collected measurements, layout of each building was prepared.

Using the survey data, Table 2.1 has been generated based on the principles of Hassan-Sözen Index, also known as the Priority Index (Hassan and Sözen, 1997). For each building, 16 parameters are presented. Each column is labeled with a number for ease of explanation. Column 1 indicates the building number. Column 2 is the name of the school. Columns 3 and 4 list the latitude and longitude of the school building. Column 5 is the Priority Index for each school building which is explained below. Columns 6, 7, 8 and 9 indicate the number of floors above ground floor, floor area at the ground level, total floor area of all above-ground floors, and the total cross-sectional area of the reinforced concrete columns at the ground story, respectively. Columns 10 and 11 provide the total cross-section area of concrete walls along the plan principal directions, expressed as north-south and east-west directions, at the ground story, respectively, and which are equal to zero, since there is no concrete wall in any of the surveyed school buildings. Columns 12 and 13 specify the total cross-sectional area of solid masonry walls along the north-south and the east-west directions of the building at the ground story. Column 14 shows the column index for each building (explained below). Columns 15 and 16 are the wall indices (explained below) along the north-south and the east west directions, respectively.

2.2 Indices used in Table 2.1

2.2.1 Priority Index (PI)

Priority Index is the sum of Column Index, CI, and minimum of Wall Index, min (WI), either along the north-south or the east-west direction for a given building (Hassan and Sozen, 1997):

$$PI = CI + WI \qquad (2\text{-}1)$$

where

PI	:	Priority Index (%)
CI	:	Column Index (%)
WI	:	minimum Wall Index in any direction

2.2.2 Column Index (CI)

Column Index is equal to half of total cross-sectional area of all reinforced concrete columns in the ground floor divided by the total area of floors above ground for a given building (Hassan and Sozen 1997):

$$CI = \frac{1}{2}\frac{A_c}{\sum A_f} \qquad (2\text{-}2)$$

where

CI	:	Column Index (%)
A_c	:	total cross-sectional area of all RC columns at ground story
$\sum A_f$	:	total area of all floors above ground

2.2.3 Wall Index (WI)

Wall Index in a given direction is sum of the area of cross-section of all concrete walls and one tenth of all masonry infill walls divided by the total area of floors above ground for a given building (Hassan and Sozen 1997):

$$WI = \frac{(A_{cw} + 0.1xA_{mw})}{\sum A_f} \qquad (2\text{-}3)$$

where

WI	:	Wall Index (%)

A_{cw} : total cross-sectional area of reinforced concrete walls along one horizontal direction at ground story

A_{mw} : total cross-sectional area of masonry infill walls along one horizontal direction at ground story

$\sum A_f$: total area of floors above ground

Based on the Principles of Hassan-Sozen Index, the provided plot in Figure 2.1 includes two boundary lines. The line named as “Boundary 1” forms a triangular section along with two axes. If the wall and column indices for a particular building fall within this region, it is considered as more vulnerable building compared to those buildings with the indices outside of “Boundary 2”, (Hassan and Sözen, 1997). There is not any absolute rule of thumb to locate these threshold lines. The first boundary may be located as close to the origin or as far away from the origin considering the risk that can be estimated as well as the availability of the resources for seismic risk reduction.

CHAPTER 3. STUDY OF RC BUILDINGS AFFECTED BY THE 2016 MEINONG, TAIWAN EARTHQUAKE

3.1 Introduction

A team of engineers and researchers surveyed reinforced concrete buildings affected by the February 2016 Meinong, Taiwan earthquake which had magnitude Mw 6.4 (USGS),. All of the information gathered during the field reconnaissance has been made available at the datacenterhub.org. The information used in this study are the dimensions of the RC columns, solid masonry infill walls, total floor area above ground floor, and damage state. Only those 50 buildings with no structural walls and within 5 km of a ground motion recording station have been considered. Based on the measurements made in each building, Column Index (%) and Wall Index (%), defined below, and are calculated. Additionally, ground motion parameters extracted from records obtained in nearby ground motion monitoring stations are used. Possible correlation between observed severe structural damage state ("severe damage") and Column Index and Wall Index scaled by peak ground acceleration (PGA) measured at nearest ground motion monitoring station is investigated.

3.2 Study of RC Buildings without RC walls in Taiwan

The 50 buildings with no concrete/structural walls range from 1 to 5 stories in height. The structural system in these buildings consists of reinforced concrete moment-resisting frames with solid brick masonry infill walls. 11 (22%) of these 50 buildings were observed to have sustained severe damage in their structural systems during the February 2016 earthquake.

The method used to identify likelihood of these buildings to sustain different levels of structural damage ("severe damage" vs. less than severe damage) is derived from the concepts used in the Priority Index (Hassan and Sozen, 1997). Ratios of the total cross-sectional area of ground story columns and masonry walls to total floor area above ground floor formed two of the key parameters. Peak ground acceleration (PGA), expressed in terms of gravitational acceleration (g), and was used as the parameter to indicate the intensity of ground shaking. One half the column-to-total floor area ratio ("Column Index") and one-tenth the masonry wall-to-total floor area ratio ("Wall Index") were divided by PGA from the nearest ground motion station to differentiate between levels of shaking intensity at different sites. The plan principal direction with lesser amount of masonry walls was chosen in calculating the Wall Index, WI. Below are the definitions of parameters used in this study to estimate likelihood of sustaining severe damage vs. lesser damage in RC buildings subject to earthquake ground motions study.

3.2.1 Wall Index, WI (%)

Wall Index of a building in a given direction is the sum of the one-tenth area of all masonry walls effective in that direction divided by the total area of floors above the ground floor:

$$WI = \frac{0.1 * A_{mw}}{\sum A_f} \qquad (3\text{-}1)$$

where

WI	:	Wall Index (%)
A_{mw}	:	total cross-sectional area of masonry infill walls in one horizontal direction at ground story; only masonry infill walls spanning full bay (column-to-column) and full story height with no openings are considered
$\sum A_f$	:	total area of floors above ground floor

3.2.2 Column Index, CI (%)

Column Index of a building is equal to half of the total cross-sectional area of columns in the ground story divided by the total area of floors above the ground floor:

$$CI = \frac{1}{2} \frac{A_c}{\sum A_f} \qquad (3\text{-}2)$$

where

CI	:	Column Index (%)
A_c	:	total cross-sectional area of columns in the ground story
$\sum A_f$	:	total area of floors above ground floor

3.3 Column and Wall Indices scaled by PGA

For each of the 50 RC buildings with no structural walls but with solid brick infill walls, the WI and CI indices were scaled by the peak ground acceleration (PGA) measured at the nearest ground motion recording station within 5 km of the building. This scaling idea is first proposed by Pujol (2016). “PGA scaled” CI vs. WI plots, i.e. CI/PGA vs. WI/PGA, were used to find simple threshold expressions that can distinguish between severely damaged buildings and lesser damaged buildings. Various linear combinations of the indices were studied to find a good and simple threshold description (Figs. 3.1, 3.3, 3.5, 3.7, 3.9, 3.11, 3.13 and 3.15). Threshold expression choice was based on 1) the success rate in identifying buildings that sustained severe damage as “more vulnerable” while 2) minimizing the likelihood of identifying buildings that did not sustain severe damage as “more vulnerable”. The approach is based on the work by Pujol (2016). The primary objective is to avoid loss of life while the secondary objective is to avoid establishing a threshold that would be too costly to implement. Another objective is to find a way to scale the “threshold” expression obtained for buildings affected by an earthquake so that projections could be made for different levels of earthquake hazard (often stated in terms of PGA).

Figs. 3.2, 3.4, 3.6, 3.8, 3.10, 3.12, 3.14 and 3.16 illustrate how successful various thresholds with different combination of Column and Wall Indices are. In these figures, the straight line (red colored) is the baseline illustrating the hypothetical “perfect” threshold expression which would identify only those buildings with observed severe as more vulnerable. Given the nature of ground motion and building response, however, the “perfect” threshold expression is not achievable. The piecewise linear graphs illustrate for different combinations of Column to Wall Indices. When compared with the baseline for the “perfect” threshold, these graphs indicate the success level of the thresholds considered. Each graph indicates while identifying a certain percentage of the observed severely damaged buildings as “more vulnerable to severe damage”, how many buildings which were not severely damaged are diagnosed by the respective threshold criterion as “more vulnerable to severe damage”.

For the 50 RC frame buildings with solid brick infill walls and no concrete walls, it is found that the threshold formed by connecting the points (0.70, 0) and (0, 0.70) on the “PGA scaled” Column Index vs. “PGA scaled” Wall Index worked best (see Fig. 3.3). Namely, the line expressed as

$$\frac{CI}{PGA} + \frac{WI}{PGA} = 0.70 \qquad (3\text{-}3)$$

defines the threshold separating the “more vulnerable” and “less vulnerable” to severe damage. A building with CI/PGA and WI/PGA values falling below this threshold line (Eq. 3-3) is deemed more vulnerable to severe damage than a building falling above this threshold line. This threshold identifies 21 buildings (out of 50) as "more vulnerable" to severe damage. Additionally, the threshold expression suggests that for a given PGA level, judged per unit cross-sectional area, columns contribute five times to the survivability of the considered RC buildings as solid brick masonry infill walls.

It is also found that another threshold formed by connecting the points (0.75, 0) and (0, 0.375) on the "PGA scaled" Column Index vs. "PGA scaled" Wall Index (Fig. 3.1) worked just as good. This second threshold line is expressed as

$$\frac{CI}{PGA}+\frac{2WI}{PGA}=0.75 \qquad (3\text{-}4)$$

This threshold identifies 20 buildings (out of 50) as "more vulnerable" to severe damage. This second threshold expression suggests that, for a given PGA level, judged per unit cross-sectional area, columns contribute 2.5 times more to the survivability of the considered RC buildings than solid brick masonry infill walls.

3.4 Column and Wall Indices without scaling by PGA

WI and CI pairs for each of the 50 RC buildings with no structural walls but with solid brick infill walls within 5 km to closest ground motion recording stations were also studied without considering PGA information. Various linear combinations of the indices were studied to find a good threshold (Figs. 3.21, 3.23, 3.25, 3.27, 3.29, 3.31, 3.33 and 3.35) separating the buildings with severe damage and those with lesser damage, in their structural systems.

Figs. 3.22, 3.24, 3.26, 3.28, 3.30, 3.32, 3.34 and 3.36 illustrate how successful various thresholds with different column and wall index combinations are. Like before, the straight line (red color) illustrates the hypothetical "perfect" threshold expression which would have identified as "more vulnerable to severe damage" only those buildings that were observed to have sustained severe damage in their structural systems.

For the 50 RC frame buildings with solid brick infill walls and no concrete walls, it is found that the threshold formed by connecting the points (0.25, 0) and (0, 0.25) on the Column Index vs. Wall Index worked best, shown in Fig. 3.23. Namely, the line expressed as

$$CI+WI=0.25 \qquad (3\text{-}5)$$

defines the threshold falling below which suggests a building is more vulnerable to severe damage than a building falling above the threshold line. This threshold identifies 28 buildings (out of 50) as more vulnerable to sustain severe damage in their structural systems. This threshold expression suggests that, when compared in terms of per unit cross-sectional area, columns contribute five times to the survivability of the considered RC buildings as solid brick masonry infill walls.

3.5 Summary

Figure 3.20 shows the best-fit thresholds for CI/PGA-to-WI/PGA ratio of 1:1 and 1:0.5. The success rate of these thresholds are similar. Accordingly, due to its better success rate in sorting out most vulnerable buildings and for sake of simplicity, CI/PGA + WI/PGA = 0.7 is chosen. This threshold can be also expressed as CI + WI = 0.7 PGA. CI + WI is known as the Priority Index (PI) (Hassan and Sozen, 1997).

Comparison of CI/PGA + WI/PGA = 0.7 with a best-fit threshold obtained from CI-to-WI (no PGA scaling) ratio of 1:1 ratio is given in Fig. 3.39. It can be seen that when PGA information is ignored, the optimal threshold overestimates the total number of “more vulnerable” buildings by about 15%. Accordingly, it is deemed tht scaling Column and Wall Indices by PGA would also work in identifying whether a RC frame building is more vulnerable to severe damage or not, just like the Column to Wall Indices without PGA scaling. It should be noted that given the uncertainties and the limited number of observations, all of which were from the region affected by the 2016 Meinong earthquake Taiwan, further studies and data are needed to make a final judgement.

Scaling CI and WI by PGA, i.e. using CI/PGA and WI/PGA, allows projection of a threshold expression obtained using building survey data collected in an area following an earthquake to different levels of ground shaking hazard (expressed in terms of PGA) at the same region or elsewhere. Accordingly, in the next chapter, the threshold CI/PGA + WI/PGA = 0.7 (in its equivalent form, CI + WI = 0.7 PGA) obtained from studying the 50 RC frame buildings with solid brick infill walls and no RC walls will be used to study the vulnerability of school buildings surveyed in Kabul, Afghanistan, which are all RC frame buildings with no RC walls, to different levels of ground shaking.

CHAPTER 4. ESTIMATING SEISMIC VULNERABILITY OF SCHOOL BUILDINGS IN KABUL, AFGHANISTAN

4.1 Study of School Buildings in Kabul

The 51 reinforced concrete (RC) school buildings, ranging from 1 to 3 stories, with masonry infill walls and no structural wall as described in Chapter 2 are studied using insight gained from studying the 50 similar type buildings in Taiwan surveyed following the 2016 Meinong earthquake.

To rank the school buildings in vulnerability and to identify which ones, if any, would need to be upgraded to avoid high likelihood of severe damage at various levels of ground shaking, the approach applied to buildings in Taiwan is used. The relative contributions of columns and solid brick masonry infill walls to seismic performance of a building, at a given constant PGA level, have been found from the best-fit threshold expression developed for the Taiwan buildings.

The surveyed school buildings in Kabul have not experienced any strong ground shaking yet. Therefore, the threshold relationship, calibrated using the 2016 Meinong earthquake building survey, was applied to estimate possible cases of severe damage under different levels of ground motion shaking. The ground motion shaking intensity is expressed in terms of PGA (g). The best-fit threshold line for the Taiwan buildings was given in Chapter 3 as

$$\frac{CI}{PGA} + \frac{WI}{PGA} = 0.70 \quad \left[\frac{\%}{g}\right] \tag{4-1}$$

In 2016 Meinong, Taiwan earthquake building survey, PGA values varied between different structures. In the case of school buildings in Kabul, however, because future earthquakes are considered, same PGA value can be considered for all buildings. Accordingly, it is more convenient to use the following expression to identify the "more vulnerable" buildings:

$$CI + WI \leq PGA \text{ x } 0.70\% \tag{4-2}$$

So, for example, for a hazard level of PGA = 0.5g, the threshold separating buildings more vulnerable to severe damage from those that are less vulnerable can be expressed as

$$CI + WI = 0.35\,\% \tag{4-3}$$

This threshold forms the line connecting (0.35, 0) and (0, 0.35) on a column index (CI) vs. wall index (WI) graph.

Estimates of vulnerable Kabul school buildings with higher likelihood of suffering "severe damage" are made for five PGA levels: 0.1 g, 0.2 g, 0.3 g, 0.4 g, and 0.5 g. Figure 4.1 shows the results. The results indicate the high likelihood of observing severe damage, particularly in taller buildings, when the ground shaking level exceeds 0.1 g.

Given the uncertainties involved in projecting observations made in Taiwan to buildings in Kabul, Afghanistan, in order to make a safer judgment when deciding on the vulnerability of existing school buildings (and buildings with similar properties), the threshold lines described by Eq. (4-2) are scaled up by 50% (Figure 4.2). That is,

$$CI + WI \leq 1.5 \text{ x } 0.70\,PGA = 1.1PGA \quad (4\text{-}3)$$

Accordingly, the following estimates can be made for existing school buildings in Kabul:

- For 0.5g PGA, the threshold identifying "more vulnerable to severe damage" buildings is given by $CI + WI \leq 0.52\%$ .Using this threshold all of the three-story two-story buildings and one of the single-story buildings, totaling 35 out of the 51 surveyed school buildings, are identified to fall into the "more vulnerable to severe damage" zone.

- For PGA of 0.4g, the threshold is $CI + WI \leq 0.42\%$ and it is found that 34 of the surveyed buildings (all of the three-story and all of the two-story school buildings) are within the "more vulnerable to severe damage" zone.

- For PGA of 0.3g, the threshold becomes $CI + WI \leq 0.32\%$. 32 of the surveyed buildings (all of the three-story and all but two of the two-story school buildings) are within the "more vulnerable to severe damage" zone.

- For PGA of 0.2g, the threshold is $CI + WI \leq 0.21\%$ and it indicates that 8 of the surveyed buildings (four three-story and four of the two-story school buildings) are within the "more vulnerable to severe damage" zone.

- For 0.1g PGA, it is seen that none of the surveyed school buildings falls within the danger zone defined as $CI + WI \leq 0.11\%$.

4.2 Recommendation for Existing Buildings

It is important to rank existing buildings in vulnerability to earthquake ground motions. For a constant PGA, a ranking based on the sum of column index (CI) and wall index (WI), known as the Priority Index (Hassan and Sozen, 1997), is recommended. Based on this method, among the buildings estimated to be more vulnerable, priority should be given to those buildings which have lesser of:

$$CI + WI \qquad (4\text{-}4)$$

where

CI : Column Index

WI : Wall Index

Using the expression given in (4-4), all vulnerable buildings within PGA based thresholds have been labeled in decreasing order of priority (Figs. 4.3).

4.3 Recommendations for New School Buildings in Kabul

USGS (2007) states that in Kabul, the level of PGA which has 10% probability of exceedance over 50 years (i.e. shaking intensity with a return period of about 500 years) is 0.25g. Using this information, and considering that 1) in Afghanistan, school buildings are considered as important structures; 2) in times of disaster, school buildings may need to be used as emergency shelters; and 3) the seismic hazard level estimates have relatively high level uncertainty due to limited availability of field data and historic records, in design of new school buildings in Kabul, it is recommended that the following threshold be used in deciding whether a proposed school structure is more vulnerable or less vulnerable to severe damage:

$$CI + WI \leq 0.5\% \qquad (4\text{-}4)$$

It should be noted that from previous studies using reconnaissance data (e.g. Hassan and Sozen, 1997; Donmez and Pujol, 2016; Gur et al. 2010), it is known that properly designed and constructed reinforced concrete structural walls contribute very highly to good performance of RC buildings during earthquakes. Accordingly, it is recommended that in the design of future school buildings and other critical buildings, as well as residential buildings in high seismic zones, structural walls be included.RC walls can be included in Wall Index (WI) calculation directly as given in Eq. 2-3.

CHAPTER 5. SUMMARY AND CONCLUSION

Afghan school buildings surveyed in Kabul are representative of all newly built school buildings across Afghanistan after the establishment of new administration in 2001. The Afghan Ministry of Education and various NGOs have used very similar, template school plans almost all over Afghanistan. These new schools have been built based on the principles of modern design codes.

Comparing the school buildings in Kabul which have not yet experienced severe ground shaking with those buildings surveyed in Taiwan after the 2016 Meinong earthquake and for which ground motion records within 5 km exist, the following conclusion can be made:

Future earthquakes resulting in peak ground accelerations in the order of 0.2g and above can pose considerable threat to school buildings (and similar buildings) in Afghanistan. Accordingly, in addition to considering all design codes and provisions, properly proportioned and constructed walls and columns need to be used to improve the likelihood of good performance of school buildings during earthquakes in the future.

Based on Afghan school building survey done in June 2017, it was found that regardless of the number of stories, typical column cross-section of 35x35 cm was used in all buildings and at all stories. Particularly in buildings taller than single story, these small cross-section columns may not sufficient. Almost in all of the buildings surveyed, there are large openings in one plan direction, compared to the other direction, to bring natural light into the rooms. These large openings not only result in a more flexible structural system but also weaken the RC frames by causing captive column condition (e.g. Sozen and Roesset, 1976). It is best to avoid captive column condition by not building partial height walls or walls with openings adjacent to columns, and for the existing ones, to fill the openings in walls adjacent to columns.

To tackle the weaknesses in existing buildings deemed to be more vulnerable to sustain severe damage, retrofit approach seems a very reasonable undertaking (see Appendix C for a simple retrofit example).

For new school buildings, it is recommended that reinforced concrete structural walls be used.

Overall, in deciding for upgrade of existing RC buildings as well as design of new RC buildings in Kabul, $CI + WI > 0.5\%$ is recommended as a simple objective to achieve. Column Index (CI) and Wall Index (WI) are defined in Eq. (2-2) and Eq. (2-3), respectively.

TABLES

Table 1.1: List of major historical earthquakes in Afghanistan

Date, C.E.	Magnitude, M_s	Latitude	Longitude	Description
819	7.4	36.4°	65.4°	Took place in west Mazar Sharif, heavy causalities and damages were reported.
849	5.3	34.3°	62.2°	Took place near Herat city, had caused causalities, damage reported to be severe.
1505	7.3	34.5°	69.1°	Took place in Kabul. Heavy fatalities and damage were reported. It was originally occurred on the Paghman fault.
1818	7.5	36.8°	66.2°	Took place in Hindukush, caused heavy causalities and severe damage
1832	7.4	36.5°	71.0°	Location was in Badakhshan, killed thousands of people. Several villages were damaged. Landslides were took place in several area. The shocks were felt in Kabul and Lahore
1942	7.5	35.0°	71.0 °	The location was close to Jalalabad, northeast of the country.
1874	7.0	35.1°	69.2°	Took place 70km in the north of Kabul city. Reports indicate causalities and damages
1892	6.5	30.9°	66.5°	The location was near Pakistan border. It caused surface rupture.
1909	7.5	36.5°	70.5°	Took place in Badakhshan, northeast of Afghanistan. Severe damages have been reported
1911	7.1	36.5°	66.5°	Took place in the northern part of Afghanistan. Damages and causalities have been recorded.
1935	7.7	28.9°	66.4°	Took place in the southeastern part of Afghanistan. It claimed 35000 lives. Some areas were totally damaged.
1956	7.4	35.1°	67.5°	The center was 160 km northwest of Kabul city. Destroyed several villages.
1975	6.8	30.2°	66.3°	Took place in the southeast part of the country.

Table 1.1: Continued

1982	6.5	36.1°	69.0°	The center was 170km far from north of Kabul. Claimed 450 lives and damaged more than 7000 houses.
1983	7.2	36.37°	70.34°	Took place in Hindukush, 26 deaths, 483 injured (Wikipedia)
1998	5.9	37.1°	70.1°	Took place in the north part of Afghanistan. Claimed 2300 lives.
1998	6.5	37.1°	70.1°	Took place in the north part of Afghanistan. Claimed 4000 lives.
2002	7.4	36.5°	70.48°	The center was in Hindukush region. Hundreds of people were killed.
2015	7.5	36.52°	70.37°	Took place in Hindukush, 399 death, 2536 injured (Wikipedia)

Table 1.2: List of major earthquakes near the borders of Afghanistan

Date, C.E.	Magnitude, M	Latitude	Longitude	Description
1935	7.7 Mw	29.5°	66.8°	Took place in Quetta, Pakistan. Caused 60000 deaths and severe damage. (USGS)
1721	7.7 Ms	36.07°	46.28°	Took place in East Azerbaijan, Iran. Caused 8000-250000 deaths. (USGS)
2017	6.1 Mw	35.77°	60.44°	Took place in Torbat-e-Jam, Iran. At least 2 people were killed, 11 injured and 4 villages damaged in the Sefid Sang area. (USGS)
2013	7.7 Mw	26.95°	65.50°	Took place near Balochistān, Pakistan. Caused severe damage and causalities. (USGS)
1819	8.2 Mw	23.0°	71.0°	Took place in Allahbund, Sindh, Pakistan. More than 1543 deaths. Heavy damage to several villages. (USGS)
2015	7.2 Mw	38.26°	72.77°	Took place in Gorno-Badakhshan Autonomous Region, Tajikistan. Two people were died, many homes were destroyed. (USGS)
1948	7.5 Mw	39.17°	70.89°	Took place in Rasht, Tajikistan. Caused heavy damage to several villages. (USGS)
1992	7.3 Mw	42.14°	73.57°	Took place in Toktogul, Jalal-Abad, Kyrgyzstan. 75 people were killed and several villages were destroyed. (USGS)
1984	7.0 Mw	40.32°	63.35°	Took place in western Uzbekistan. At least 100 people were injured, caused moderate damage to homes. (USGS)
1978	7.4 Mw	33.38°	57.43°	Took place in Mashhad, Iran. Heavy causalities and damages were reported (USGS).

Table 1.3: Faults name and location in Afghanistan (modified from Wheeler and others, 2005)

No.	**Fault Name**	**Abbreviation**	**Location**
1	Alburz	AM	Samangan
2	Andarab	AN	Andarab
3	Bande Bayan	BB	Bande Bayan
4	Chaman	CH	Chaman
5	Central Badakhshan	CB	Badakhshan
6	Dorafshan	DS	Badakhshan
7	Darvaz	DZ	Badakhshan
8	Dosi Mirzavalan	DM	Sarpul
9	Gardez	GA	Paktia
10	Hari Rud	HR	Hari Rud
11	Helmand	HM	Helmand
12	Henjvan	HV	Henjvan
13	Kaj Rod	KR	Kaj Rod
14	Konar	KO	Konar
15	Onay	ON	Onay
16	Paghman	PM	Paghman
17	Punjshir	PJ	
18	Qarghanaw	QA	Qarghanaw
19	Sarobi	SA	Sarobi
20	Spinghar	SP	Spinghar

Table 2.1. Data of the School Buildings Surveyed in Kabul.

1	2	3	4	5	6	7	8	9	10	11	12	13	14	15	16
ID	School Name	Latitude	Longitude	Priority Index [%]	No. Floors	Floor Area [m^2]	Total Floor Area [m^2]	Column Area [m^2]	Concrete Wall Area (NS) [m^2]	Concrete Wall Area (EW)	Masonry Wall Area (NS) [m^2]	Masonry Wall Area (EW) [m^2]	Column Index [%]	Wall Index (NS) [%]	Wall Index (EW) [%]
1	Kabul School 1	NA	NA	0.24	2	602	1204	3.68	0	0	28.00	10.00	0.15	0.23	0.08
2	Kabul School 2	NA	NA	0.24	2	602	1204	3.68	0	0	28.00	10.00	0.15	0.23	0.08
3	Kabul School 3	NA	NA	0.24	2	602	1204	3.68	0	0	28.00	10.00	0.15	0.23	0.08
4	Kabul School 4	NA	NA	0.23	2	602	1204	3.68	0	0	28.00	10.00	0.15	0.23	0.08
5	Kabul School 5	NA	NA	0.23	2	602	1204	3.68	0	0	28.00	10.00	0.15	0.23	0.08
6	Kabul School 6	NA	NA	0.23	2	602	1204	3.68	0	0	28.00	10.00	0.15	0.23	0.08
7	Kabul School 7	NA	NA	0.23	2	602	1204	3.68	0	0	28.00	10.00	0.15	0.23	0.08
8	Kabul School 8	NA	NA	0.23	2	602	1204	3.68	0	0	28.00	10.00	0.15	0.23	0.08
9	Kabul School 9	NA	NA	0.23	2	602	1204	3.68	0	0	28.00	10.00	0.15	0.23	0.08
10	Kabul School 10	NA	NA	0.23	2	602	1204	3.68	0	0	28.00	10.00	0.15	0.23	0.08
11	Kabul School 11	NA	NA	0.23	2	602	1204	3.68	0	0	28.00	10.00	0.15	0.23	0.08
12	Kabul School 12	NA	NA	0.23	2	602	1204	3.68	0	0	28.00	10.00	0.15	0.23	0.08
13	Kabul School 13	NA	NA	0.23	2	602	1204	3.68	0	0	28.00	10.00	0.15	0.23	0.08
14	Kabul School 14	NA	NA	0.21	3	496	1488	5.15	0	0	15.54	6.30	0.17	0.10	0.04
15	Kabul School Admin 15	NA	NA	0.19	2	158	316	1.23	0	0	4.03	0.00	0.19	0.13	0.00
16	Kabul School Admin 16	NA	NA	0.19	2	158	316	1.23	0	0	4.03	0.00	0.19	0.13	0.00
17	Kabul School Admin 17	NA	NA	0.19	2	158	316	1.23	0	0	4.03	0.00	0.19	0.13	0.00
18	Kabul School Admin 18	NA	NA	0.19	2	158	316	1.23	0	0	4.03	0.00	0.19	0.13	0.00
19	Kabul School 19	NA	NA	0.13	3	440	1319	3.31	0	0	15.09	0.00	0.13	0.11	0.00
20	Kabul School 20	NA	NA	0.46	1	824	824	5.64	0	0	36.75	10.08	0.34	0.45	0.12
21	Kabul School 21	NA	NA	0.46	1	824	824	5.64	0	0	36.75	10.08	0.34	0.45	0.12

Table 2.1 Continued

22	Kabul School 22	NA	NA	0.62	1	296	296	3.68	0	0	10.50	0.00	0.62	0.35	0.00
23	Kabul School 23	NA	NA	0.76	1	425	425	4.41	0	0	15.40	10.29	0.52	0.36	0.24
24	Kabul School 24	NA	NA	0.72	1	824	824	8.82	0	0	38.50	15.12	0.54	0.47	0.18
25	Kabul School 25	NA	NA	0.81	1	291	291	4.18	0	0	2.58	6.58	0.72	0.09	0.23
26	Kabul School 26	NA	NA	0.62	1	296	296	3.68	0	0	10.50	0.00	0.62	0.35	0.00
27	Kabul School 27	NA	NA	0.31	2	296	592	3.68	0	0	10.50	0.00	0.31	0.18	0.00
28	Kabul School 28	NA	NA	0.31	2	296	592	3.68	0	0	10.50	0.00	0.31	0.18	0.00
29	Kabul School 29	NA	NA	0.13	3	848	2544	6.37	0	0	53.17	0.00	0.13	0.21	0.00
30	Kabul School 30	NA	NA	0.74	1	602	602	6.86	0	0	28.00	10.08	0.57	0.47	0.17
31	Kabul School 31	NA	NA	0.71	1	600	600	6.50	0	0	28.00	10.08	0.54	0.47	0.17
32	Kabul School 32	NA	NA	0.71	1	600	600	6.50	0	0	28.00	10.08	0.54	0.47	0.17
33	Kabul School 33	NA	NA	0.71	1	602	602	6.50	0	0	28.00	10.08	0.54	0.47	0.17
34	Kabul School 34	NA	NA	0.70	1	606	606	6.50	0	0	28.00	10.08	0.54	0.46	0.17
35	Kabul School 35	NA	NA	0.70	1	605	605	6.50	0	0	28.00	10.08	0.54	0.46	0.17
36	Kabul School 36	NA	NA	0.70	1	605	605	6.50	0	0	28.00	10.08	0.54	0.46	0.17
37	Kabul School 37	NA	NA	0.70	1	605	605	6.50	0	0	28.00	10.08	0.54	0.46	0.17
38	Kabul School 38	NA	NA	0.70	1	607	607	6.50	0	0	31.50	10.08	0.54	0.52	0.17
39	Kabul School 39	NA	NA	0.31	2	376	752	3.68	0	0	19.60	5.04	0.24	0.26	0.07
40	Kabul School 40	NA	NA	0.31	2	375	750	3.68	0	0	19.60	5.04	0.25	0.26	0.07
41	Kabul School 41	NA	NA	0.19	3	1026	3078	8.58	0	0	46.20	16.04	0.14	0.15	0.05
42	Kabul School 42	NA	NA	0.29	2	1025	2050	8.58	0	0	46.20	16.04	0.21	0.23	0.08
43	Kabul School 43	NA	NA	0.38	2	734	1468	8.09	0	0	35.00	15.12	0.28	0.24	0.10
44	Kabul School 44	NA	NA	0.38	2	735	1470	8.09	0	0	35.00	15.12	0.28	0.24	0.10
45	Kabul School 45	NA	NA	0.25	3	735	2205	8.09	0	0	35.00	15.12	0.18	0.16	0.07
46	Kabul School 46	NA	NA	0.25	3	735	2205	8.10	0	0	35.00	15.12	0.18	0.16	0.07
47	Kabul School 47	NA	NA	0.76	1	736	736	8.10	0	0	35.00	15.12	0.55	0.48	0.21
48	Kabul School 48	NA	NA	0.25	3	735	2205	8.10	0	0	35.00	15.12	0.18	0.16	0.07
49	Kabul School 49	NA	NA	0.24	3	532	1596	5.64	0	0	24.50	10.08	0.18	0.15	0.06
50	Kabul School 50	NA	NA	0.24	3	532	1596	5.64	0	0	24.50	10.08	0.18	0.15	0.06
51	Kabul School 51	NA	NA	0.24	3	530	1590	5.64	0	0	24.50	10.08	0.18	0.15	0.06

FIGURES

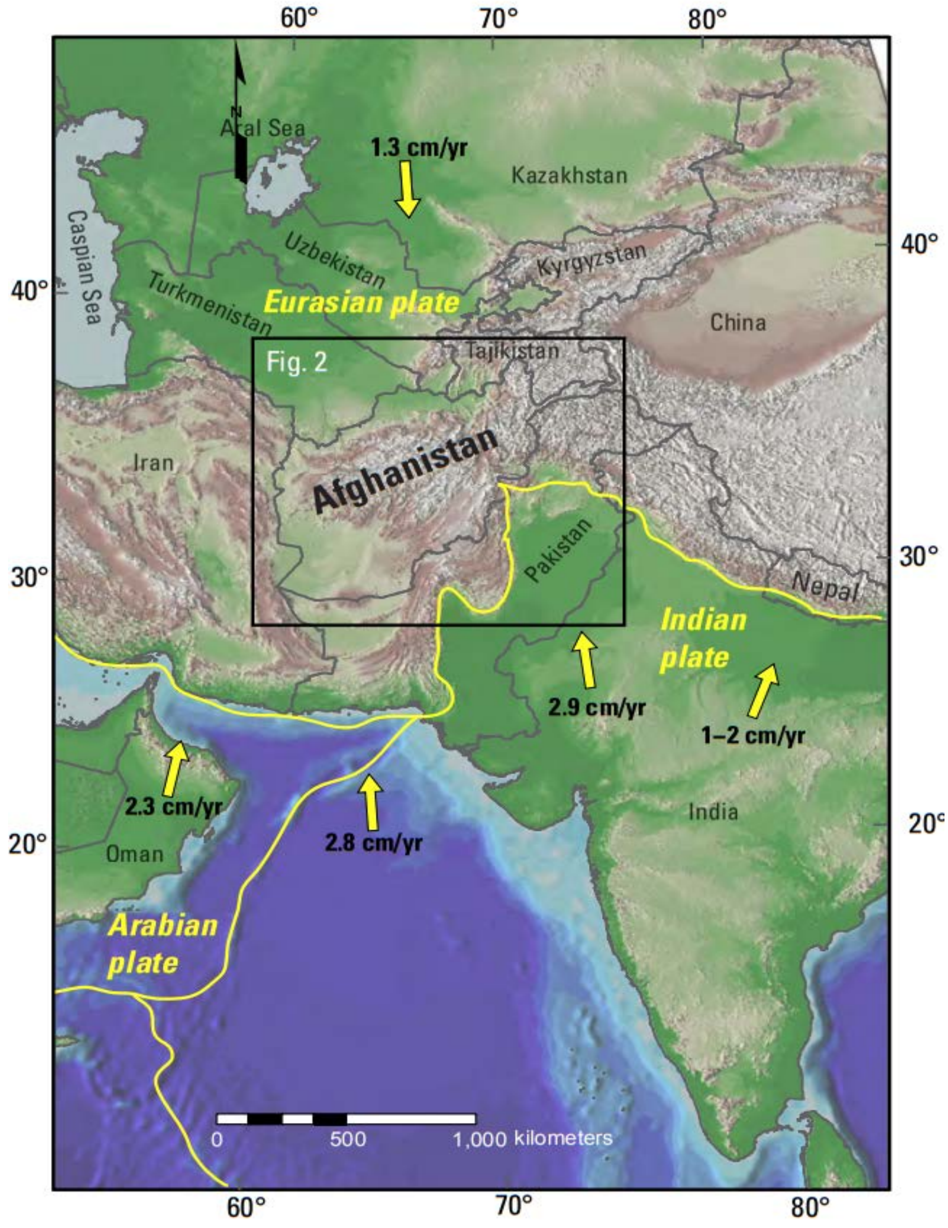

Figure 1.1: Relative plate motions between the Indian, Eurasian, and Arabian plates (Seismotectonic Map of Afghanistan, By RussellWheeler and Kenneth Rukstales 2007)

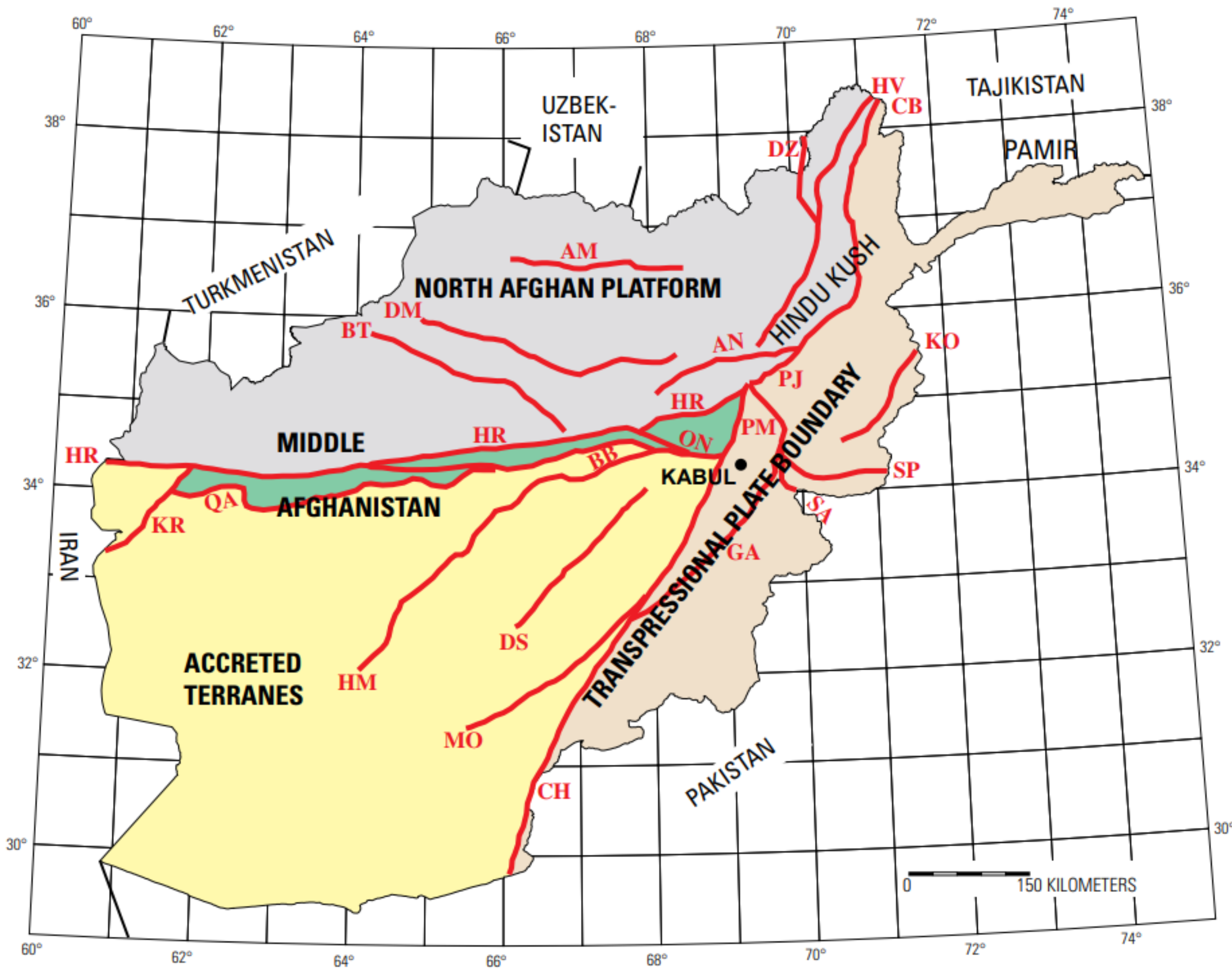

Figure 1.2: Seismotectonic provinces and major fault zones, bold red lines (USGS Seismotectonic Map of Afghanistan, 2006)

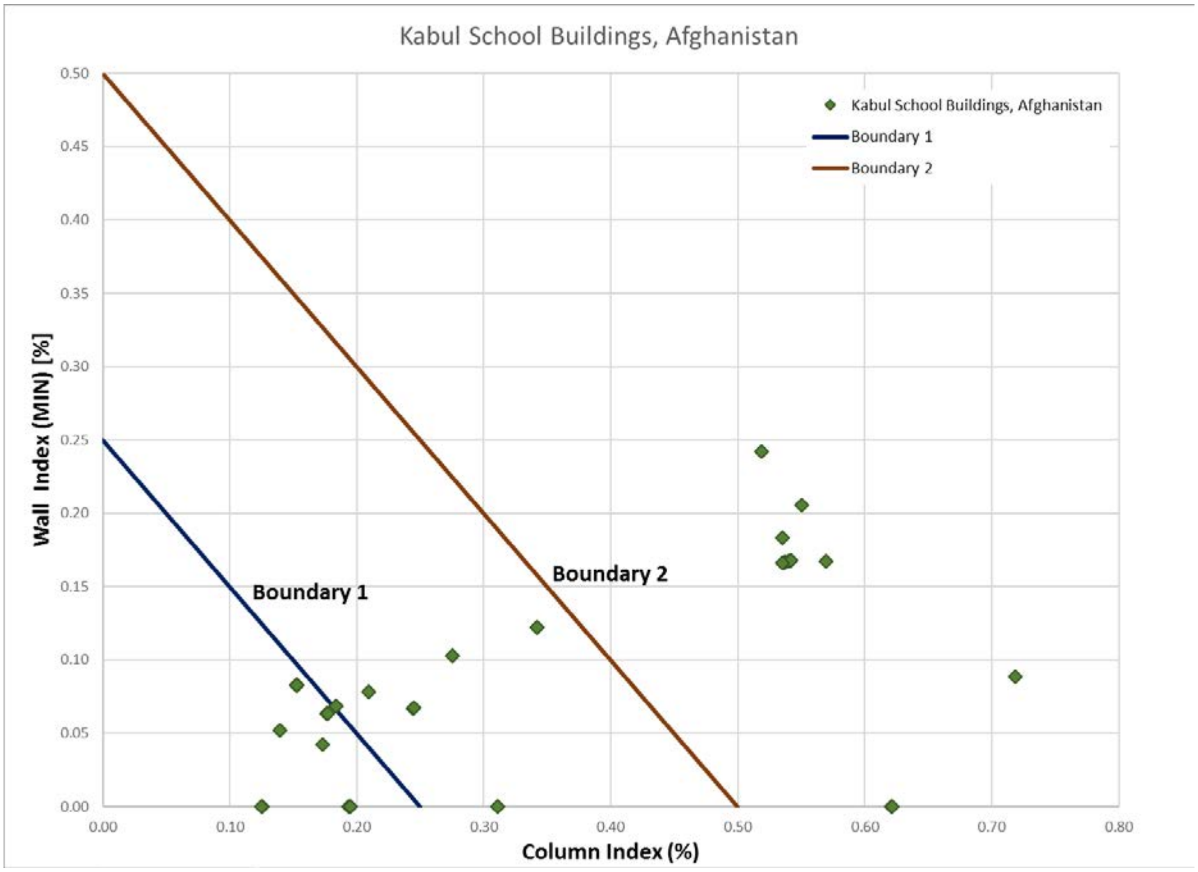

Figure 2.1. Column Index vs. Wall Index of Kabul school buildings

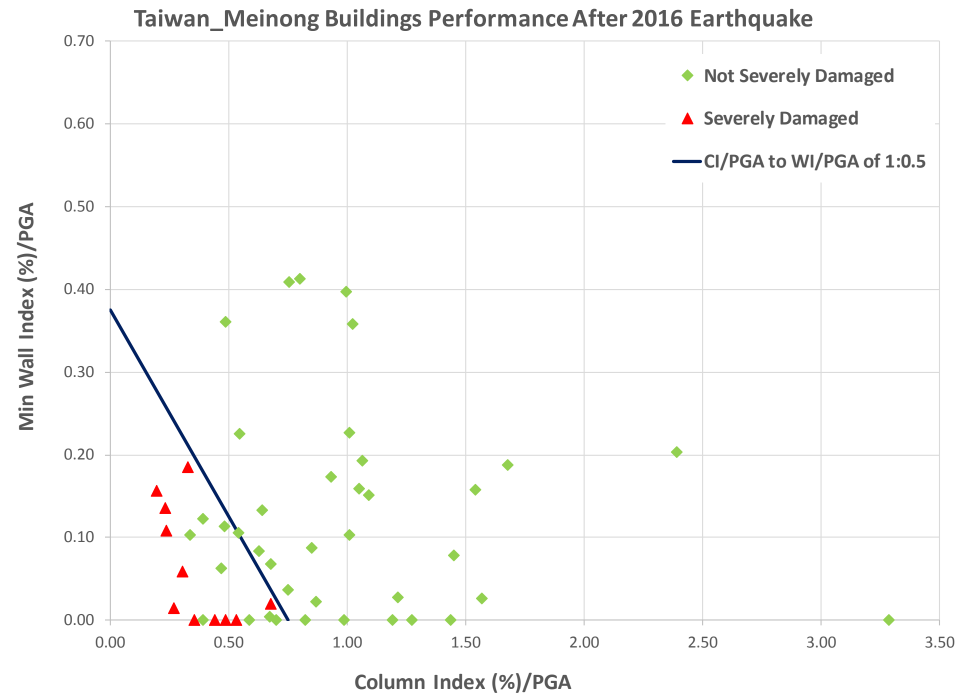

Figure 3.1. Seismic performance of Taiwan Buildings, 1:0.5 Column-Wall Index

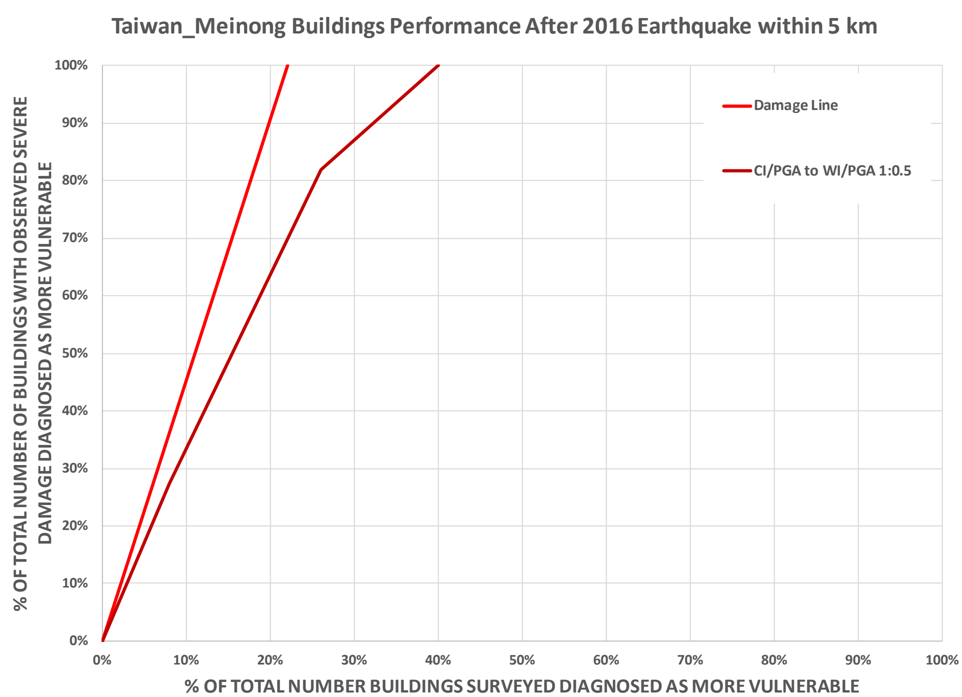

Figure 3.2. Fraction of buildings with observed severe damage successfully diagnosed as vulnerable versus fraction of total buildings diagnosed as vulnerable. 1:0.5 Column-Wall Index

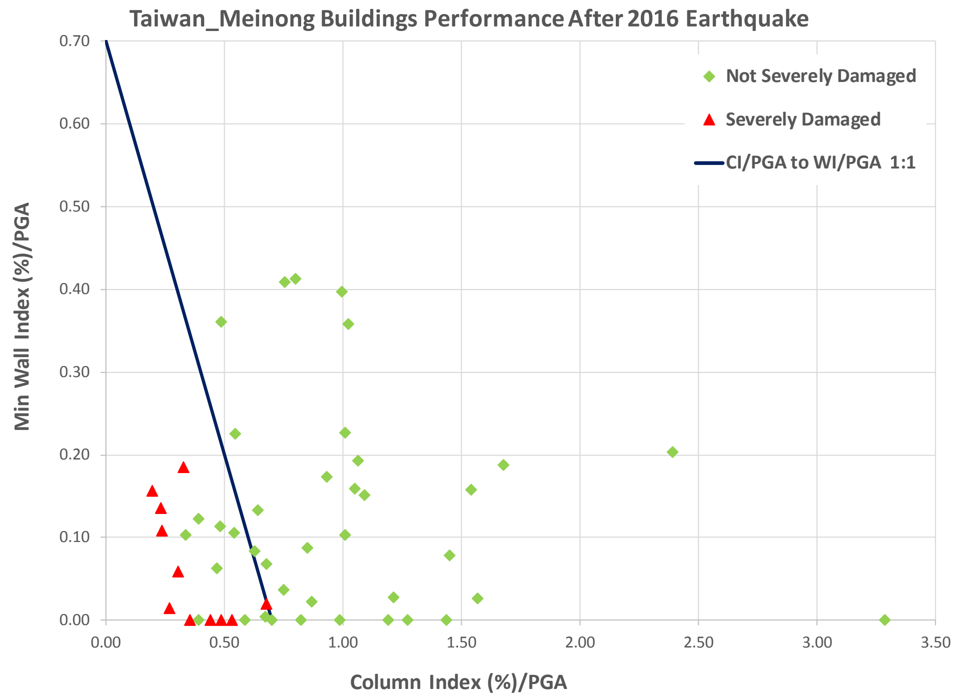

Figure 53.3. Seismic performance of Taiwan Buildings, 1:1 Column-Wall Index

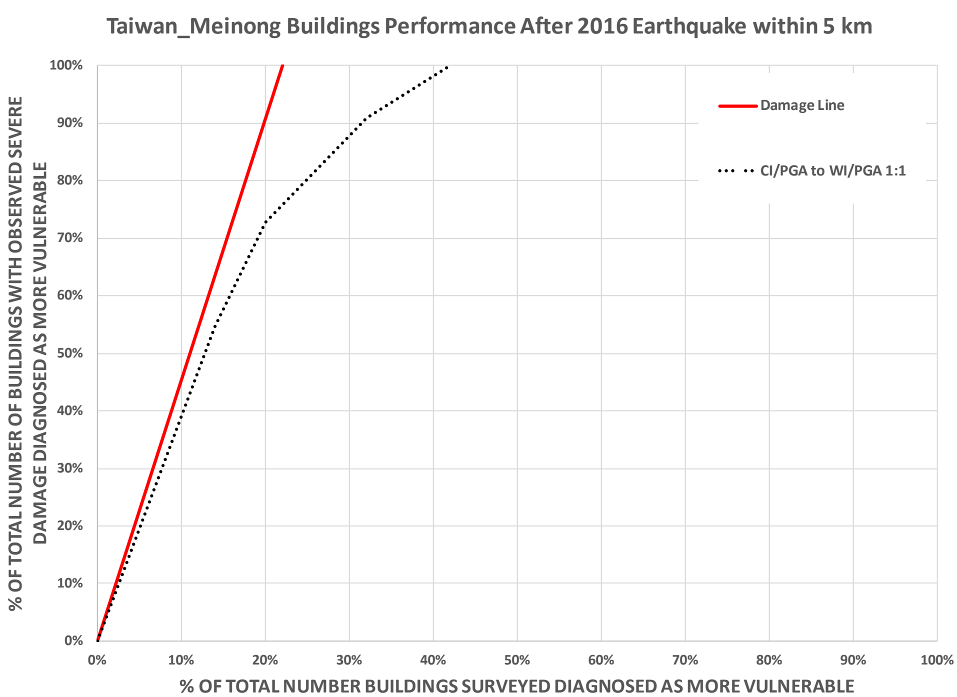

Figure 3.4. Fraction of buildings with observed severe damage successfully diagnosed as vulnerable versus fraction of total buildings diagnosed as vulnerable. 1:1 Column-Wall Index

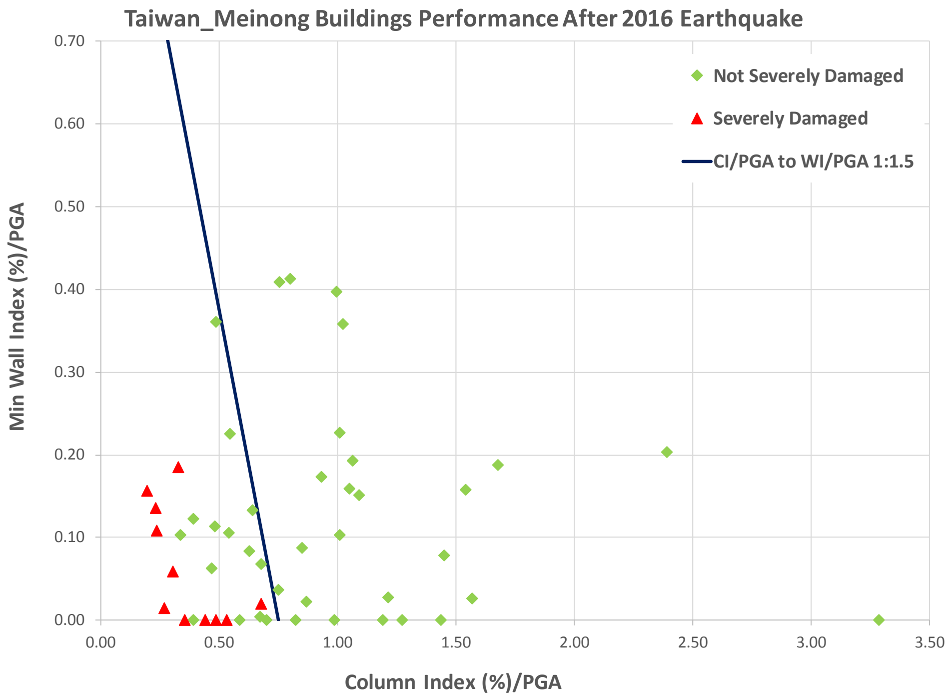

Figure 3.5. Seismic performance of Taiwan Buildings, 1:1.5 Column-Wall Index

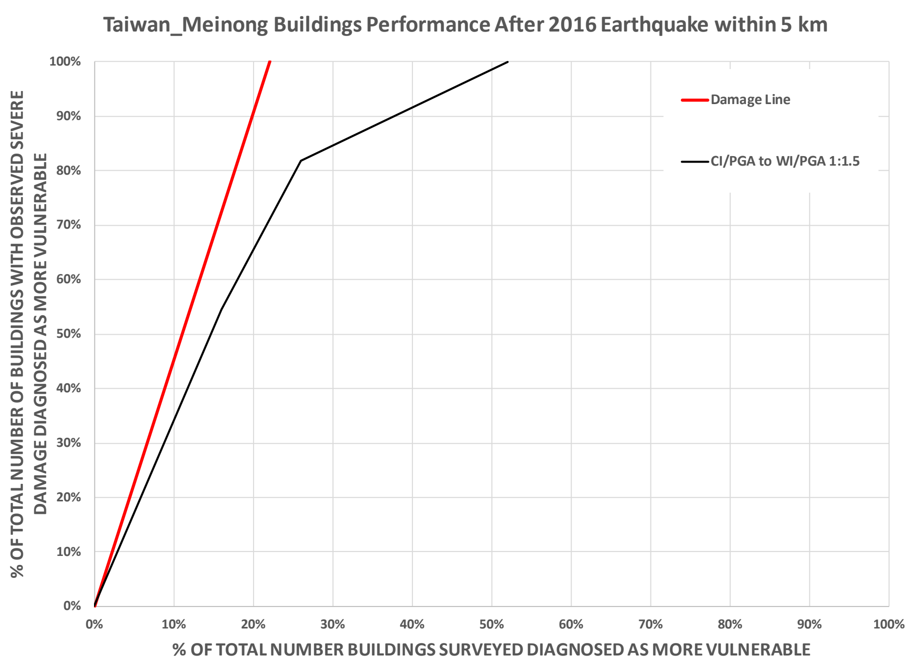

Figure 3.6. Fraction of buildings with observed severe damage successfully diagnosed as vulnerable versus fraction of total buildings diagnosed as vulnerable. 1:1.5 Column-Wall Index

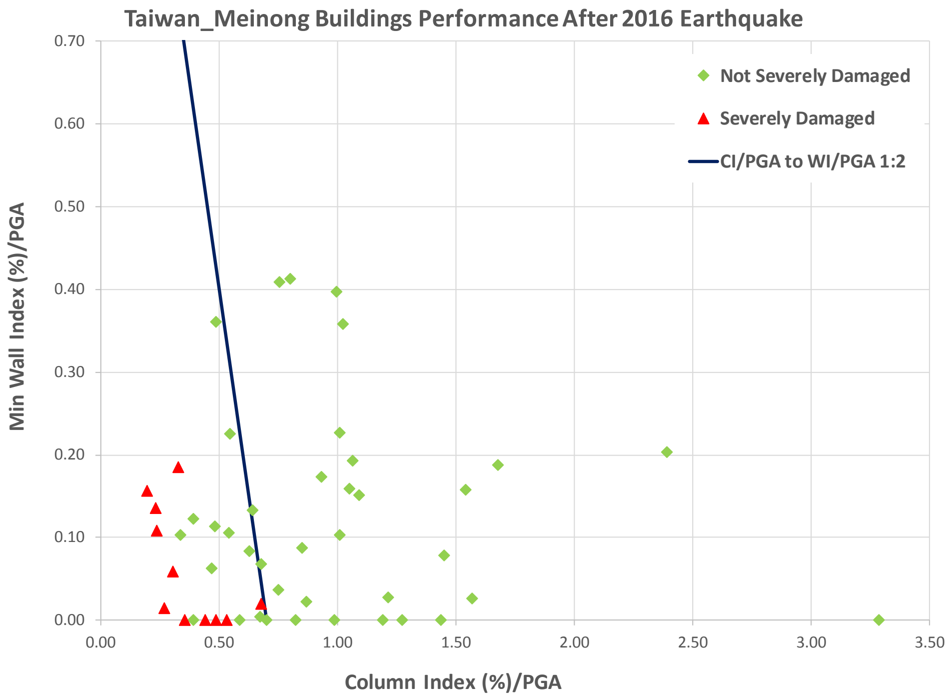

Figure 3.7. Seismic performance of Taiwan Buildings, 1:2 Column-Wall Index

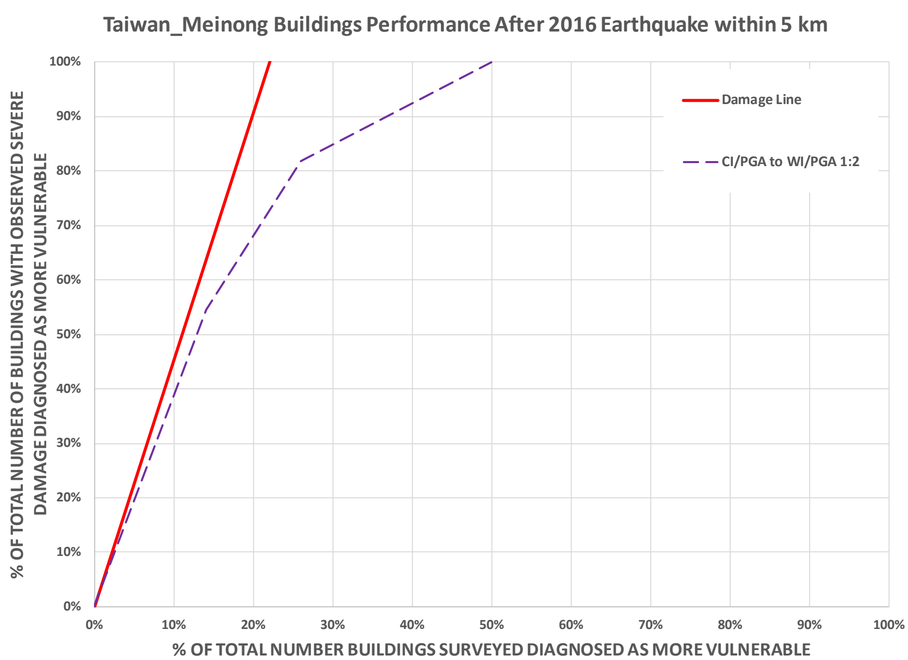

Figure 3.8. Fraction of buildings with observed severe damage successfully diagnosed as vulnerable versus fraction of total buildings diagnosed as vulnerable. 1:2 Column-Wall Index

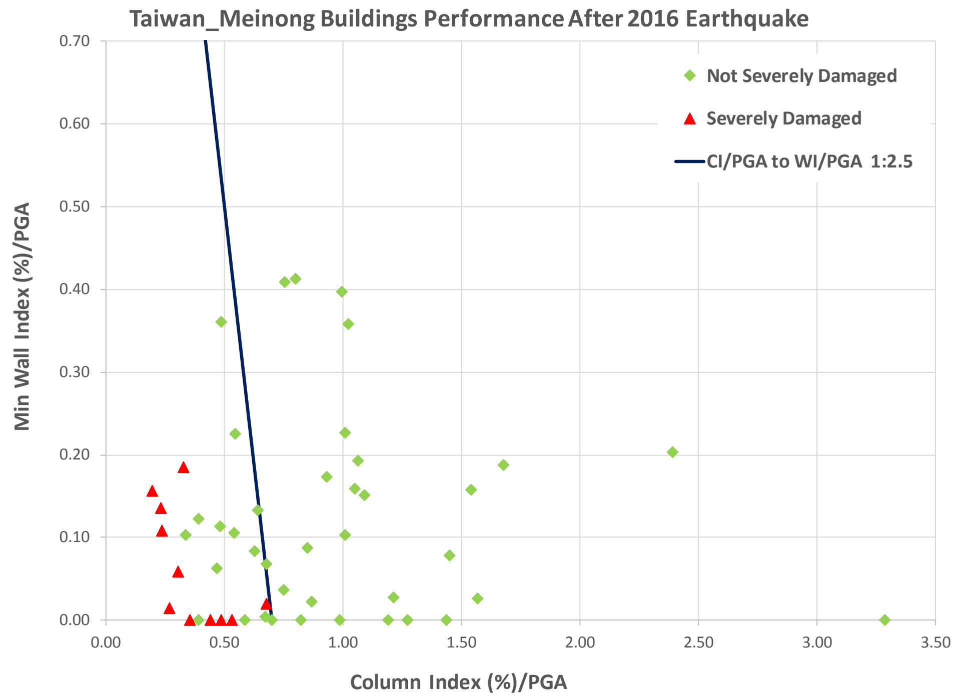

Figure 3.9. Seismic performance of Taiwan Buildings, 1:2.5 Column-Wall Index

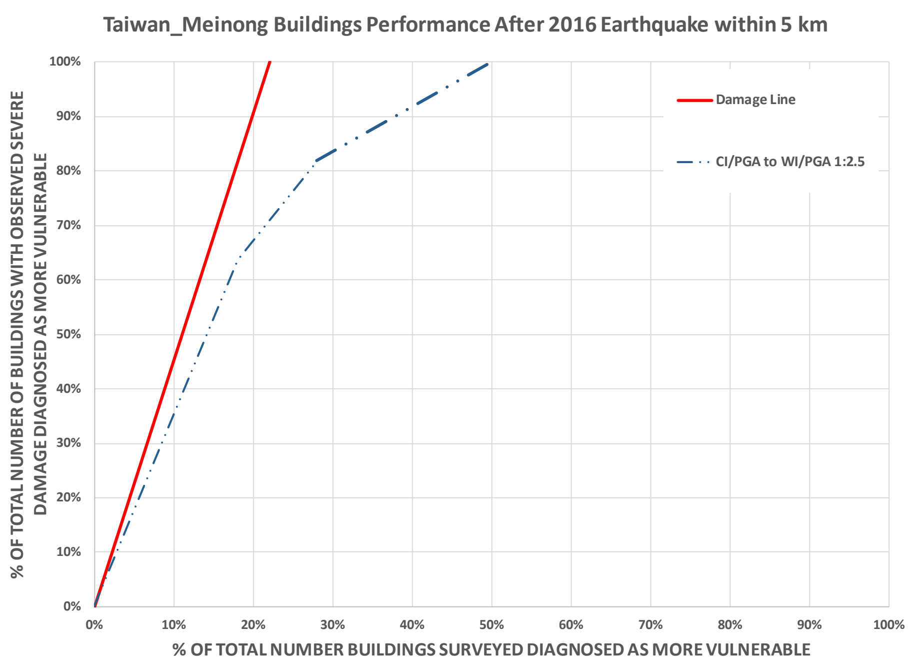

Figure 3.10. Fraction of buildings with observed severe damage successfully diagnosed as vulnerable versus fraction of total buildings diagnosed as vulnerable. 1:2.5 Column-Wall Index

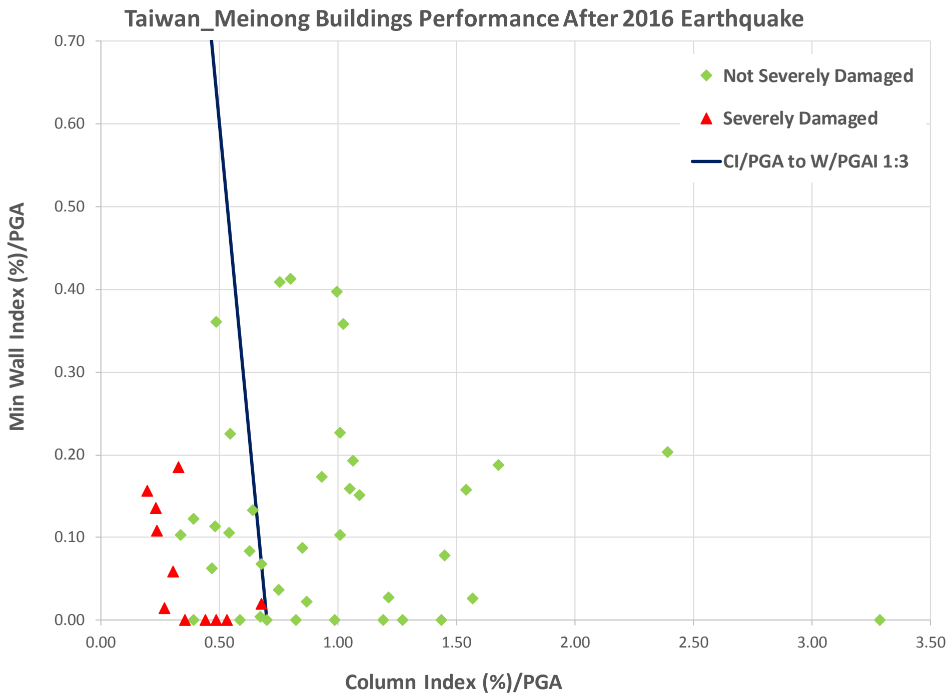

Figure 3.11. Seismic performance of Taiwan Buildings, 1:3 Column-Wall Index

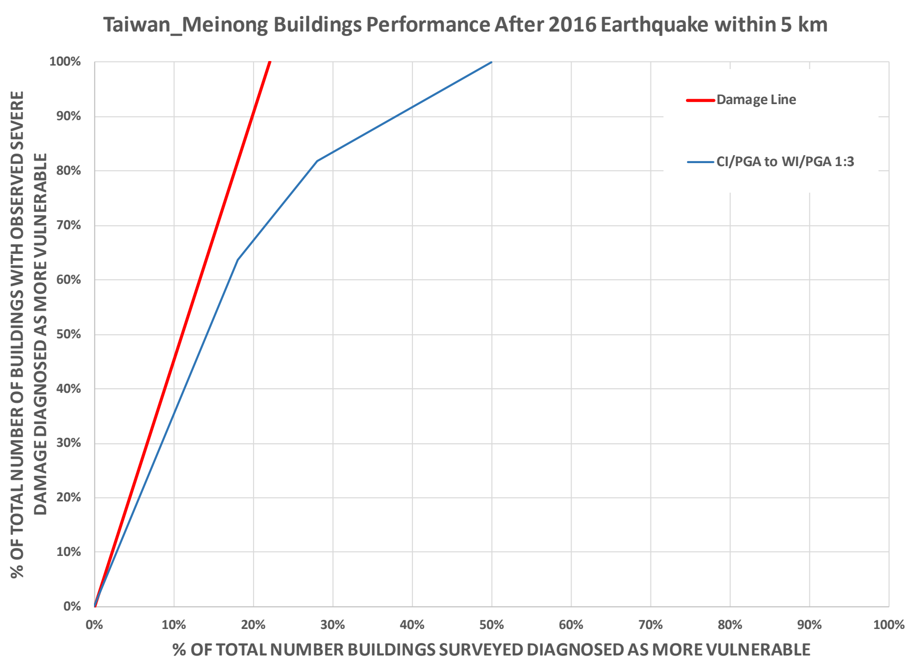

Figure 3.12. Fraction of buildings with observed severe damage successfully diagnosed as vulnerable versus fraction of total buildings diagnosed as vulnerable. 1:3 Column-Wall Index

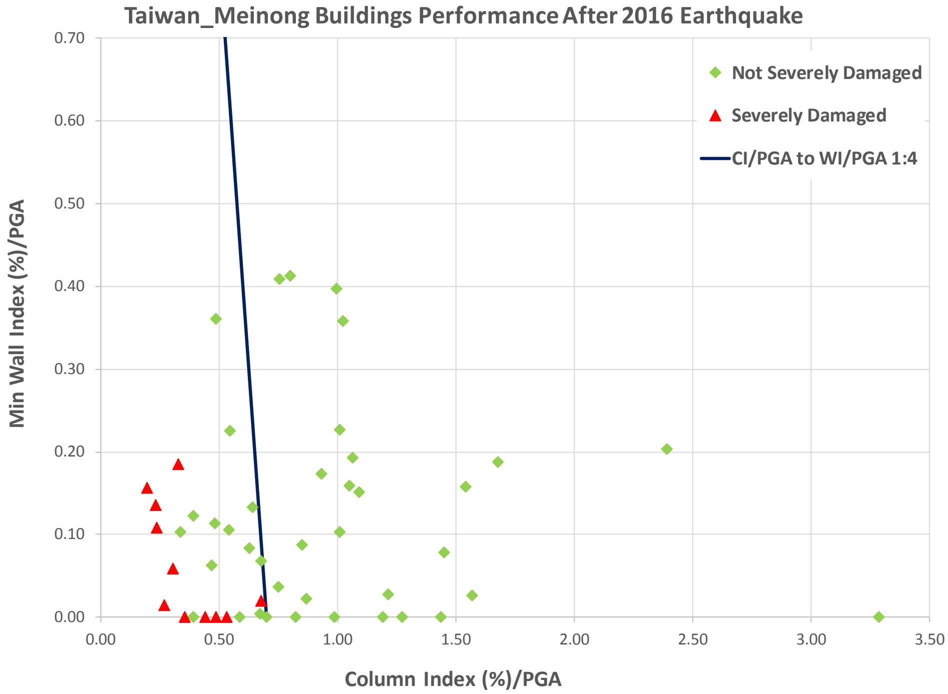

Figure 3.13. Seismic performance of Taiwan Buildings, 1:4 Column-Wall Index

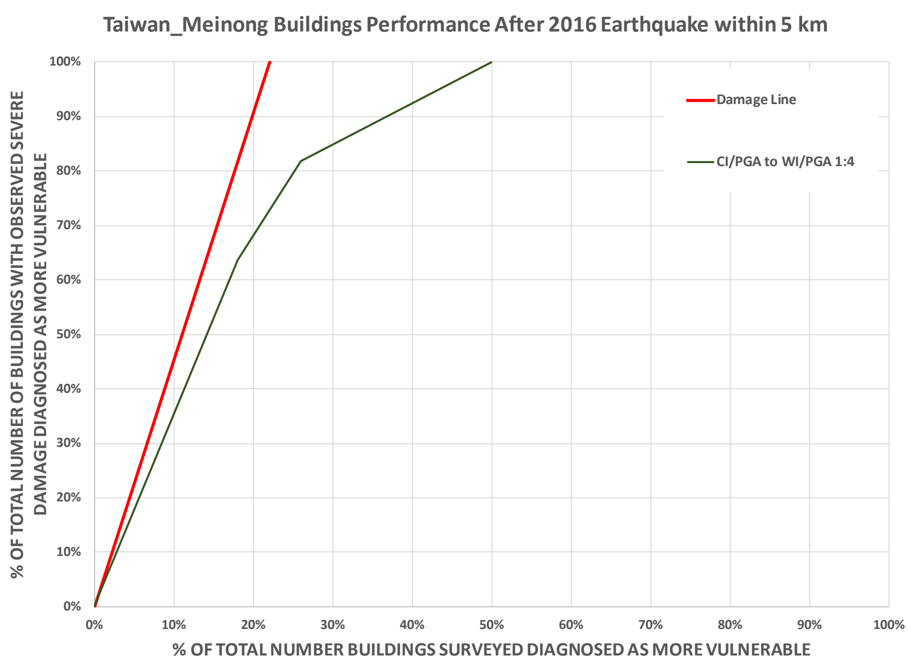

Figure 3.14. Fraction of buildings with observed severe damage successfully diagnosed as vulnerable versus fraction of total buildings diagnosed as vulnerable. 1:4 Column-Wall Index

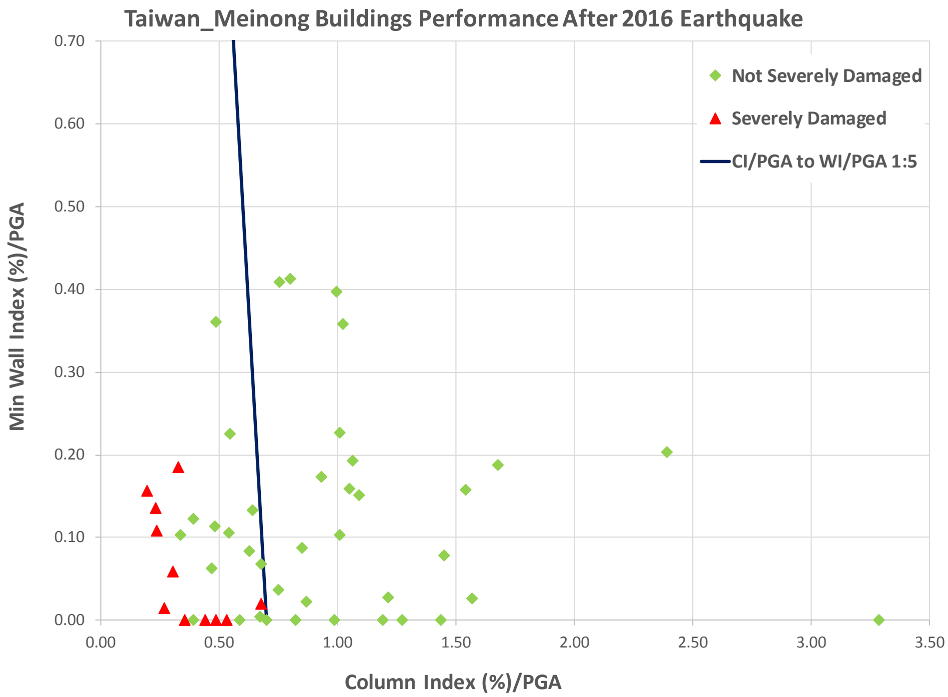

Figure 3.15. Seismic performance of Taiwan Buildings, 1:5 Column-Wall Index

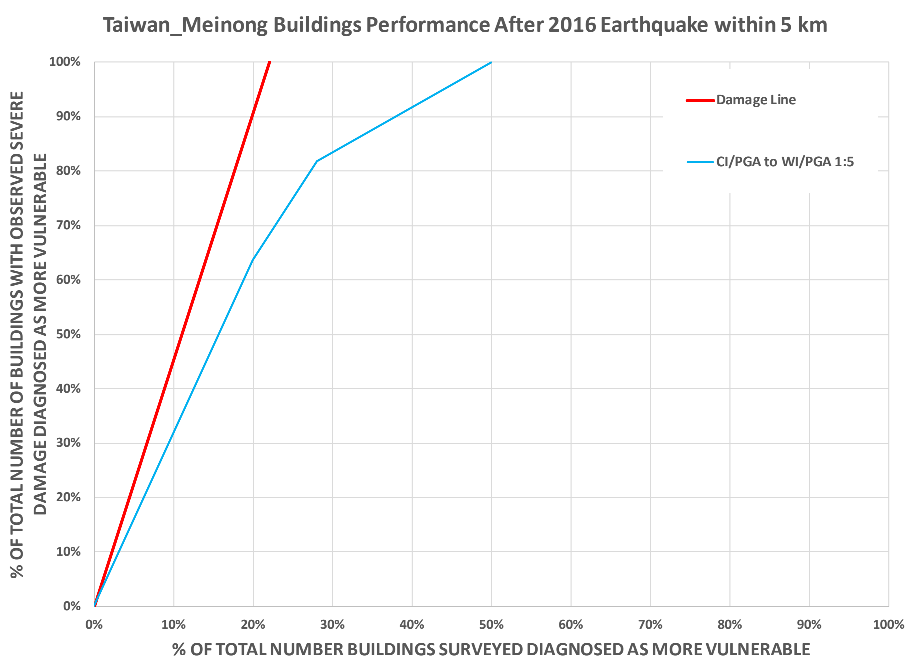

Figure 3.16. Fraction of buildings with observed severe damage successfully diagnosed as vulnerable versus fraction of total buildings diagnosed as vulnerable. 1:5 Column-Wall Index

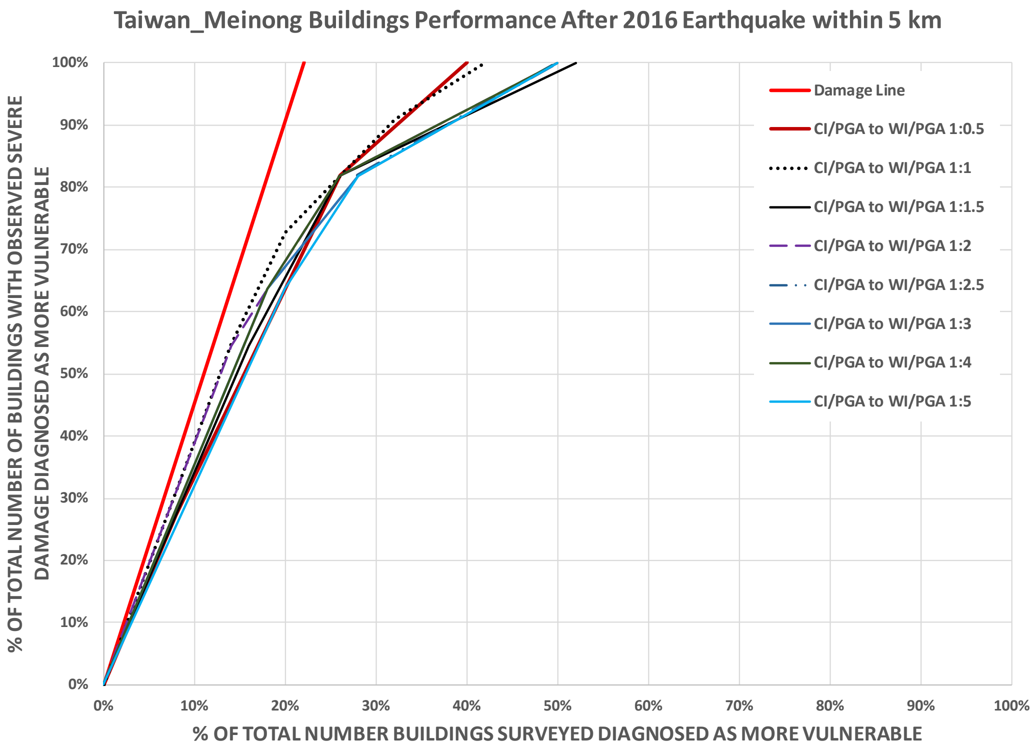

Figure 3.17. Fraction of buildings with observed severe damage successfully diagnosed as vulnerable versus fraction of total buildings diagnosed as vulnerable. Various Combinations of Column-Wall Index

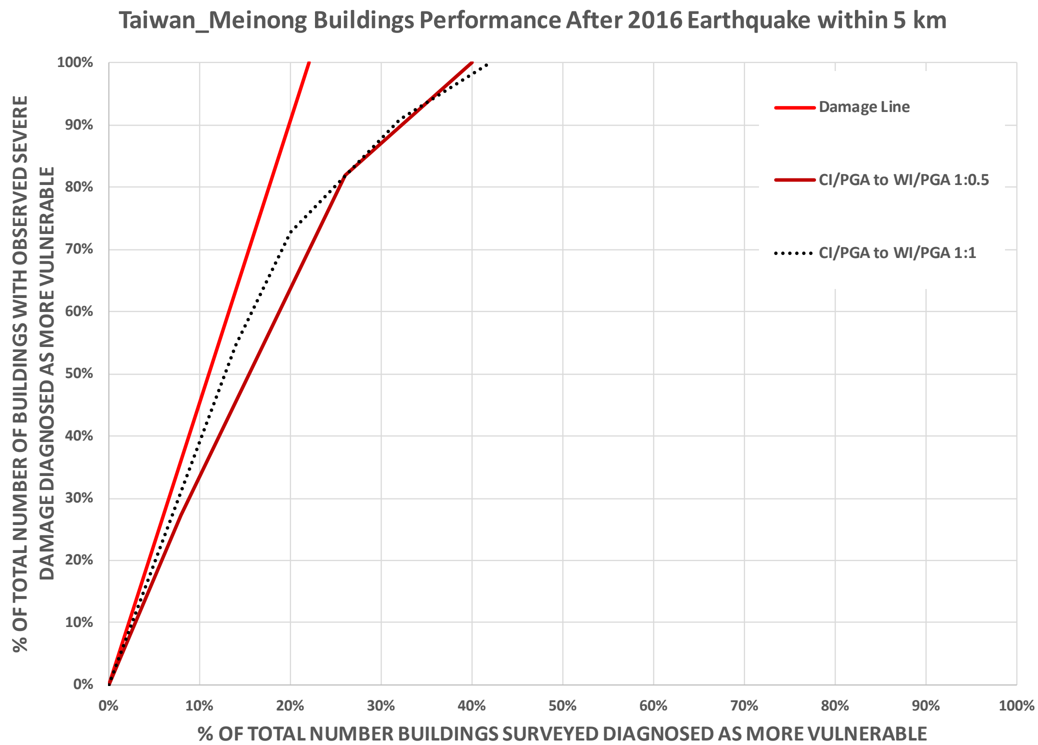

Figure 3.18. Fraction of buildings with observed severe damage successfully diagnosed as vulnerable versus fraction of total buildings diagnosed as vulnerable. 1:1 and 1:0.5 Column-Wall Index (Best Fit Thresholds)

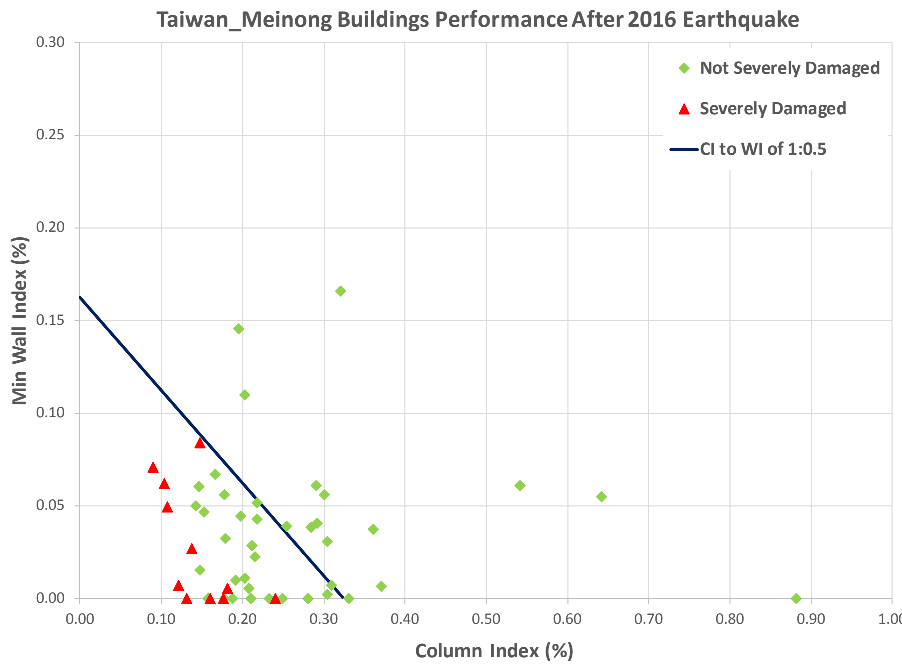

Figure 3.19. Seismic performance of Taiwan Buildings, 1:0.5 Column-Wall Index

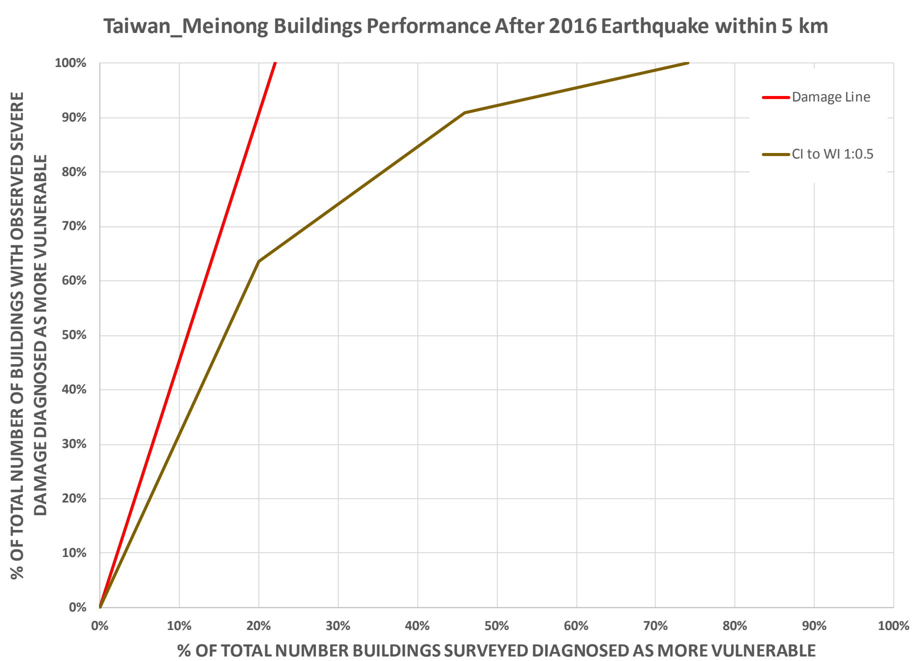

Figure 3.20. Fraction of buildings with observed severe damage successfully diagnosed as vulnerable versus fraction of total buildings diagnosed as vulnerable. 1:0.5 Column-Wall Index

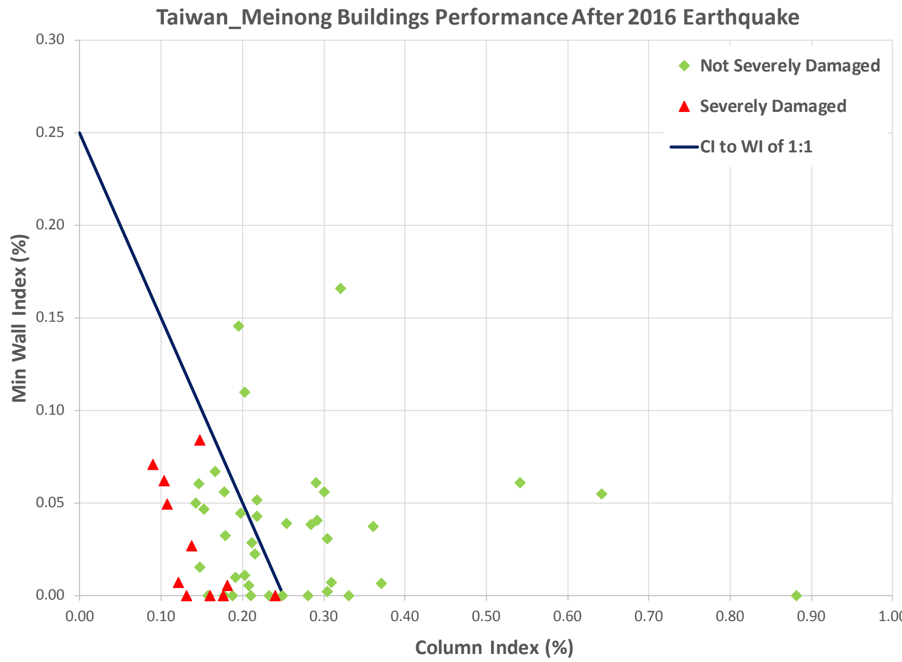

Figure 3.21. Seismic performance of Taiwan Buildings, 1:1 Column-Wall Index

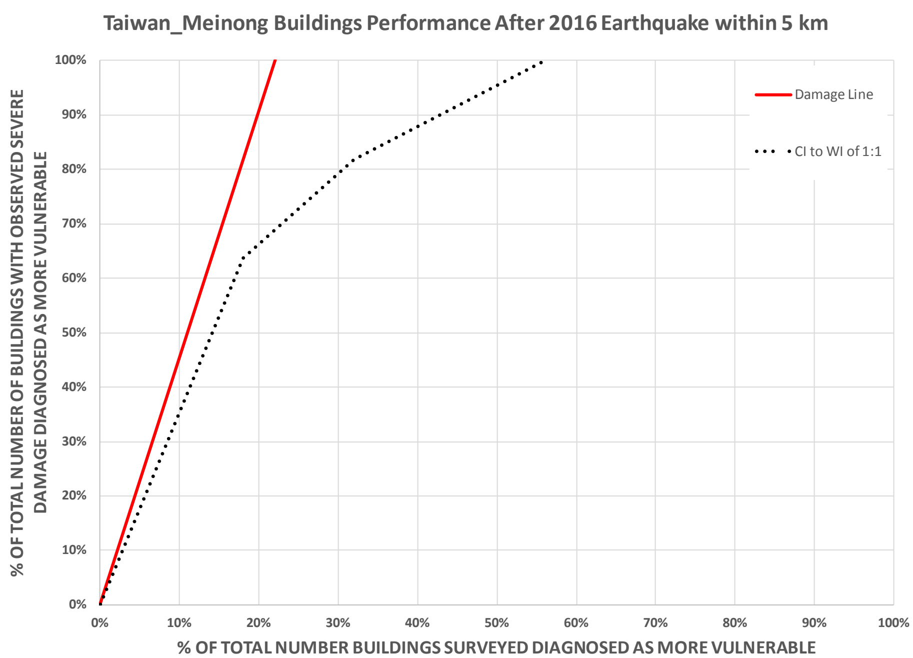

Figure 3.22. Fraction of buildings with observed severe damage successfully diagnosed as vulnerable versus fraction of total buildings diagnosed as vulnerable. 1:1 Column-Wall Index

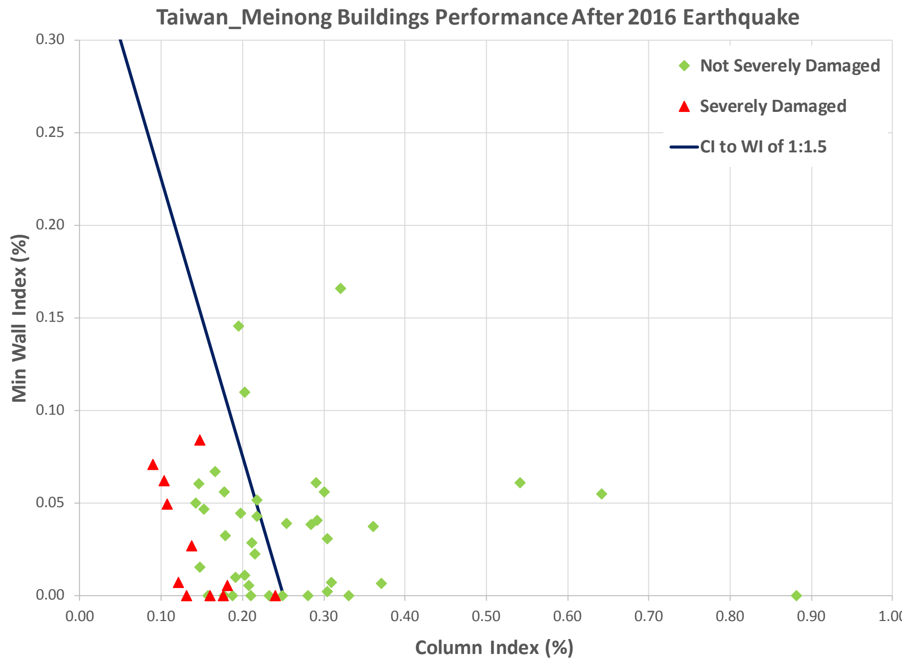

Figure 3.23. Seismic performance of Taiwan Buildings, 1:1.5 Column-Wall Index

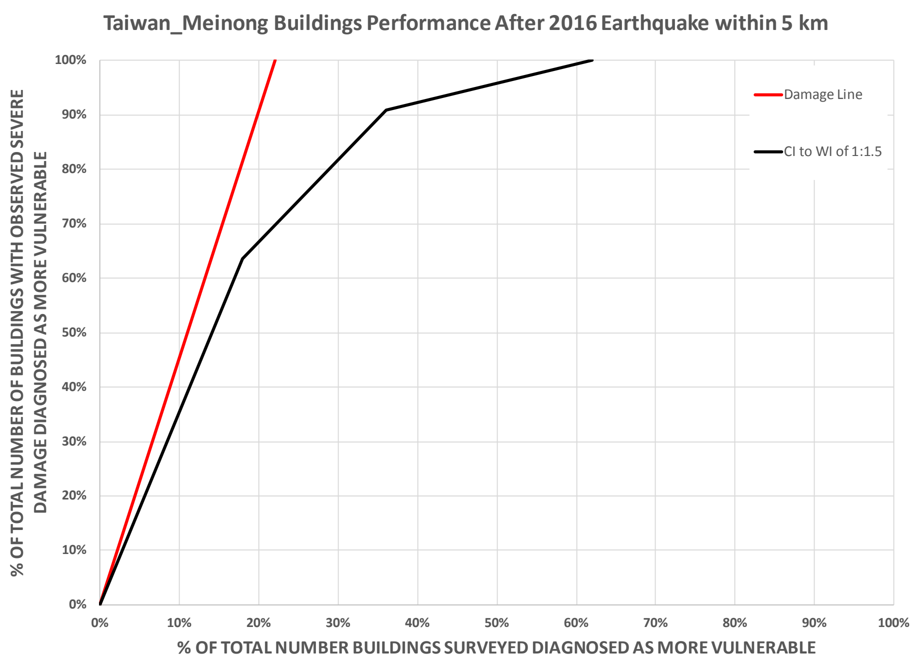

Figure 3.24. Fraction of buildings with observed severe damage successfully diagnosed as vulnerable versus fraction of total buildings diagnosed as vulnerable. 1:1.5 Column-Wall Index

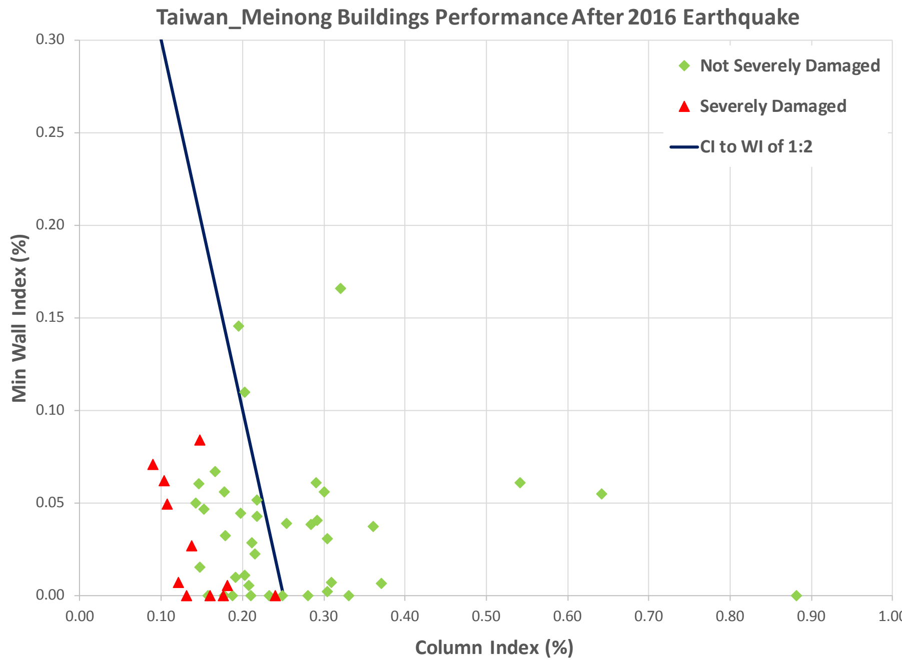

Figure 3.25. Seismic performance of Taiwan Buildings, 1:2 Column-Wall Index

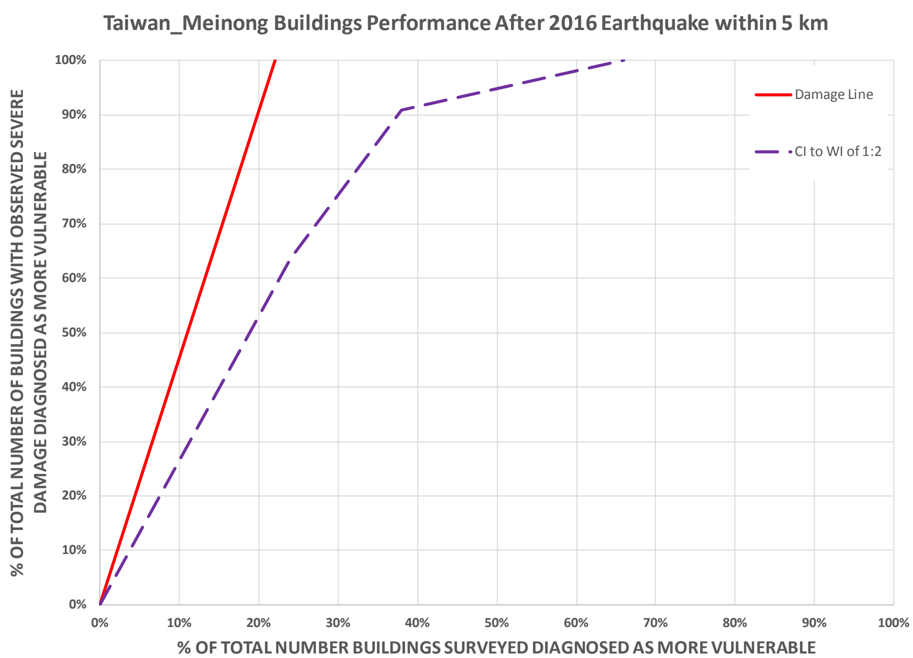

Figure 3.26. Fraction of buildings with observed severe damage successfully diagnosed as vulnerable versus fraction of total buildings diagnosed as vulnerable. 1:2 Column-Wall Index

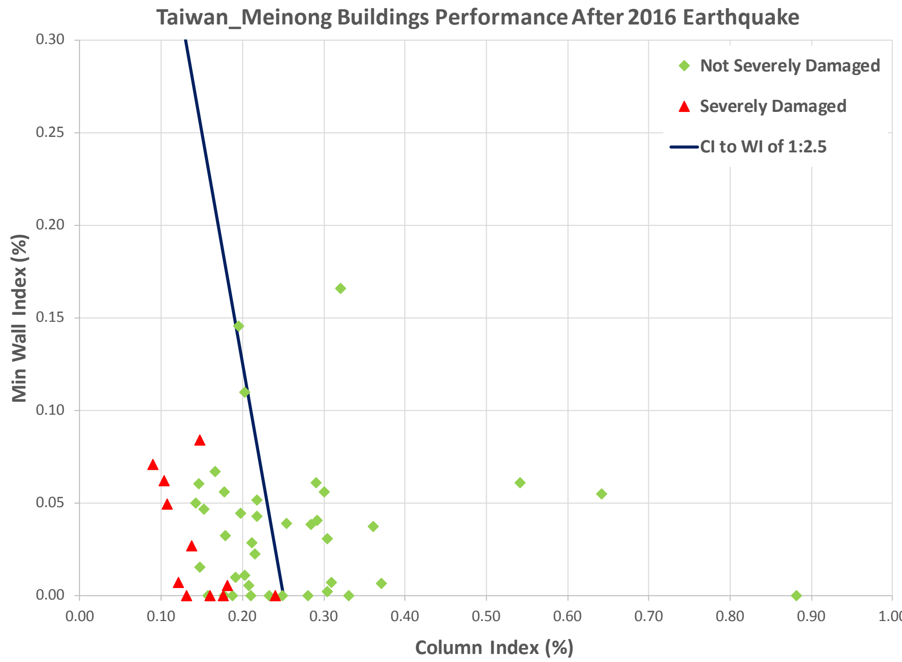

Figure 3.27. Seismic performance of Taiwan Buildings, 1:2.5 Column-Wall Index

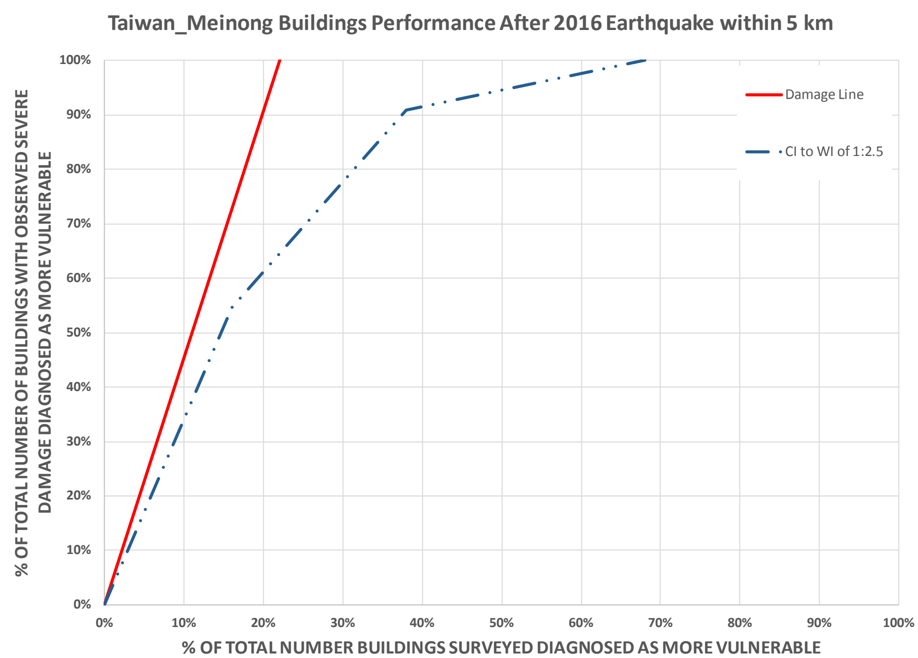

Figure 3.28. Fraction of buildings with observed severe damage successfully diagnosed as vulnerable versus fraction of total buildings diagnosed as vulnerable. 1:2.5 Column-Wall Index

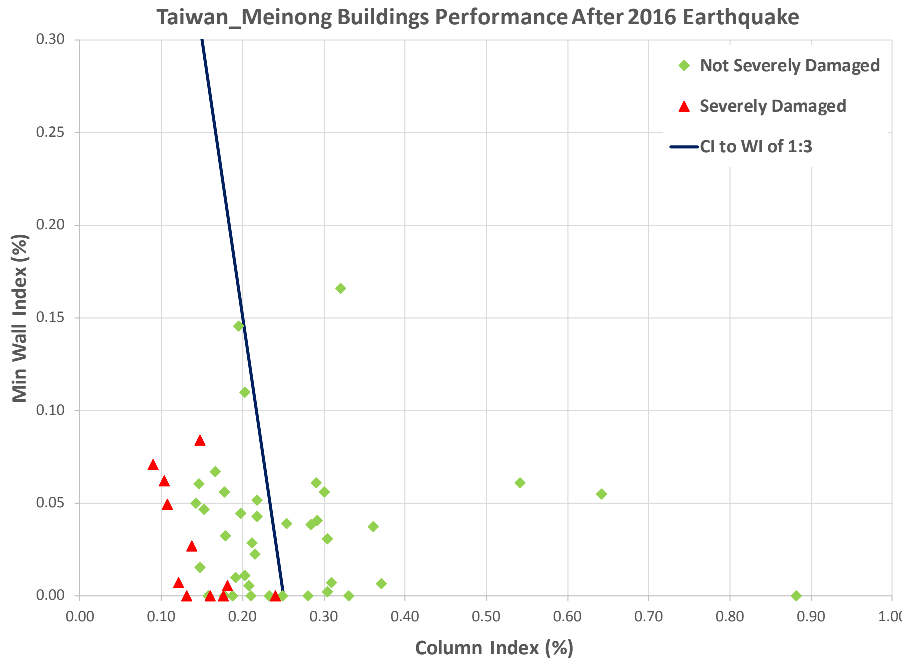

Figure 3.29. Seismic performance of Taiwan Buildings, 1:3 Column-Wall Index

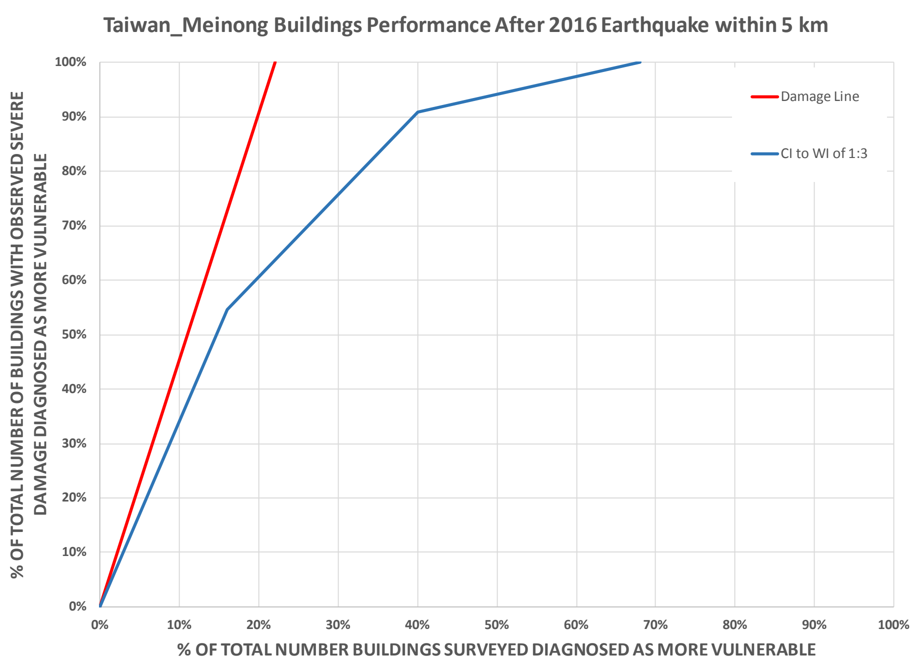

Figure 3.30. Fraction of buildings with observed severe damage successfully diagnosed as vulnerable versus fraction of total buildings diagnosed as vulnerable. 1:3 Column-Wall Index

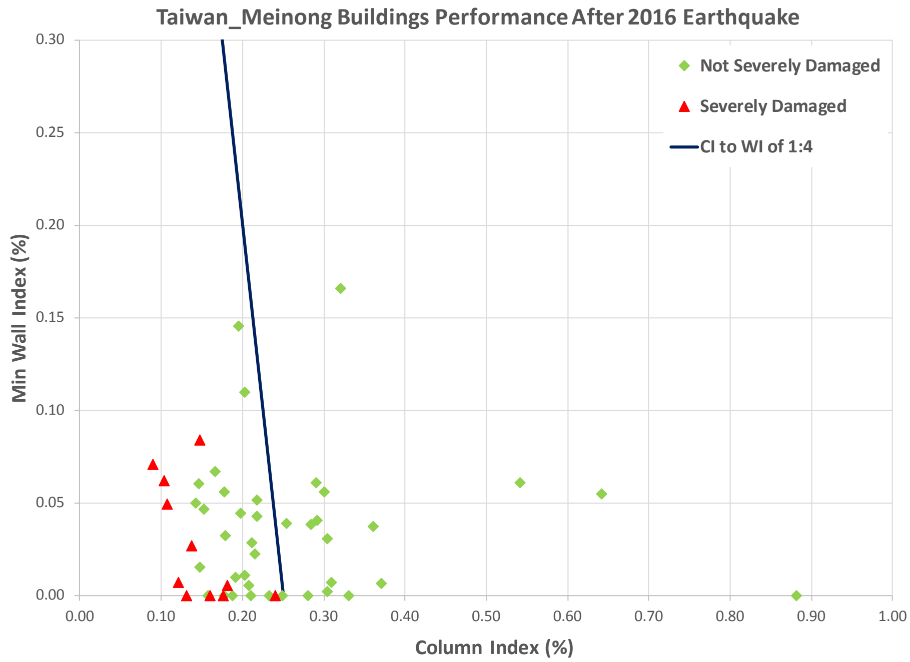

Figure 3.31. Seismic performance of Taiwan Buildings, 1:4 Column-Wall Index

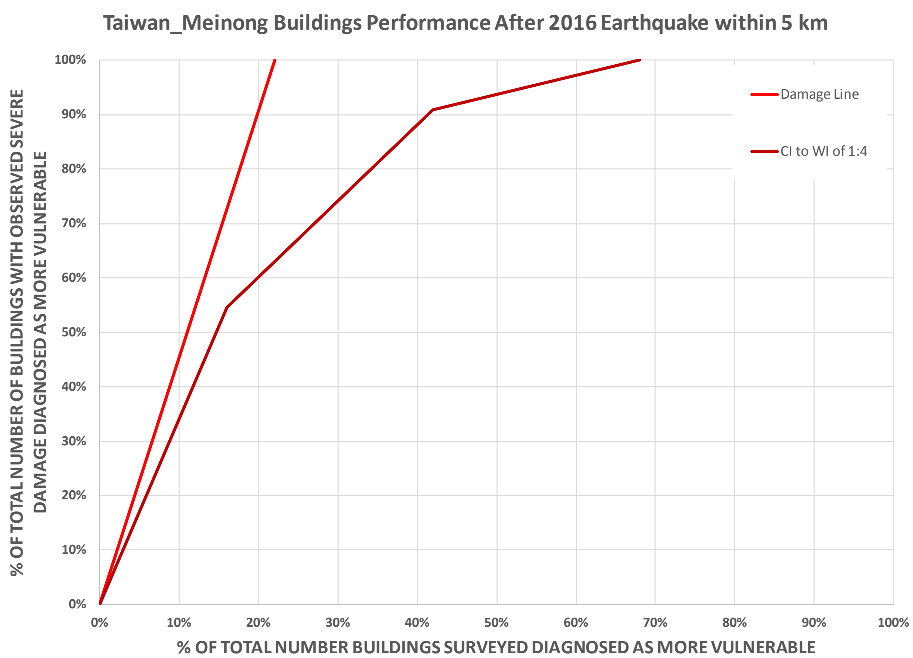

Figure 3.32. Fraction of buildings with observed severe damage successfully diagnosed as vulnerable versus fraction of total buildings diagnosed as vulnerable. 1:4 Column-Wall Index

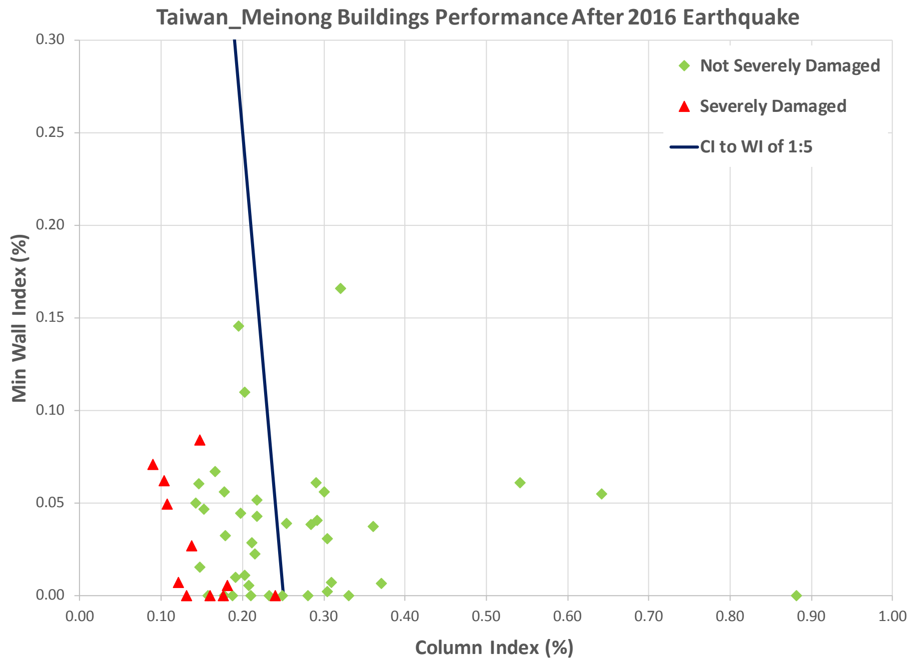

Figure 3.33. Seismic performance of Taiwan Buildings, 1:5 Column-Wall Index

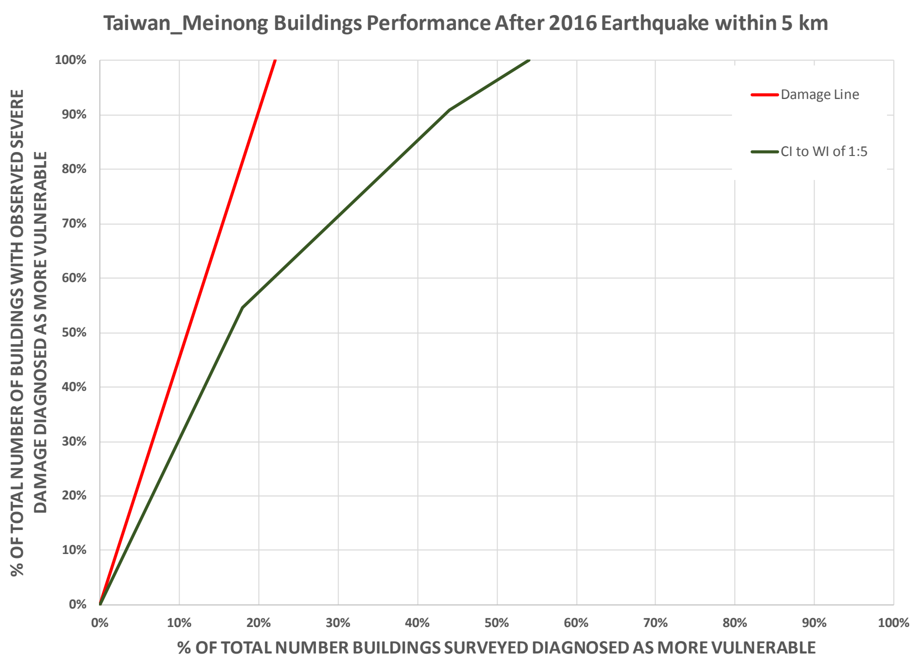

Figure 3.34. Fraction of buildings with observed severe damage successfully diagnosed as vulnerable versus fraction of total buildings diagnosed as vulnerable. 1:5 Column-Wall Index

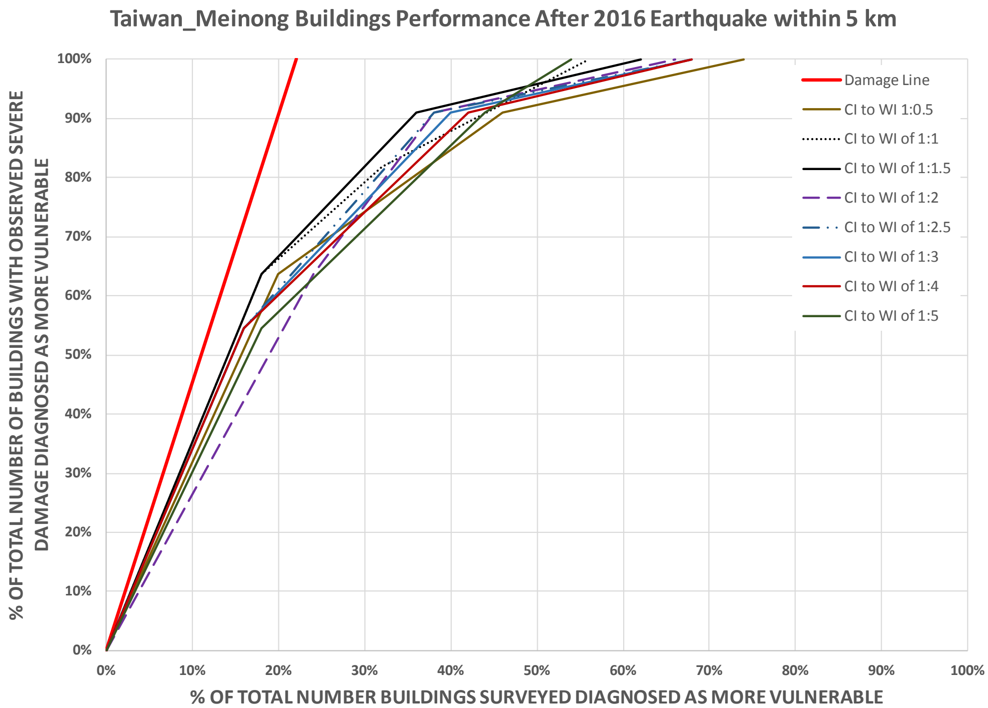

Figure 3.35. Fraction of buildings with observed severe damage successfully diagnosed as vulnerable versus fraction of total buildings diagnosed as vulnerable. Various Combinations of Column-Wall Index

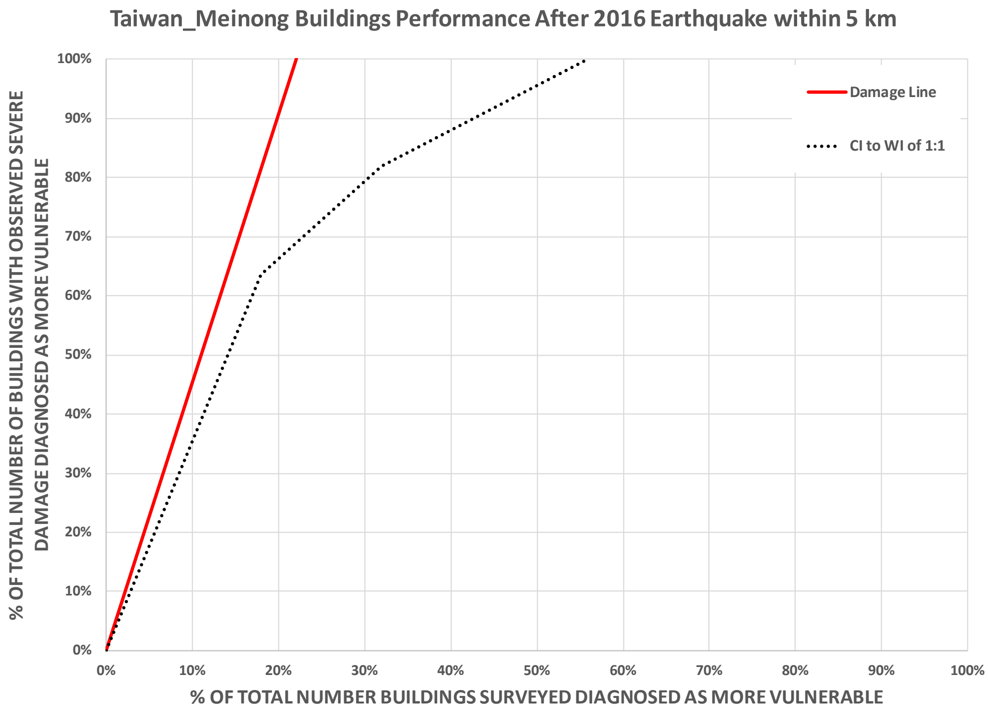

Figure 3.36. Fraction of buildings with observed severe damage successfully diagnosed as vulnerable versus fraction of total buildings diagnosed as vulnerable. 1:1 Column-Wall Index (Best Fit Threshold)

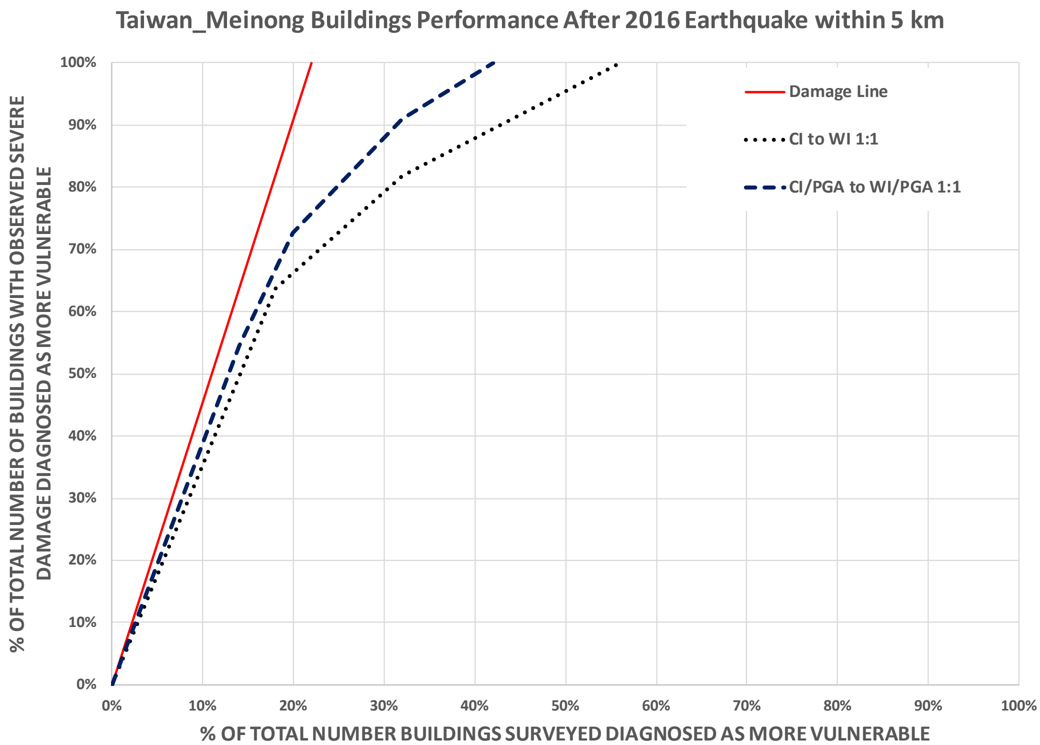

Figure 3.37. Comparison of Best Fit Threshold of 1:1 Column-Wall Index with Best Fit Threshold of 1:1 Column-Wall Index Normalized by PGA for Fraction of buildings with observed severe damage successfully diagnosed as vulnerable versus fraction of total

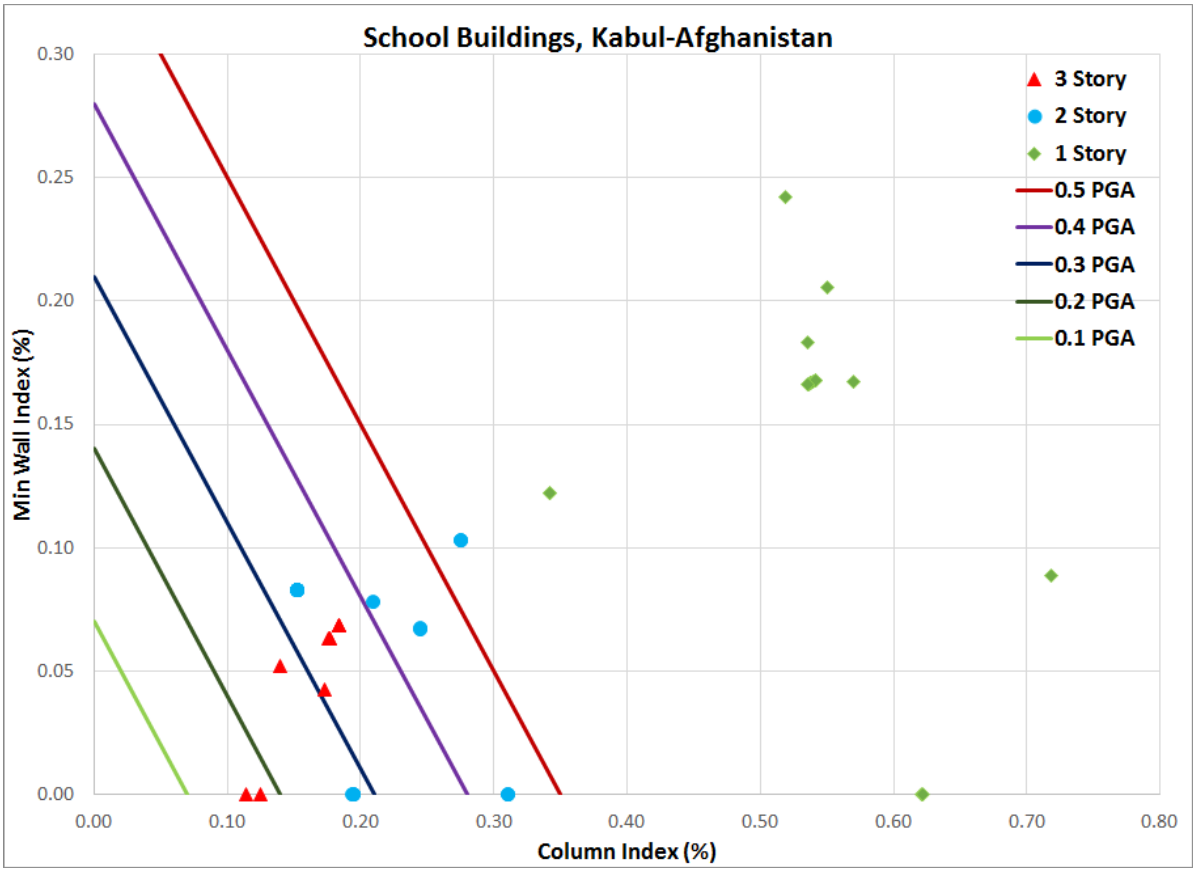

Figure 4.1. Estimated seismic performance of schools in Kabul, 1:1 column-wall index

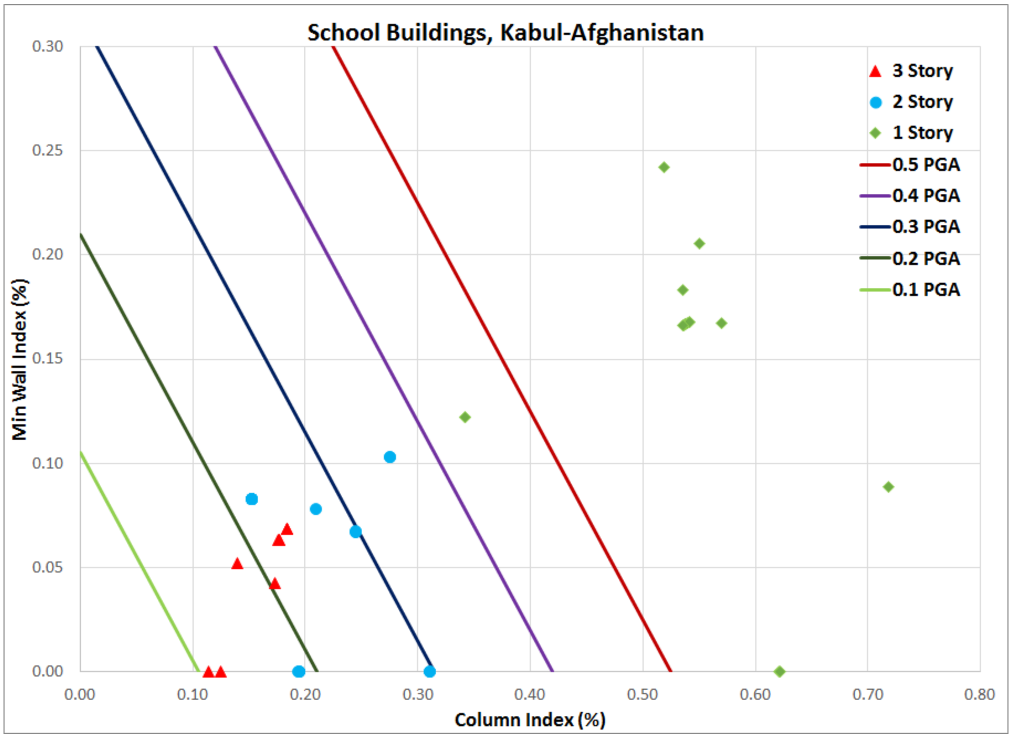

Figure 4.2. Estimated seismic performance of school buildings in Kabul, 1:1 column-wall index threshold increased by 50%

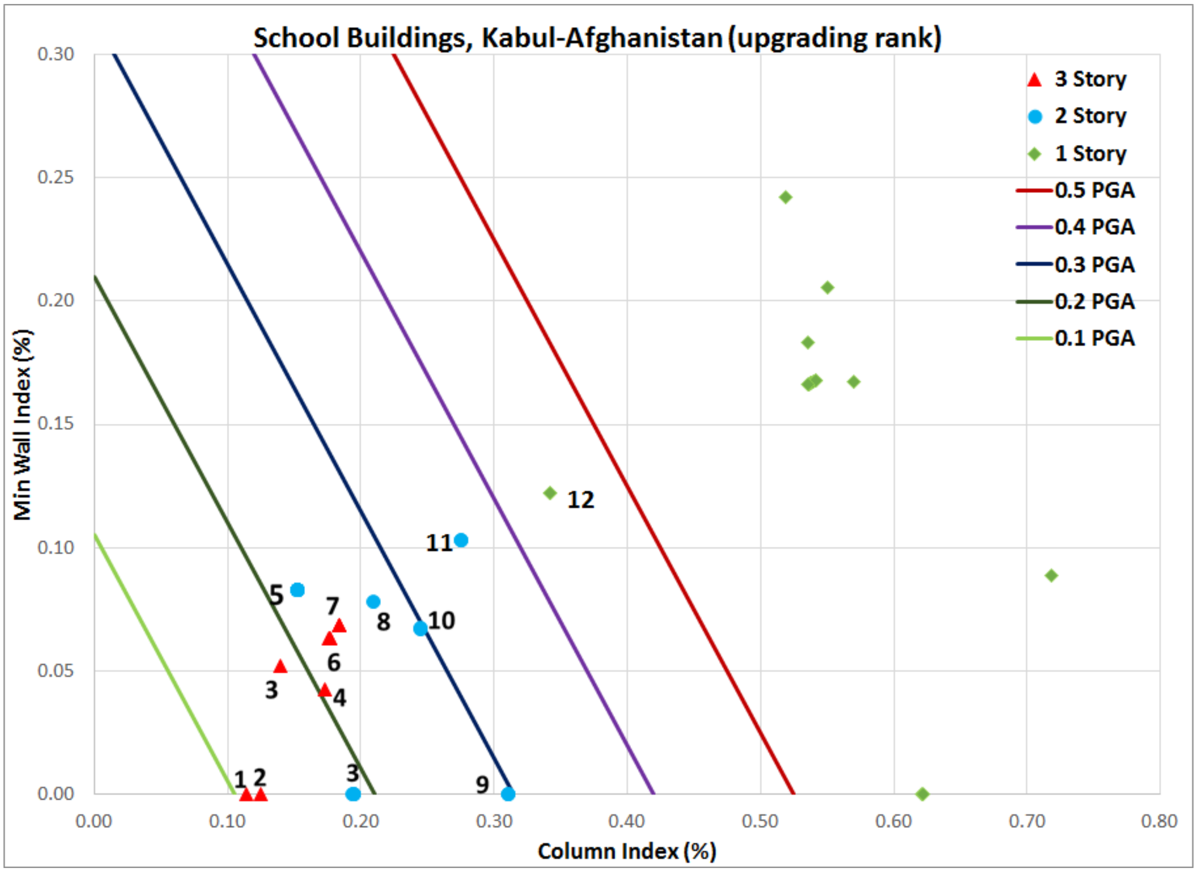

Figure 4.3. Upgrading of schools with more vulnerability, 1:1 column-wall index with threshold increased by 50%

LIST OF REFERENCES

1. Benz, H., Machette, M., Sipkin, S. and Wheeler, R., 2005. Assessing the seismic hazards of Afghanistan. US Geological Survey Publication. http://pubs. er. usgs. gov, publication/fs, 20053038.

2. Dewey, J.W., 2006. Seismicity of Afghanistan and vicinity/edited by James W. Dewey. Afghan Digital Libraries. U.S. Geological Survey Open-File Report 2006–1185, 60 p..

3. Wheeler, R.L., Bufe, C.G., Johnson, M.L., Dart, R.L. and Norton, G.A., 2005. Seismotectonic map of Afghanistan, with annotated bibliography. US Department of the Interior, US Geological Survey.

4. Boyd, O.S., Mueller, C.S. and Rukstales, K.S., 2007. Preliminary earthquake hazard map of Afghanistan. US Geological Survey Open-File Report, 2007, p.1137.

5. Ambraseys, N. and Bilham, R., 2014. The tectonic setting of Bamiyan and seismicity in and near Afghanistan for the past twelve centuries. In After the Destruction of Giant Buddha Statues in Bamiyan (Afghanistan) in 2001 (pp. 101-152). Springer, Berlin, Heidelberg.

6. Hassan, A.F. and Sozen, M.A., 1997. Seismic vulnerability assessment of low-rise buildings in regions with infrequent earthquakes. ACI Structural Journal, 94(1), pp.31-39.

7. Sozen, Mete A., and José Roesset. Structural Damage Caused by the 1976 Guatemala Earthquake. University of Illinois Engineering Experiment Station. College of Engineering. University of Illinois at Urbana-Champaign, 1976.

8. Gur, T., Pay, A., Ramirez, J.A., Sozen, M.A., Johnson, A.M., Irfanoglu, A. and Bobet, A., 2009. Performance of school buildings in Turkey during the 1999 Düzce and the 2003 Bingöl earthquakes. Earthquake Spectra, 25(2), pp.239-256.

9. Donmez, C. and Pujol, S., 2005. Spatial distribution of damage caused by the 1999 earthquakes in Turkey. Earthquake Spectra, 21(1), pp.53-69.

APPENDIX A – KABUL SCHOOL BUILDINGS FLOOR PLAN AND FRONT VIEW

Figure A-1. Kabul School 1 (front view)

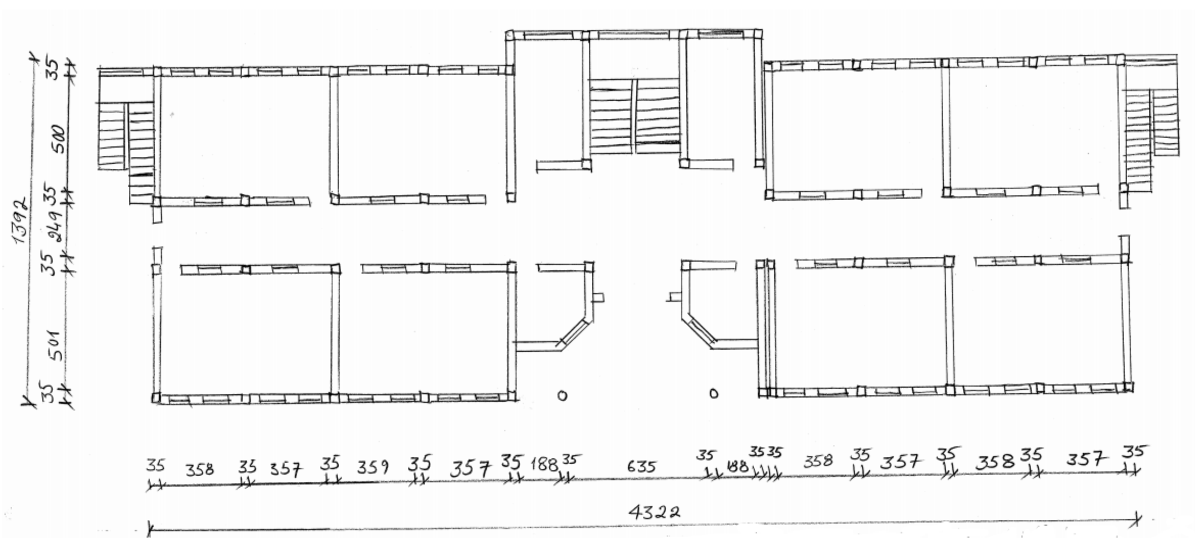

Figure A-2. Kabul School 1, typical floor plan

Figure A-3. Kabul School 2 (front view)

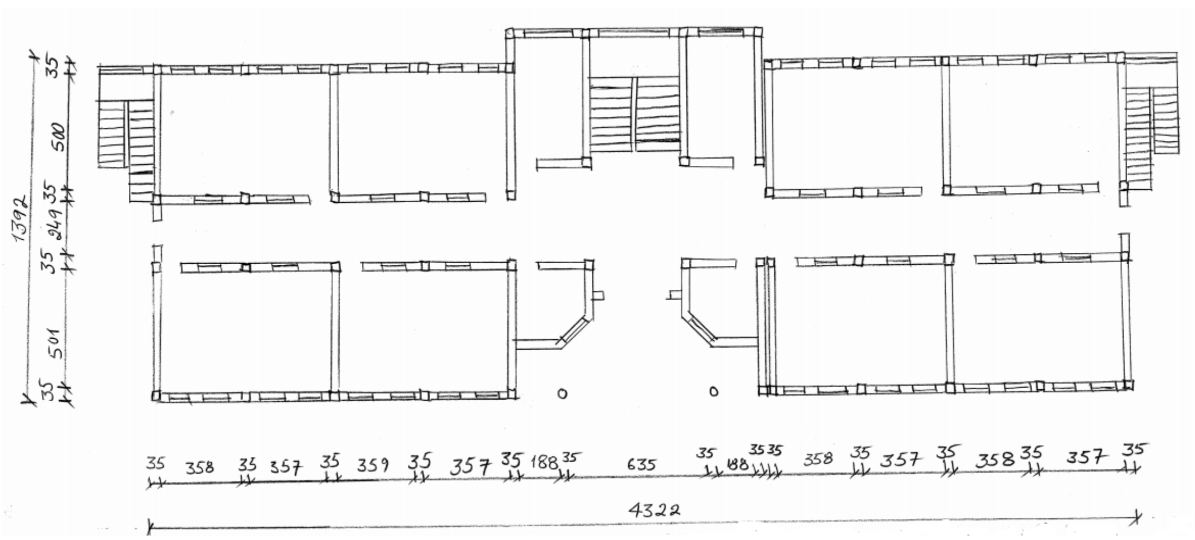

Figure A-4. Kabul School 2, typical floor plan

Figure A-5. Kabul School 3 (front view)

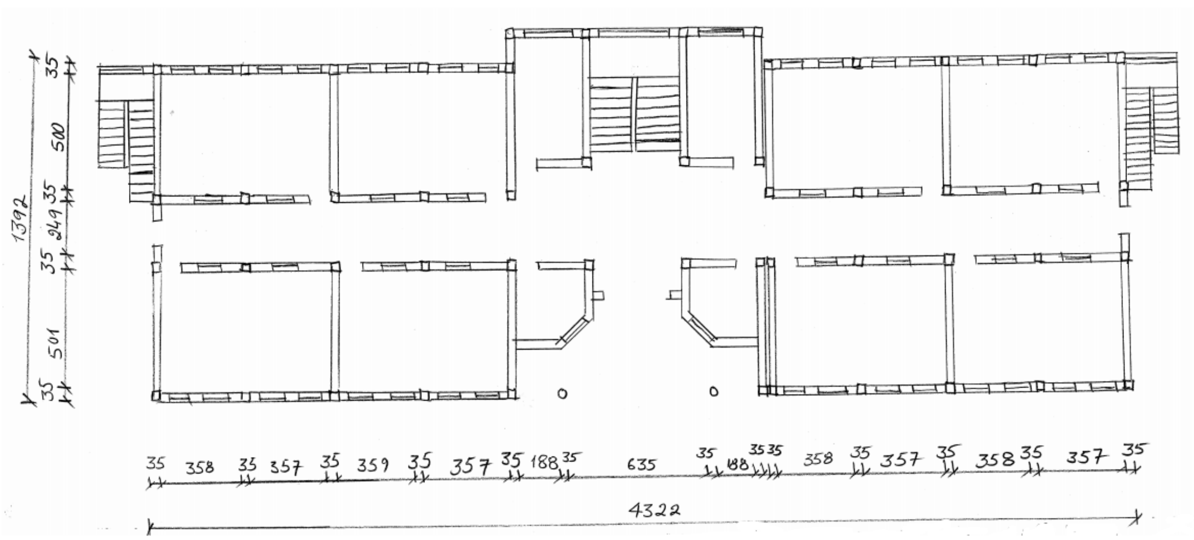

Figure A-6. Kabul School 3, typical floor plan

Figure A-7. Kabul School 4 (front view)

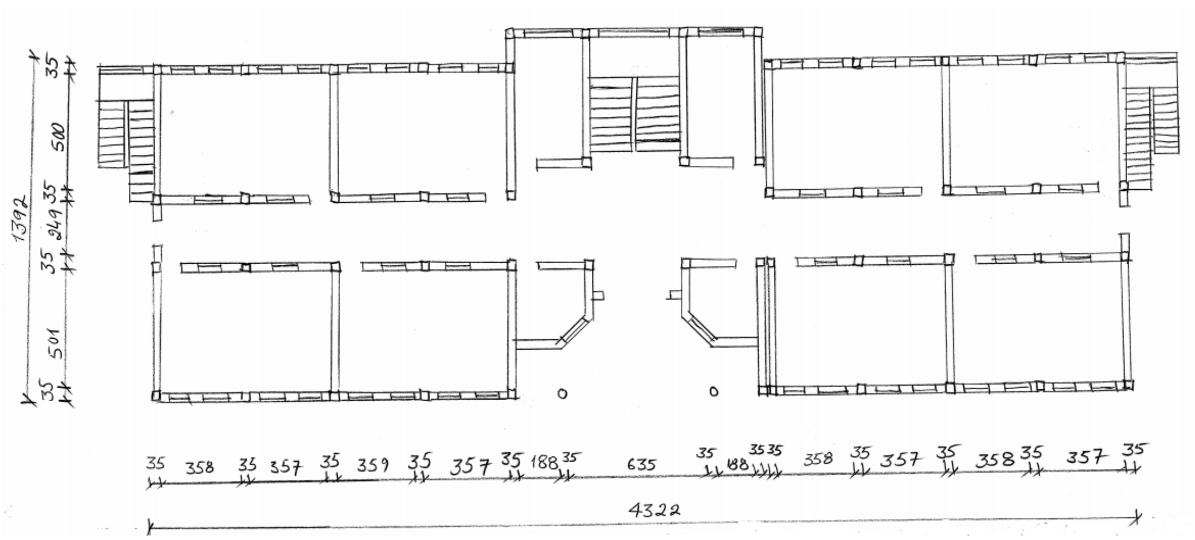

Figure A-8. Kabul School 4, typical floor plan

Figure A-9. Kabul School 5 (front view)

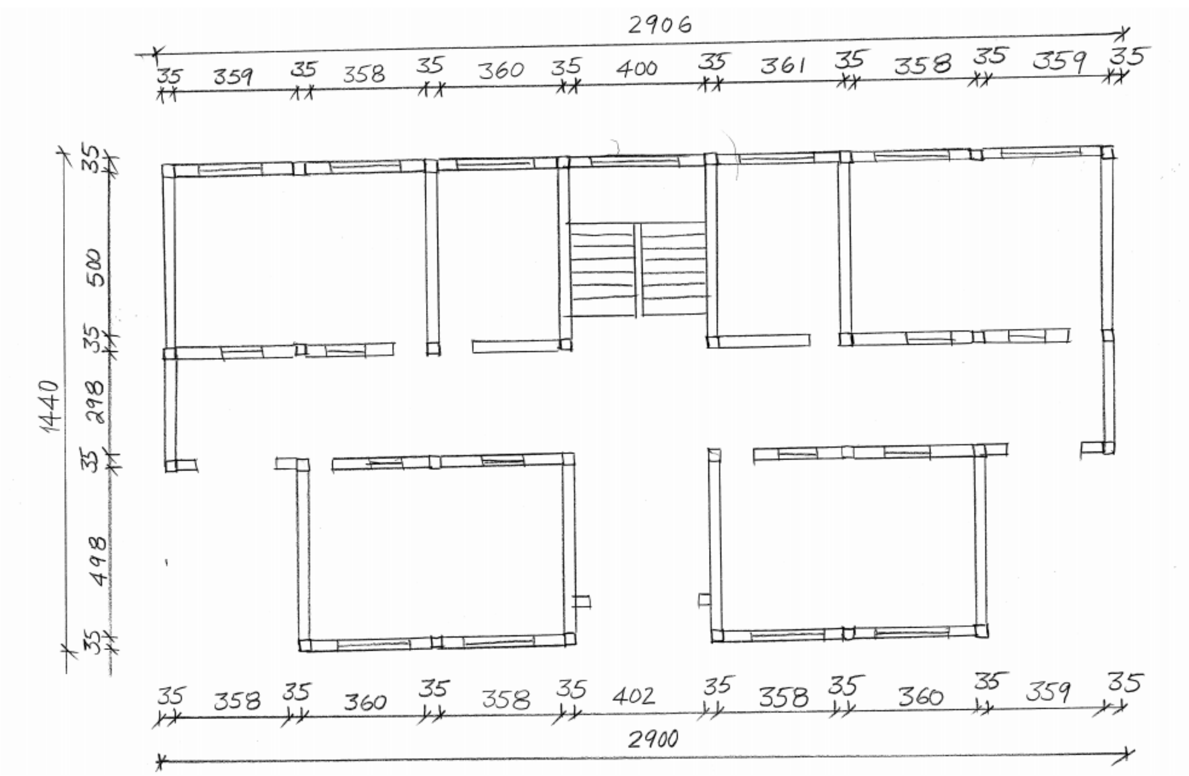

Figure A-10. Kabul School 5, typical floor plan

Figure A-11. Kabul School 6 (front view)

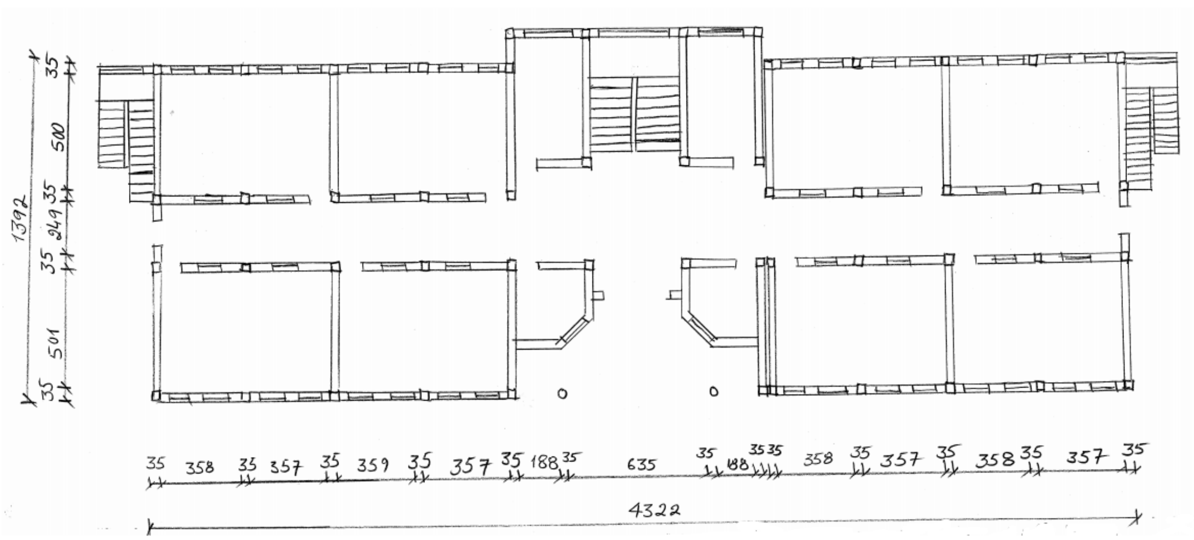

Figure A-12. Kabul School 6, typical floor plan

Figure A-13. Kabul School 7 (front view)

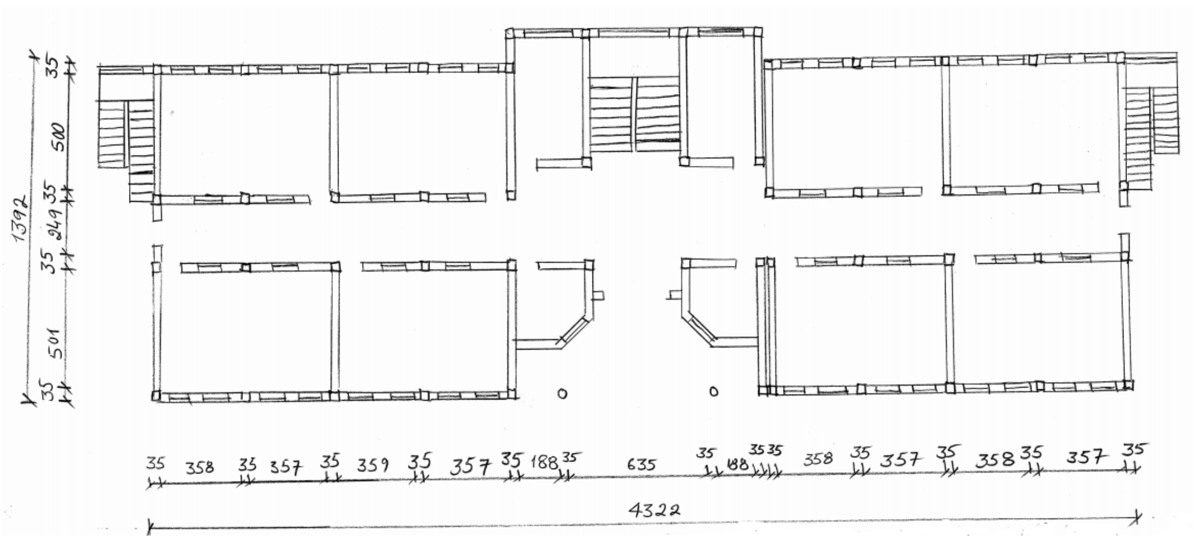

Figure A-14. Kabul School 7, typical floor plan

Figure A-15. Kabul School 8 (front view)

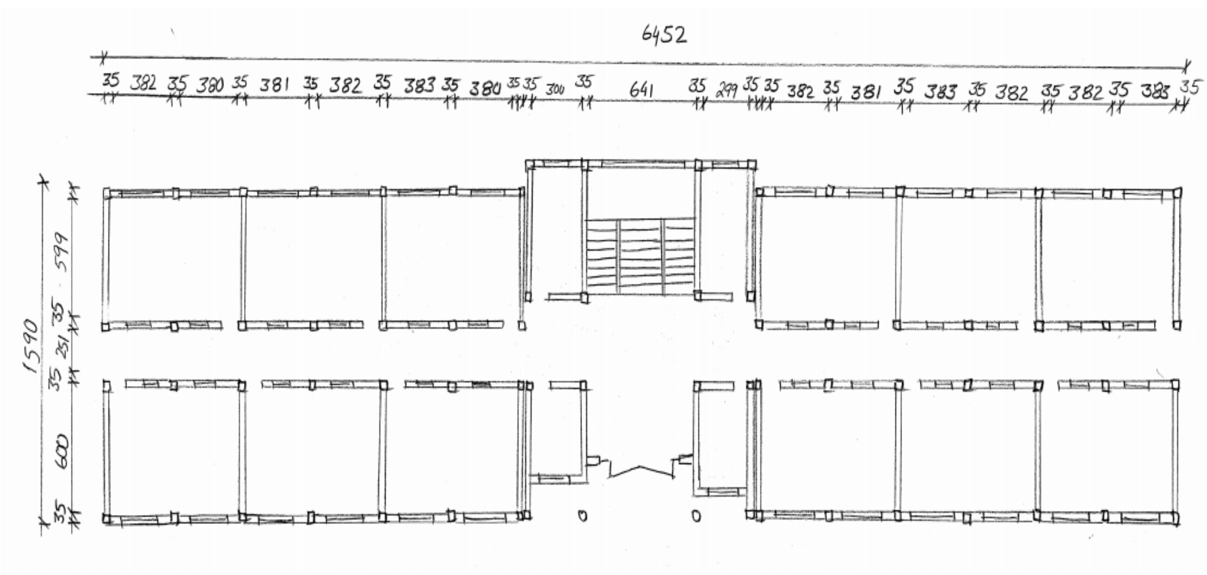

Figure A-16. Kabul School 8, typical floor plan

Figure A-17. Kabul School 9 (front view)

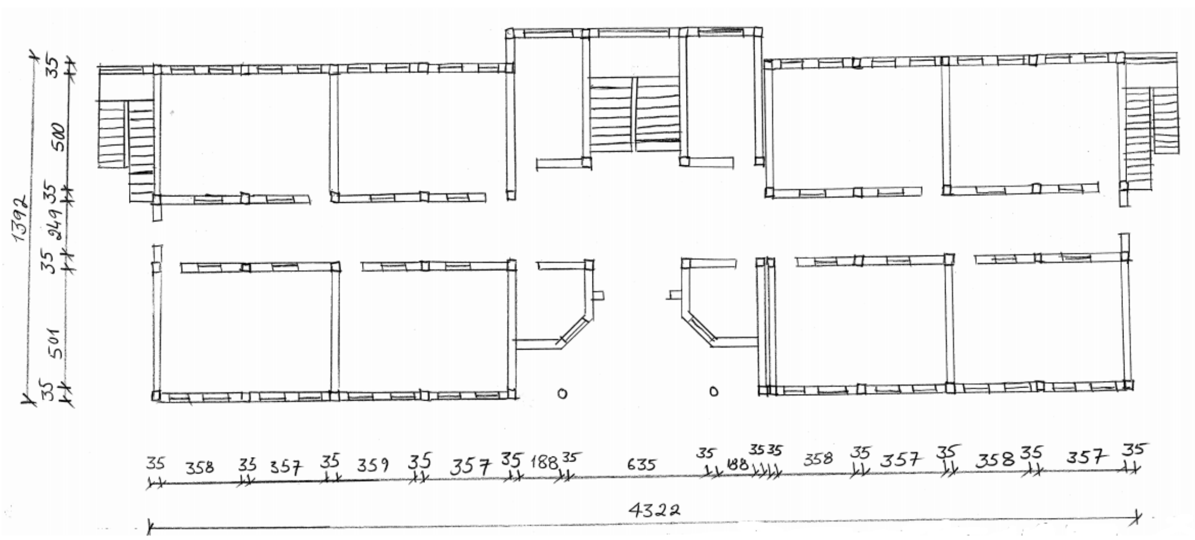

Figure A-18. Kabul School 9, typical floor plan

Figure A-19. Kabul School 10 (front view)

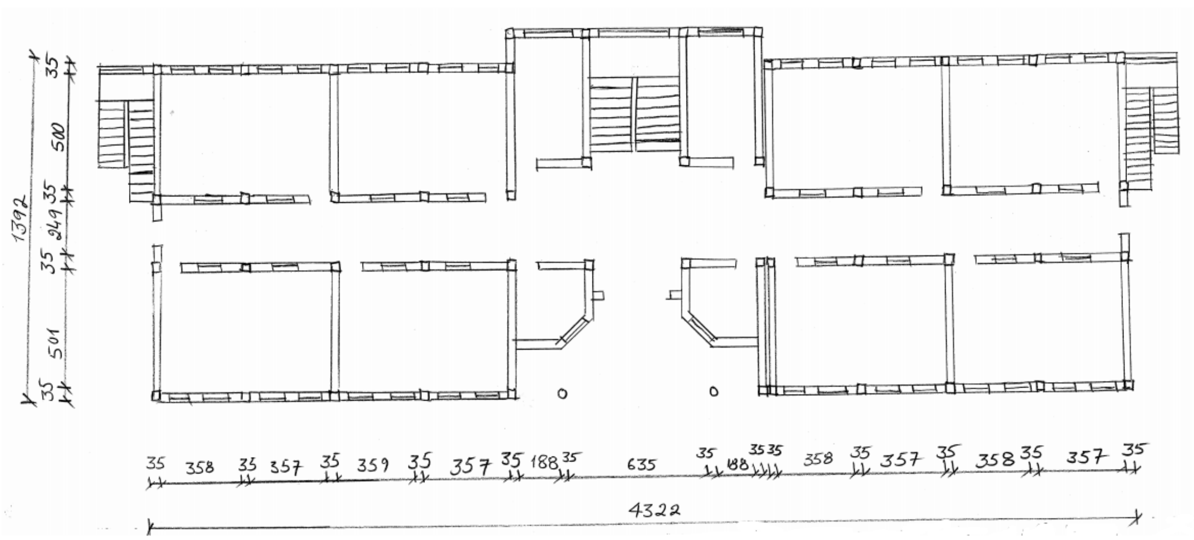

Figure A-20. Kabul School 10, typical floor plan

Figure A-21. Kabul School 11 (front view)

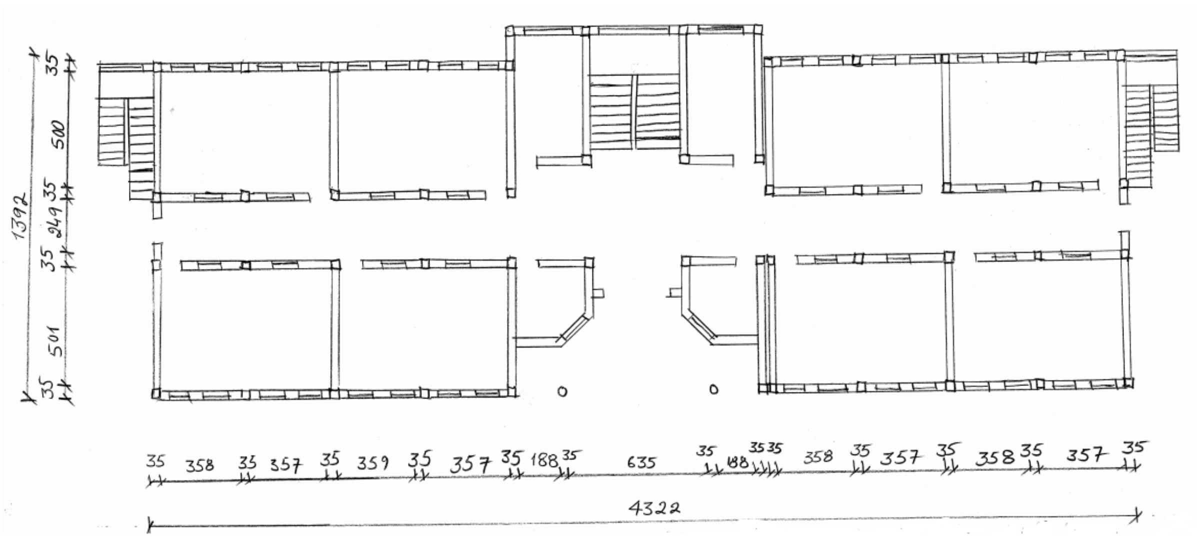

Figure A-22. Kabul School 11, typical floor plan

Figure A-23. Kabul School 12 (front view)

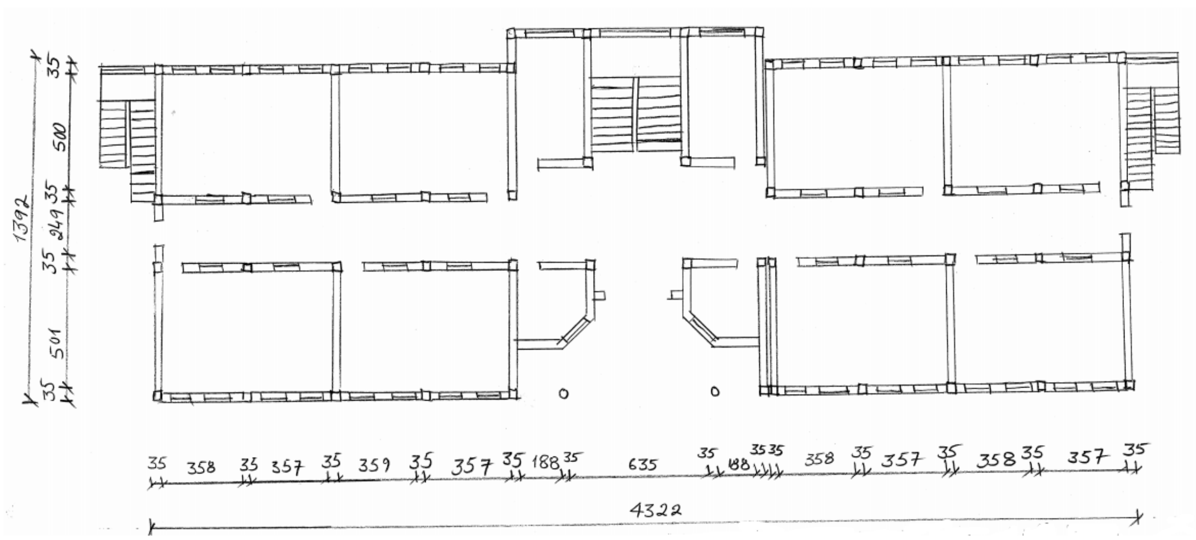

Figure A-24. Kabul School 12, typical floor plan

Figure A-25. Kabul School 13 (front view)

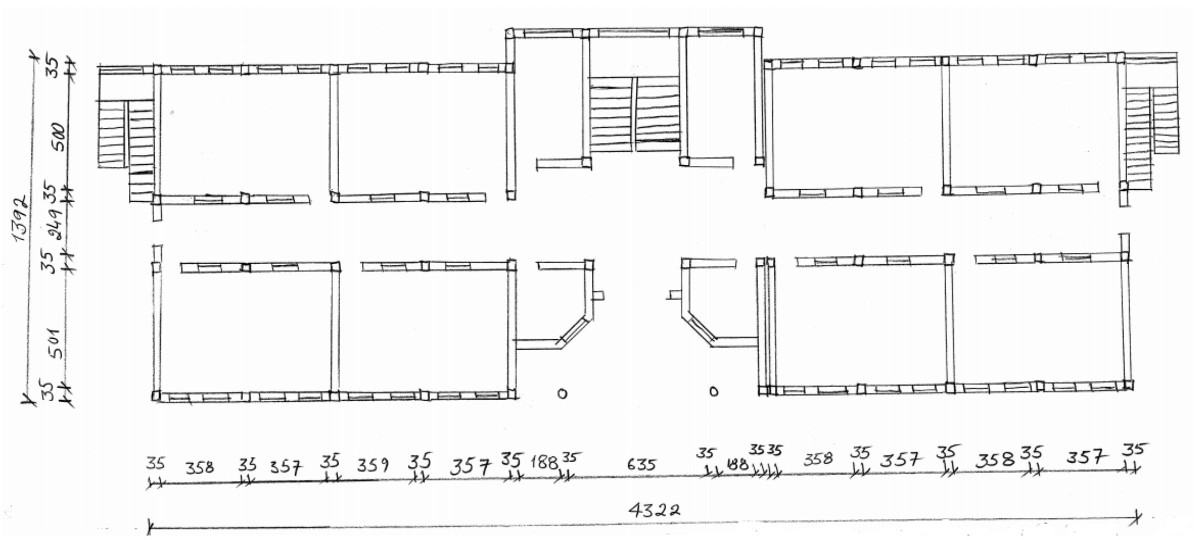

Figure A-26.Kabul School 13, typical floor plan

Figure A-27. Kabul School 14 (front view)

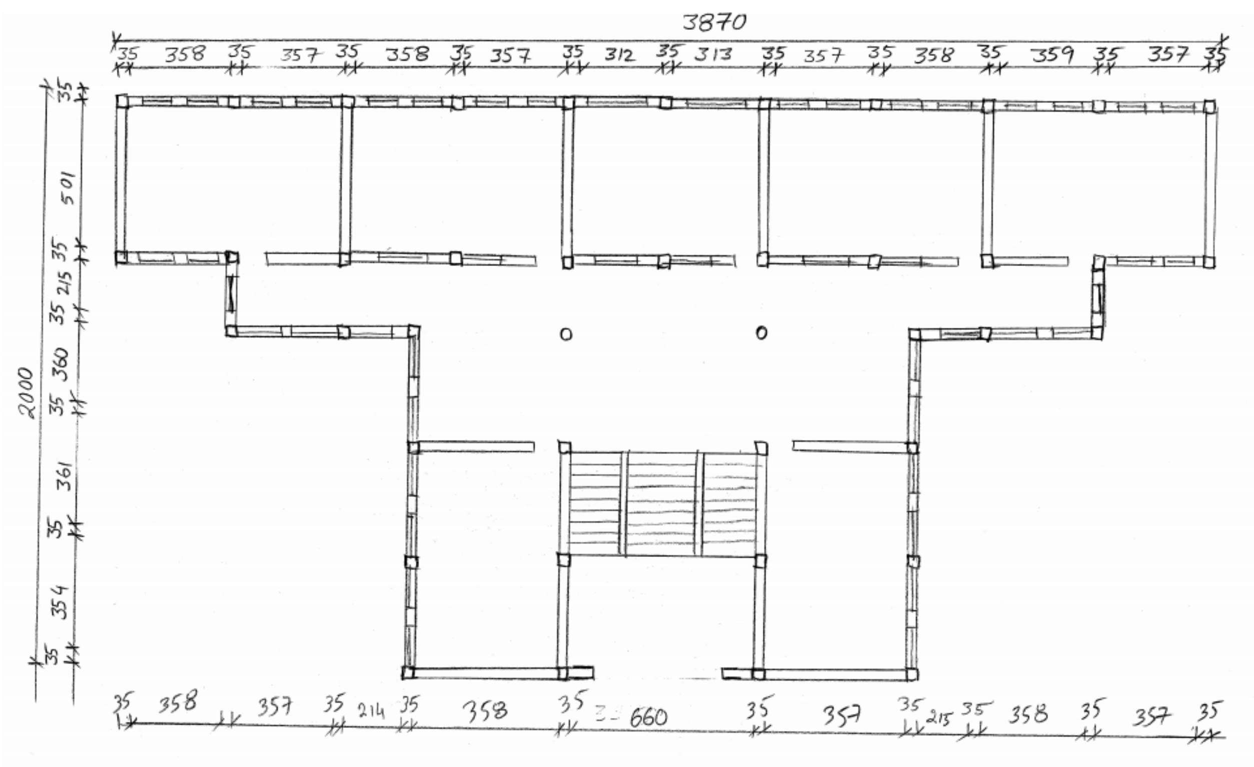

Figure A-28. Kabul School 14, typical floor plan

Figure A-29. Kabul School Admin 15 (front view)

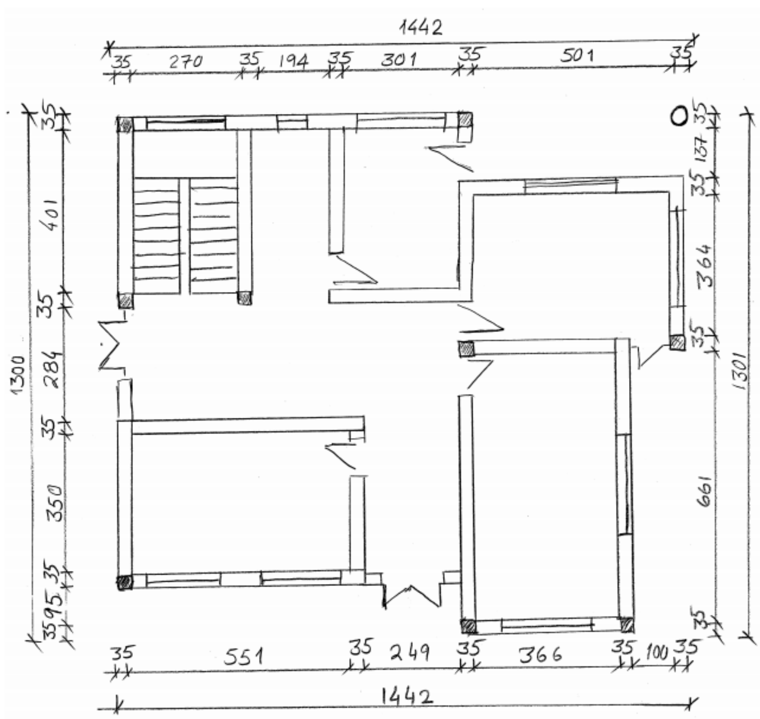

Figure A-30. Kabul School Admin 15, typical floor plan

Figure A-31. Kabul School Admin 16 (front view)

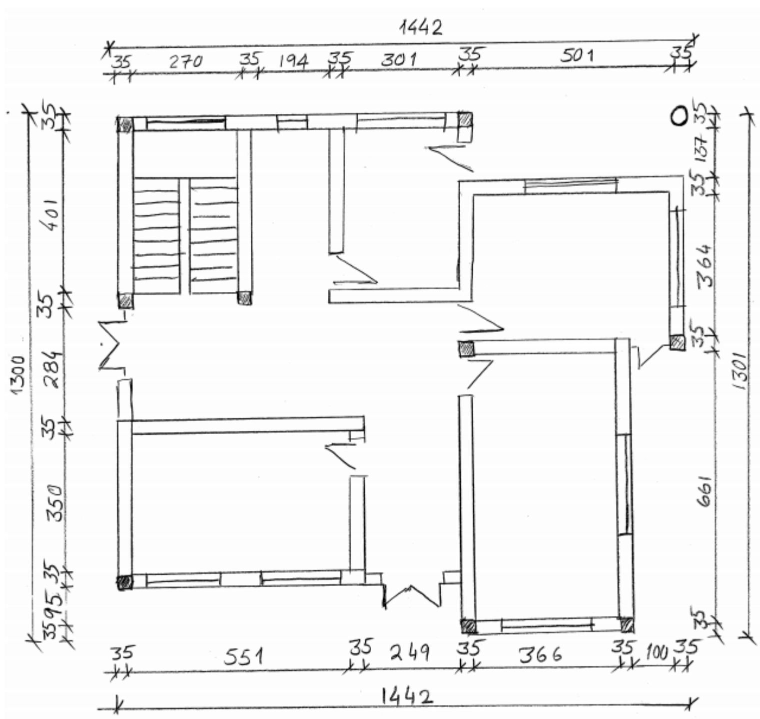

Figure A-32. Kabul School Admin 16, typical floor plan

Figure A-33. Kabul School Admin 17 (front view)

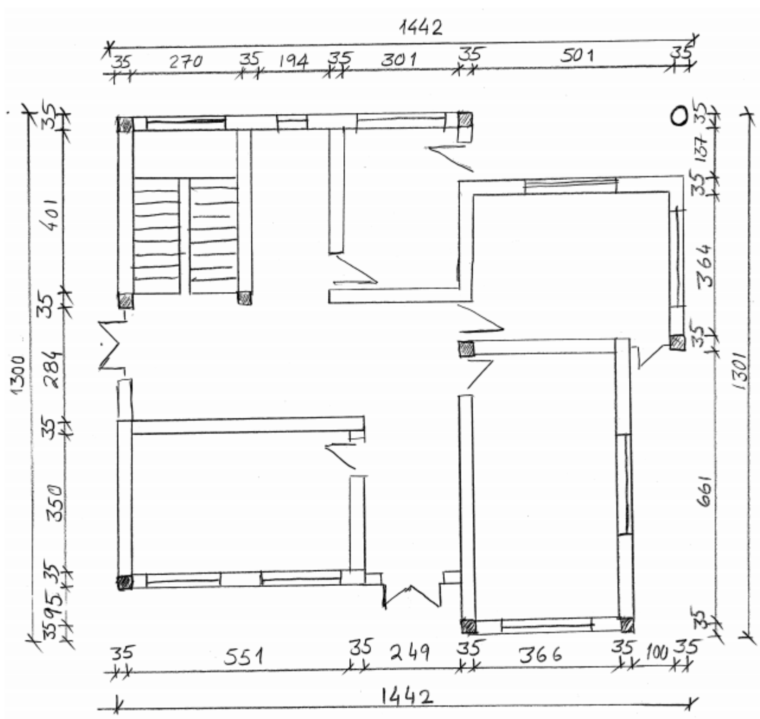

Figure A-34. Kabul School Admin 17, typical floor plan

Figure A-35. Kabul School Admin 18 (front view)

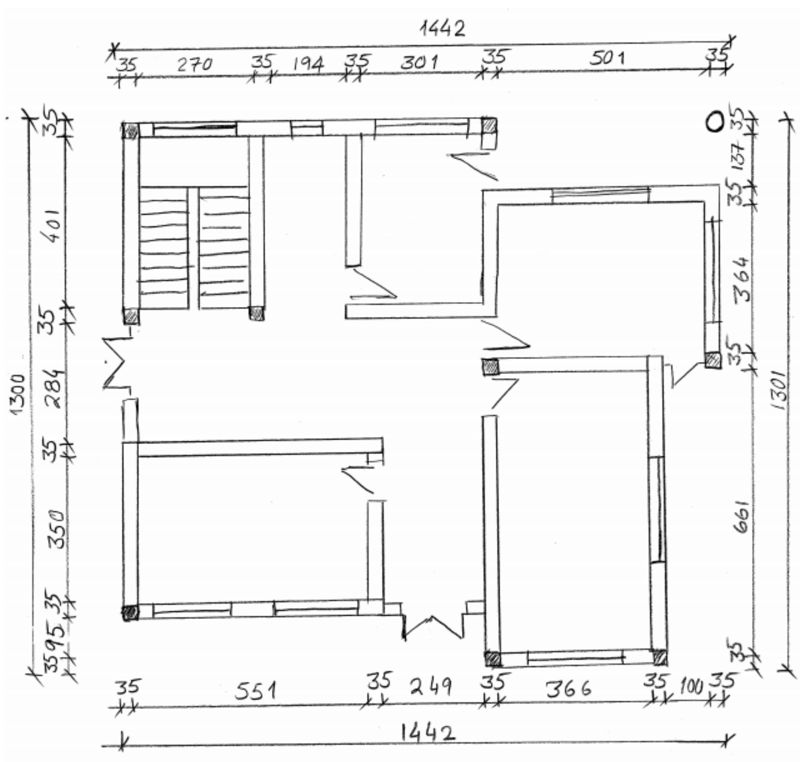

Figure A-36. Kabul School Admin 18, typical floor plan

Figure A-37. Kabul School 19 (front view)

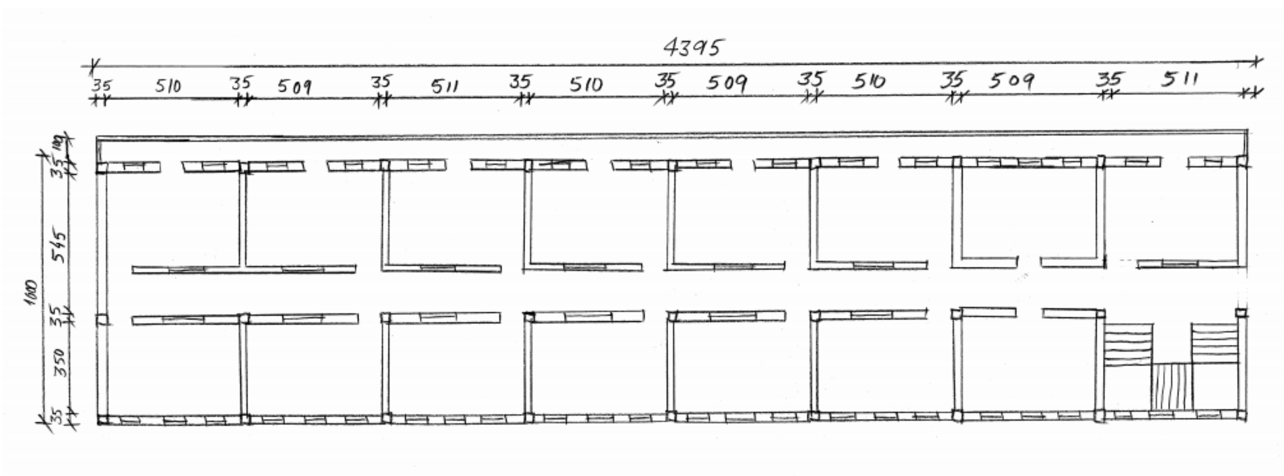

Figure A-38. Kabul School 19, typical floor plan

Figure A-39. Kabul School 20 (front view)

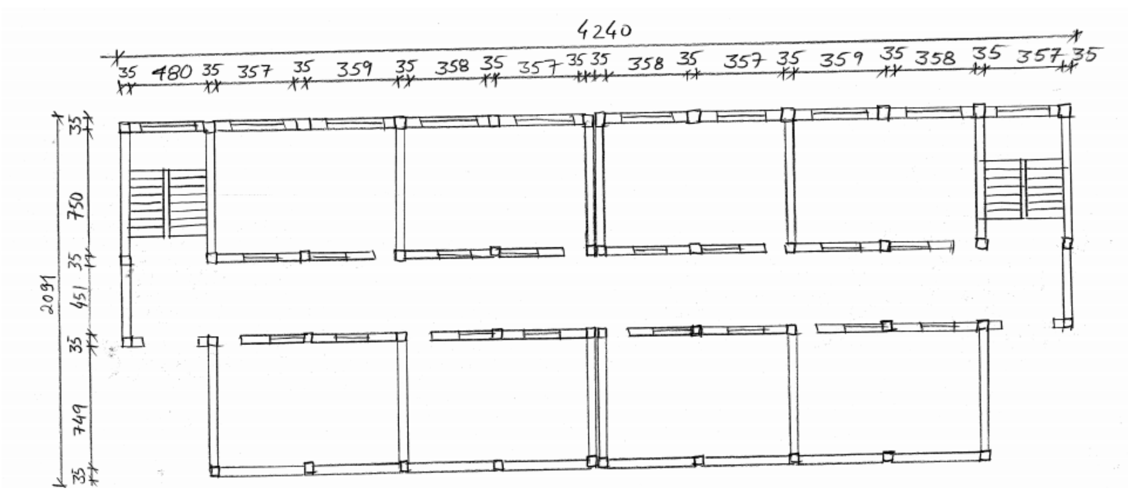

Figure A-40. Kabul School 20, typical floor plan

FigureA-41. Kabul School 21 (front view)

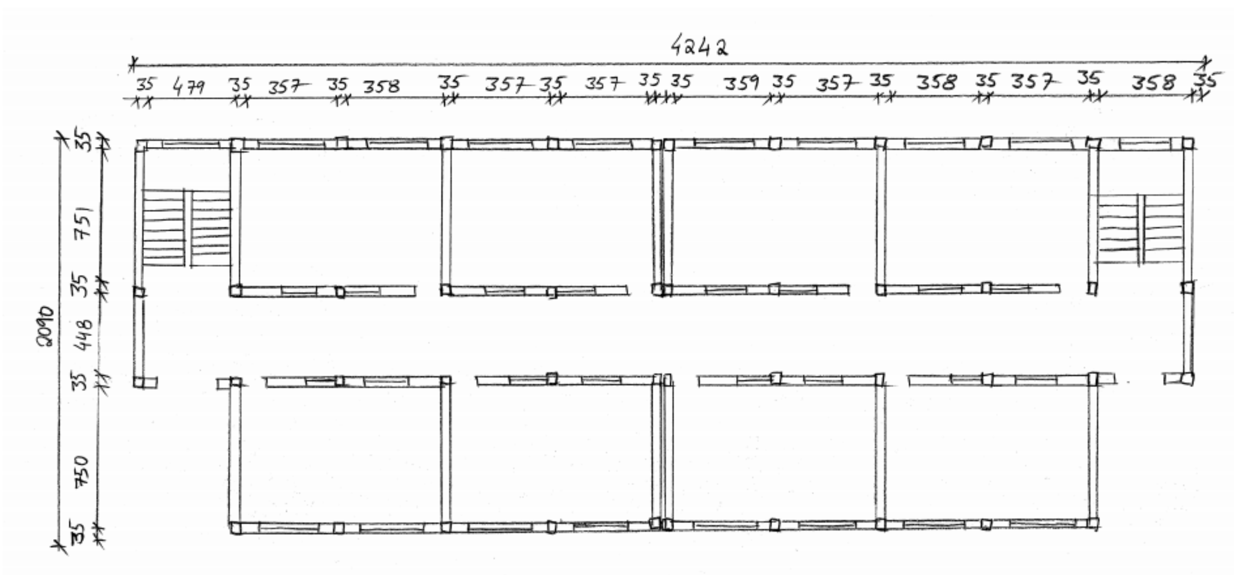

Figure A-42. Kabul School 21, typical floor plan

Figure A-43. Kabul School 22 (front view)

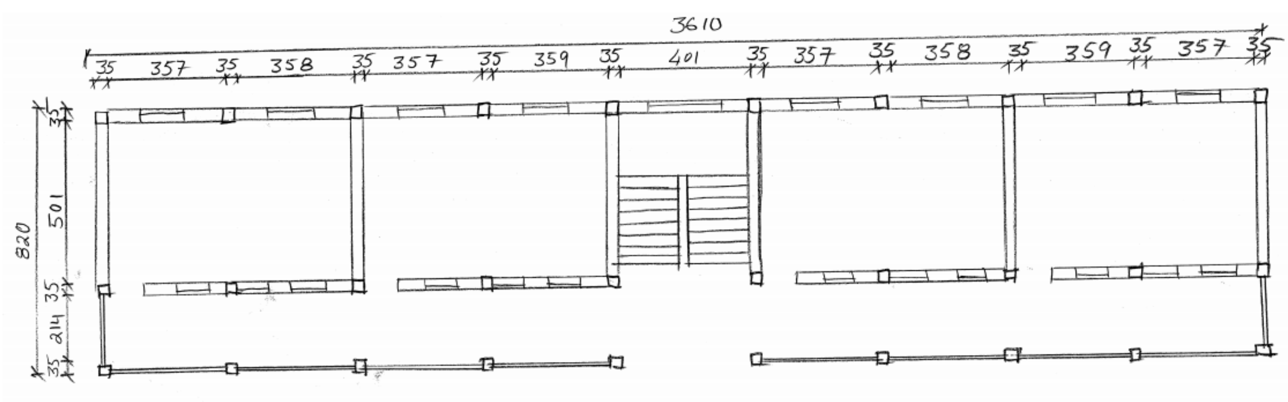

Figure A-44. Kabul School 22, typical floor plan

Figure A-45. Kabul School 23 (front view)

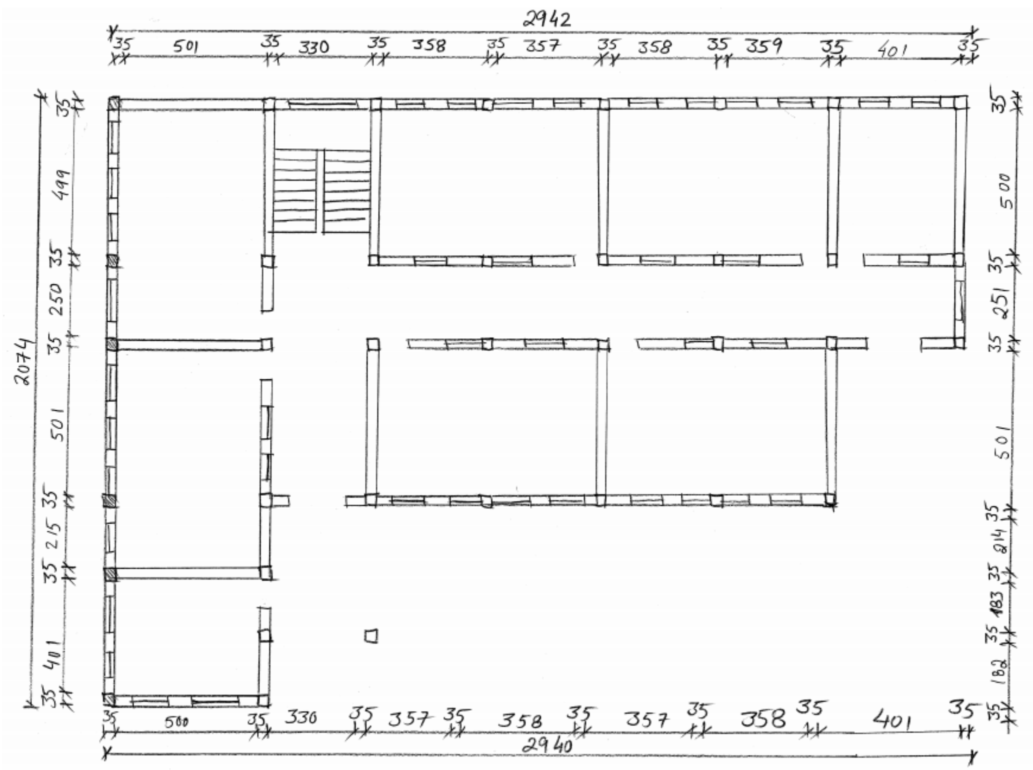

Figure A-46. Kabul School 23, typical floor plan

Figure A-47. Kabul School 24 (front view)

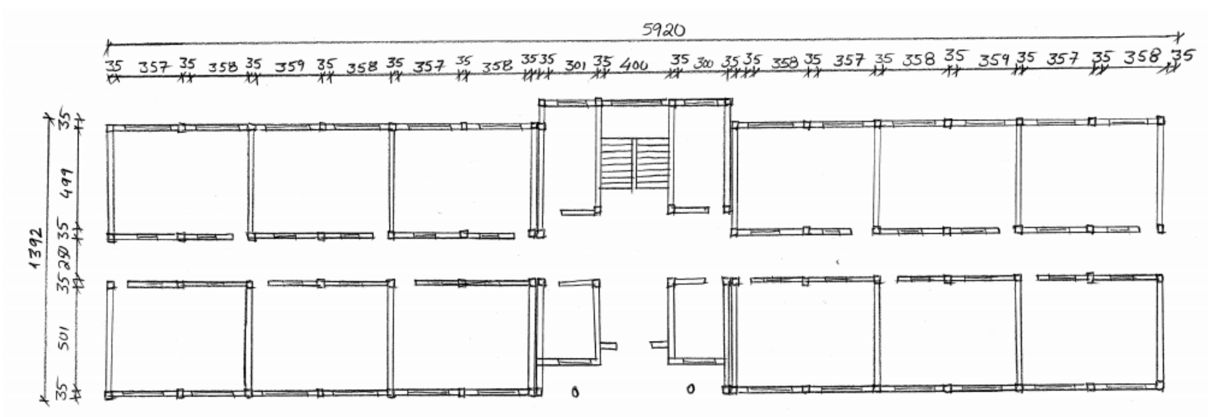

Figure A-48. Kabul School 24, typical floor plan

Figure A-49. Kabul School 25 (front view)

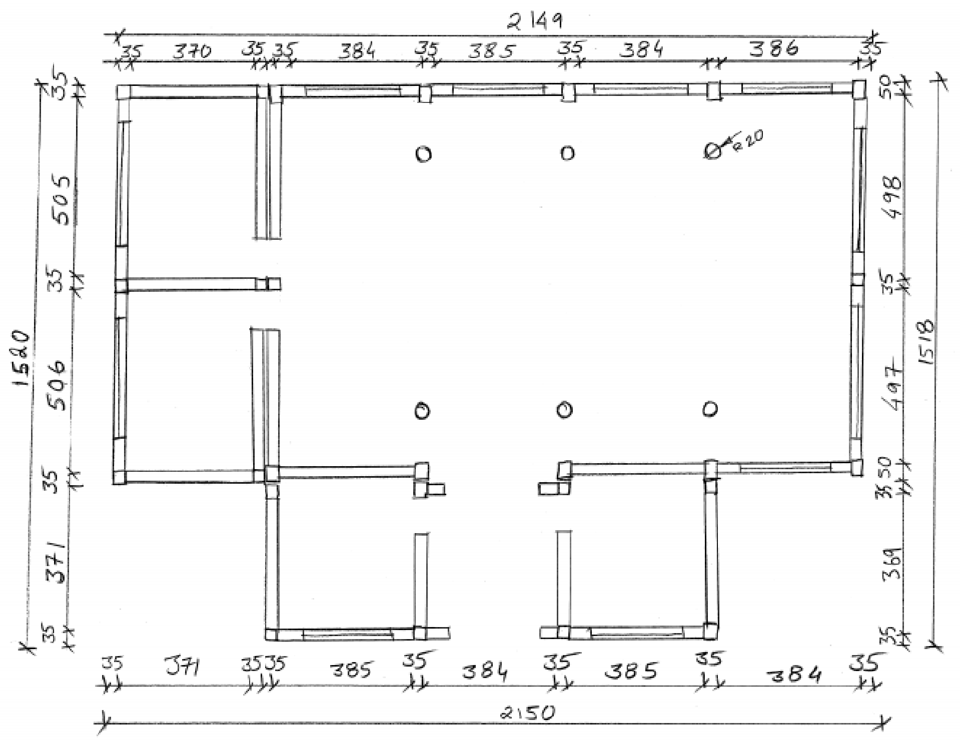

Figure A-50. Kabul School 25, typical floor plan

Figure A-51. Kabul School 26 (front view)

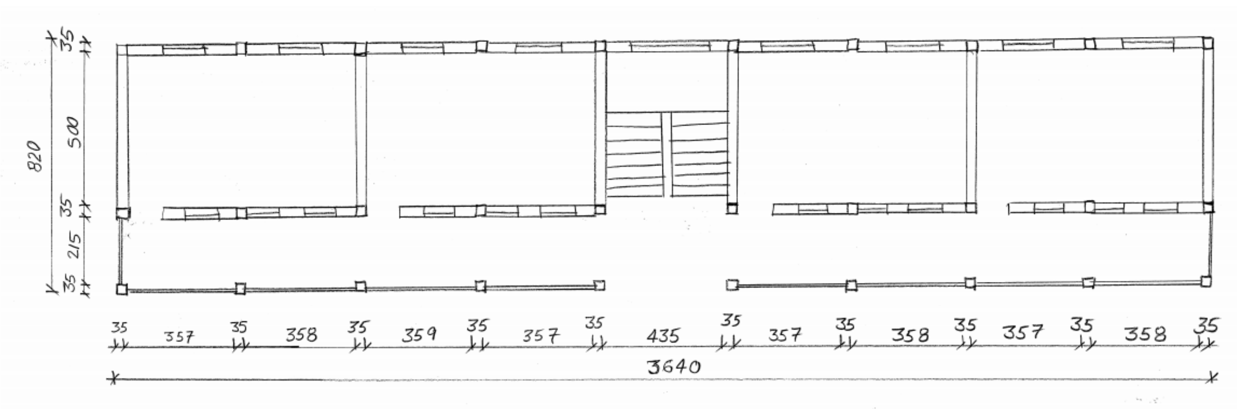

Figure A-52. Kabul School 26, typical floor plan

Figure A-53. Kabul School 27 (front view)

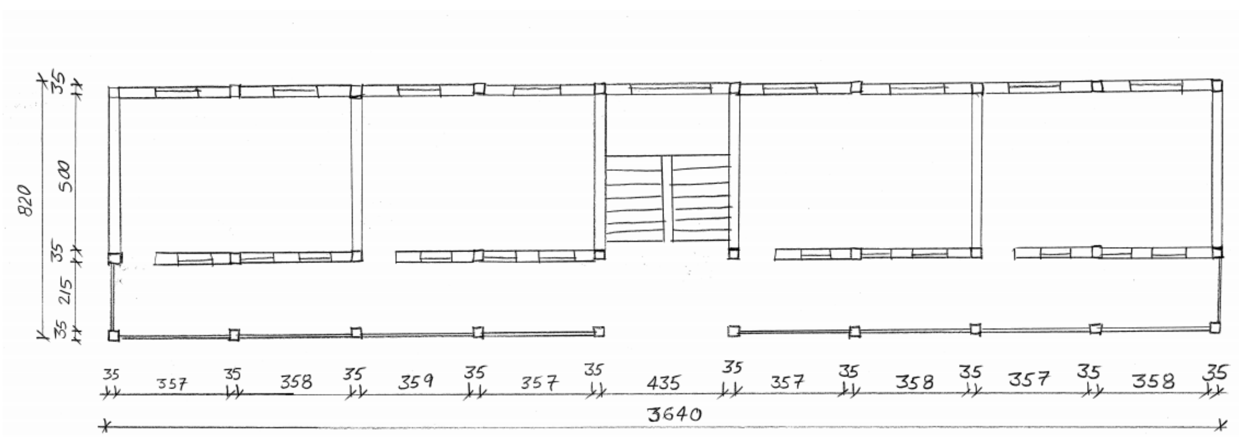

Figure A-54. Kabul School 27, typical floor plan

Figure A-55. Kabul School 28 (front view)

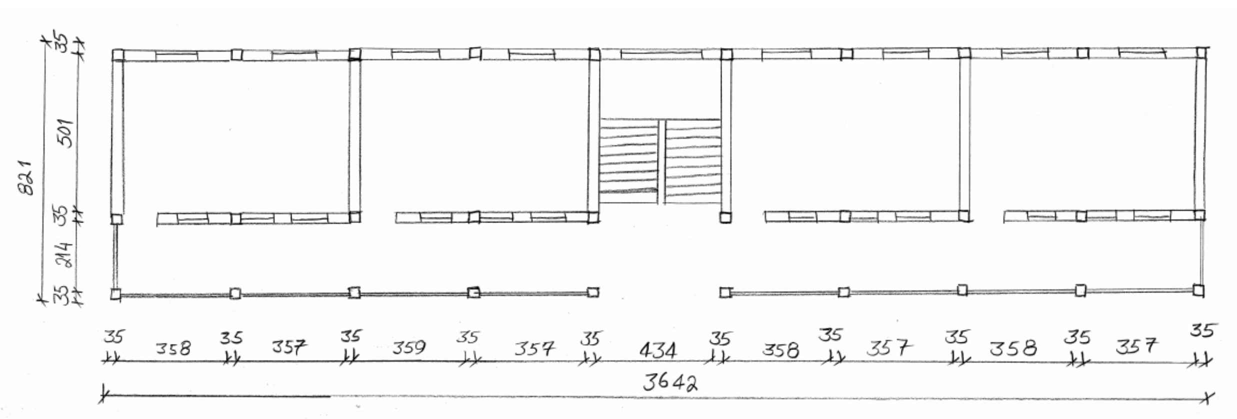

Figure A-56. Kabul School 28, typical floor plan

Figure A-57. Kabul School 29 (front view)

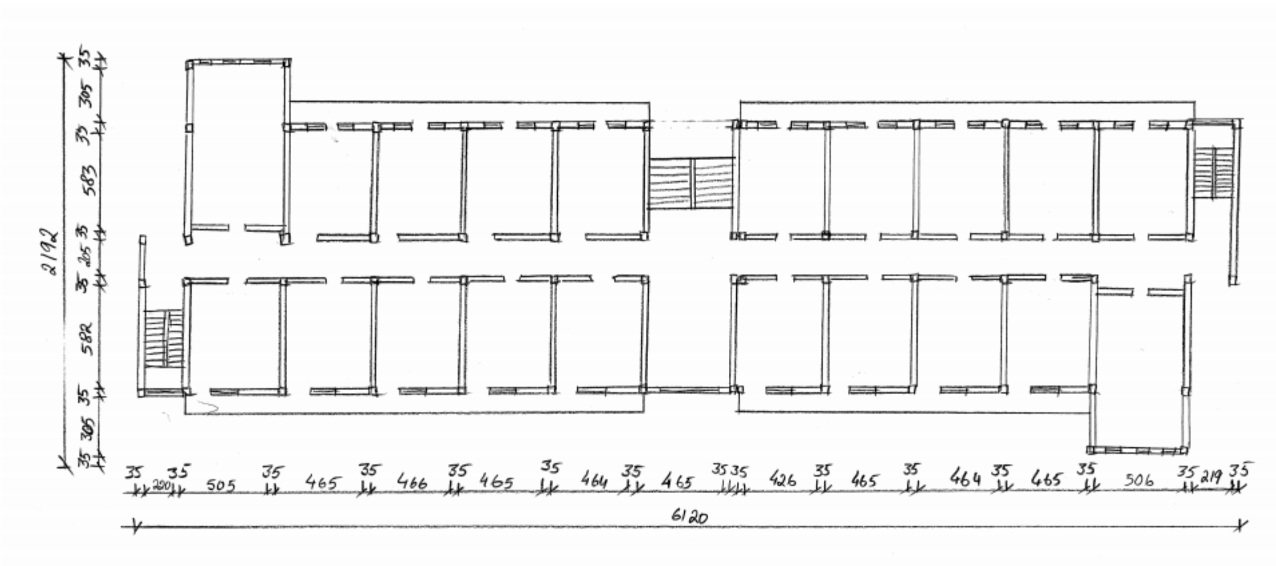

Figure A-58. Kabul School 29, typical floor plan

Figure 5A-59. Kabul School 30 (front view)

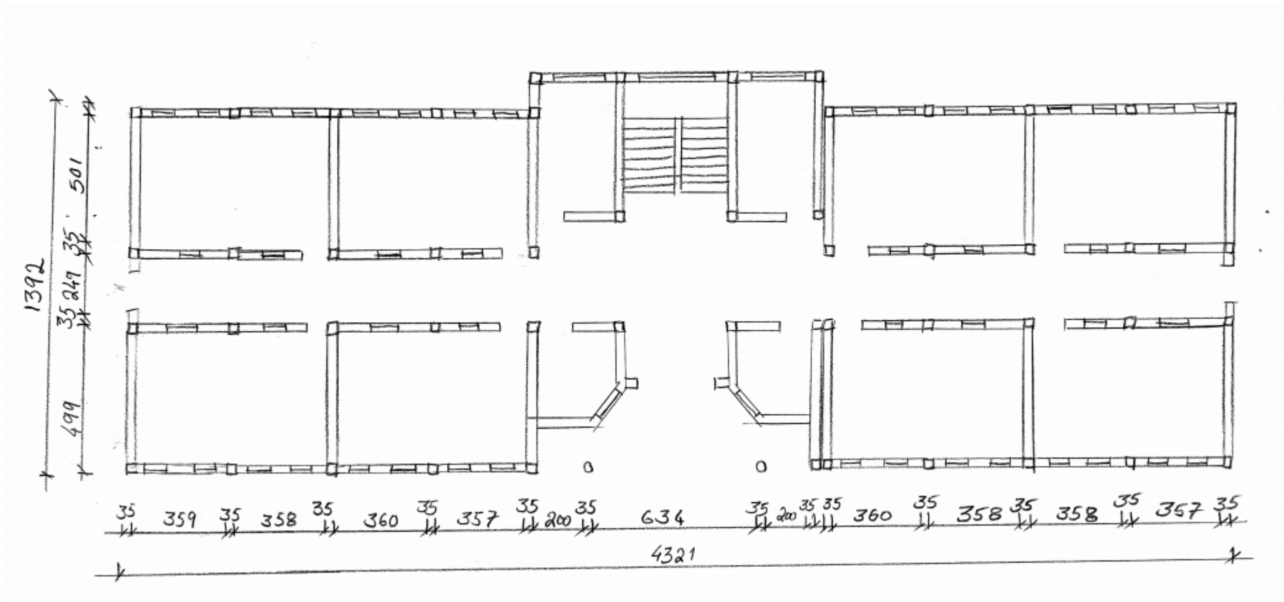

Figure A-60. Kabul School 30, typical floor plan

Figure 5A-61. Kabul School 31 (front view)

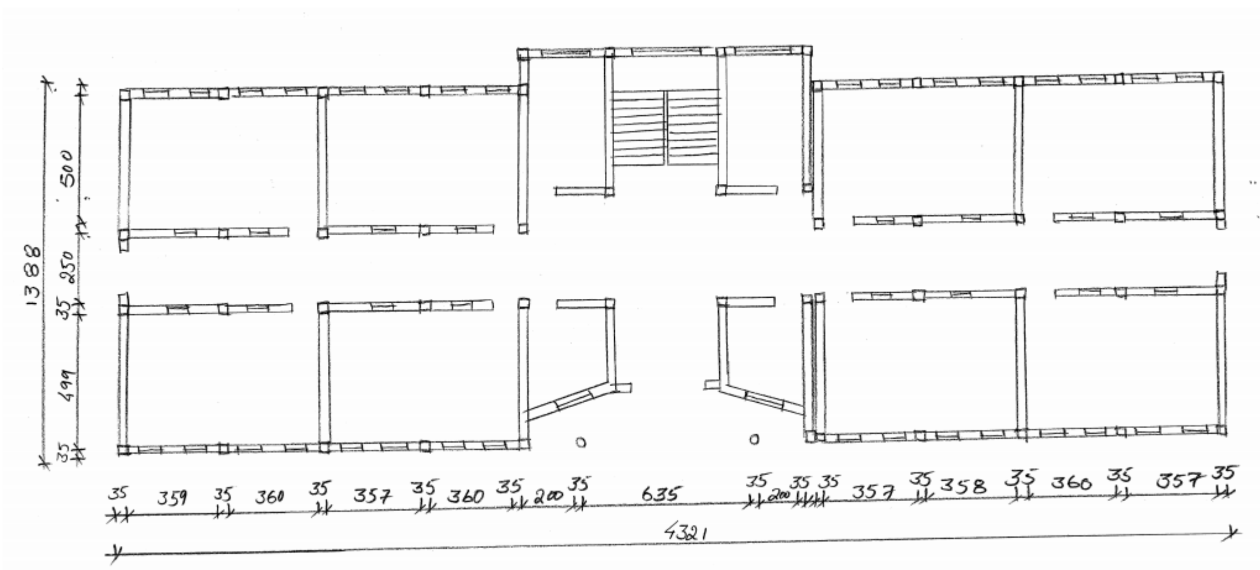

Figure A-62. Kabul School 31, typical floor plan

Figure 5 A-63. Kabul School 32 (front view)

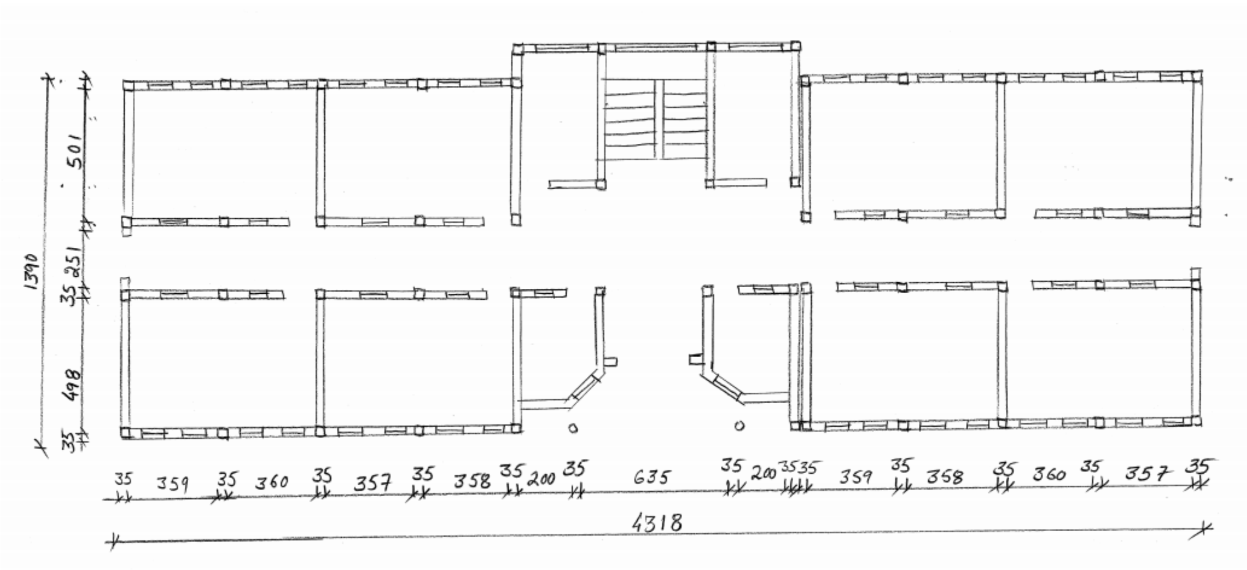

Figure A-64. Kabul School 32, typical floor plan

Figure A-65. Kabul School 33 (front view)

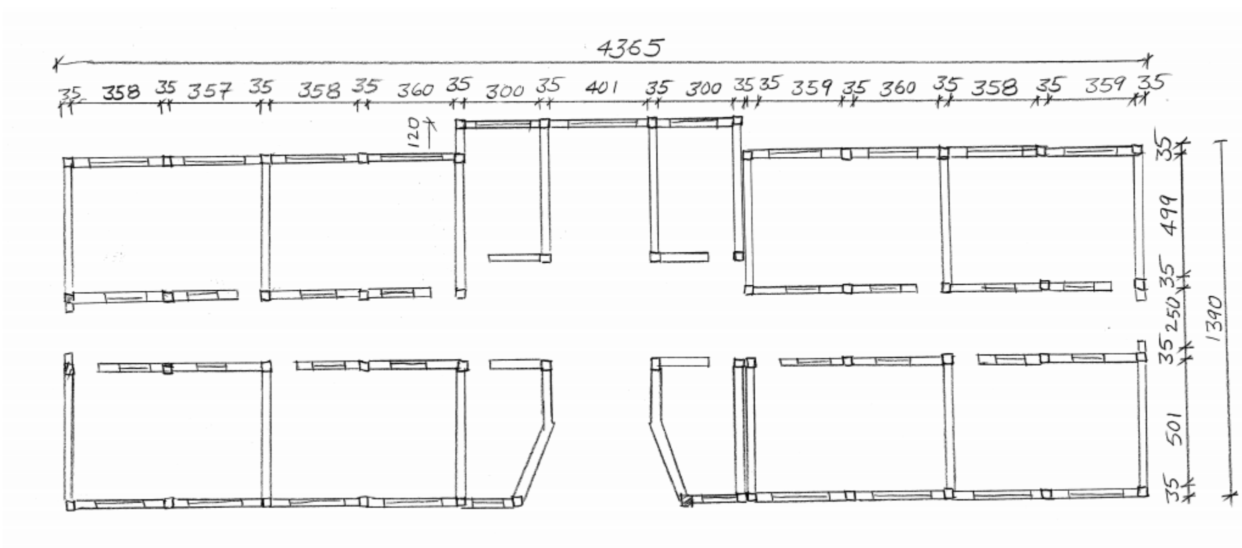

Figure A-66. Kabul School 33, typical floor plan

Figure A-67. Kabul School 34 (front view)

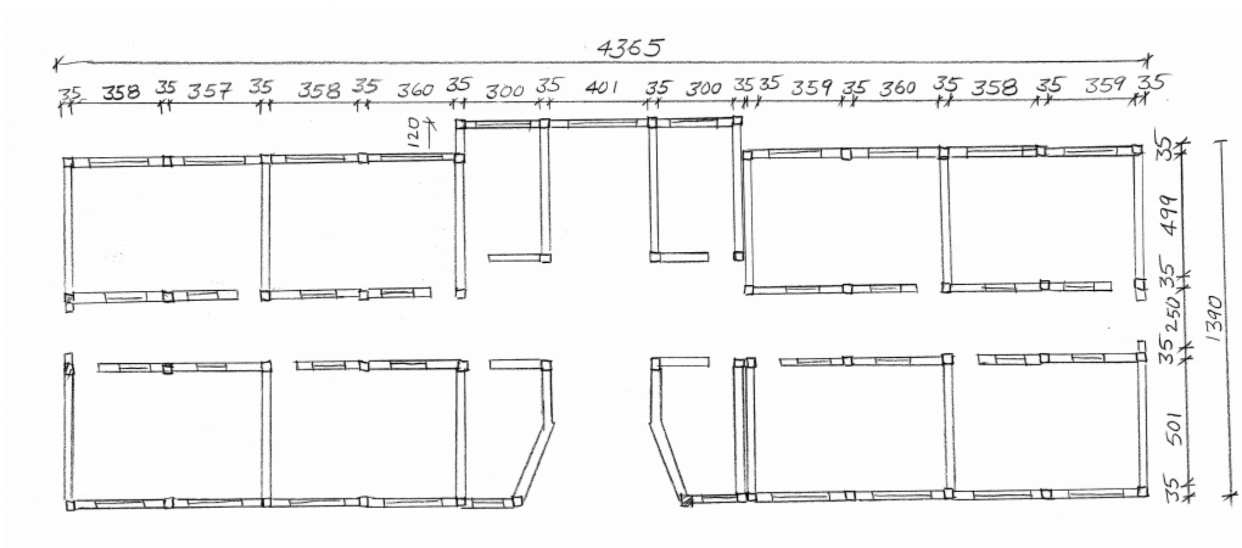

Figure A-68. Kabul School 34, typical floor plan

Figure 5A-69. Kabul School 35 (front view)

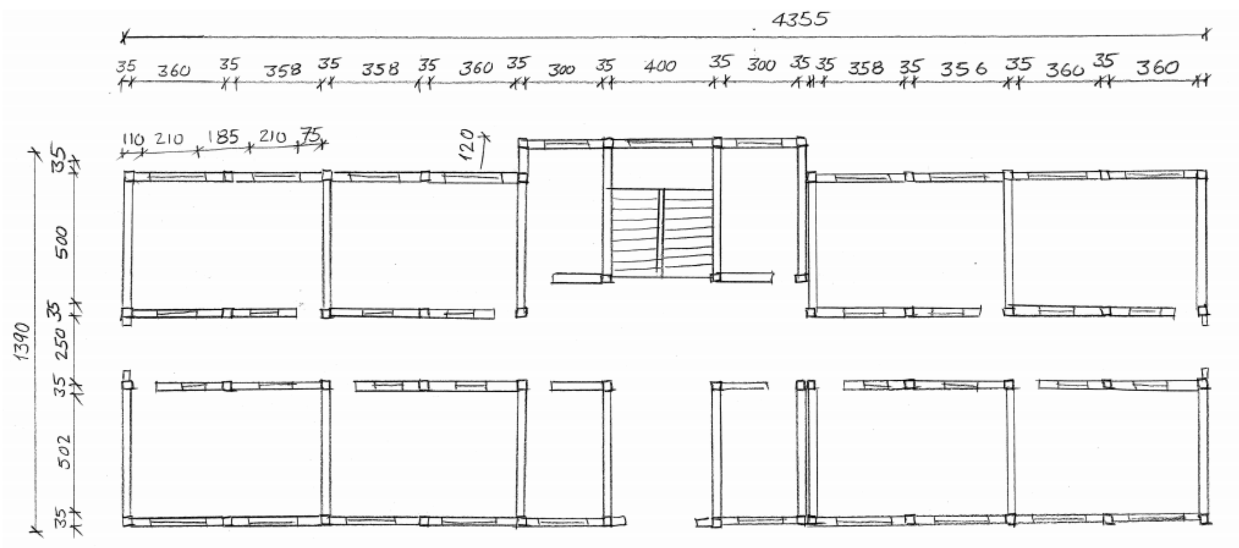

Figure A-70. Kabul School 35, typical floor plan

Figure 5A-71. Kabul School 36 (front view)

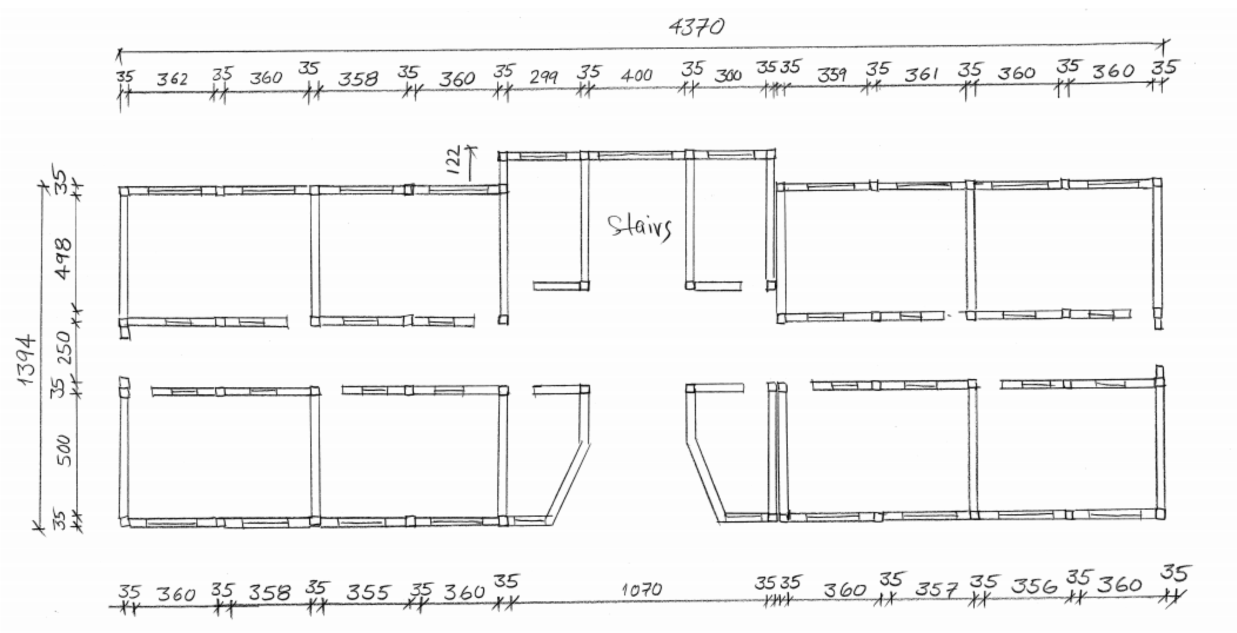

Figure A-72. Kabul School 36, typical floor plan

Figure 5A-73. Kabul School 37 (front view)

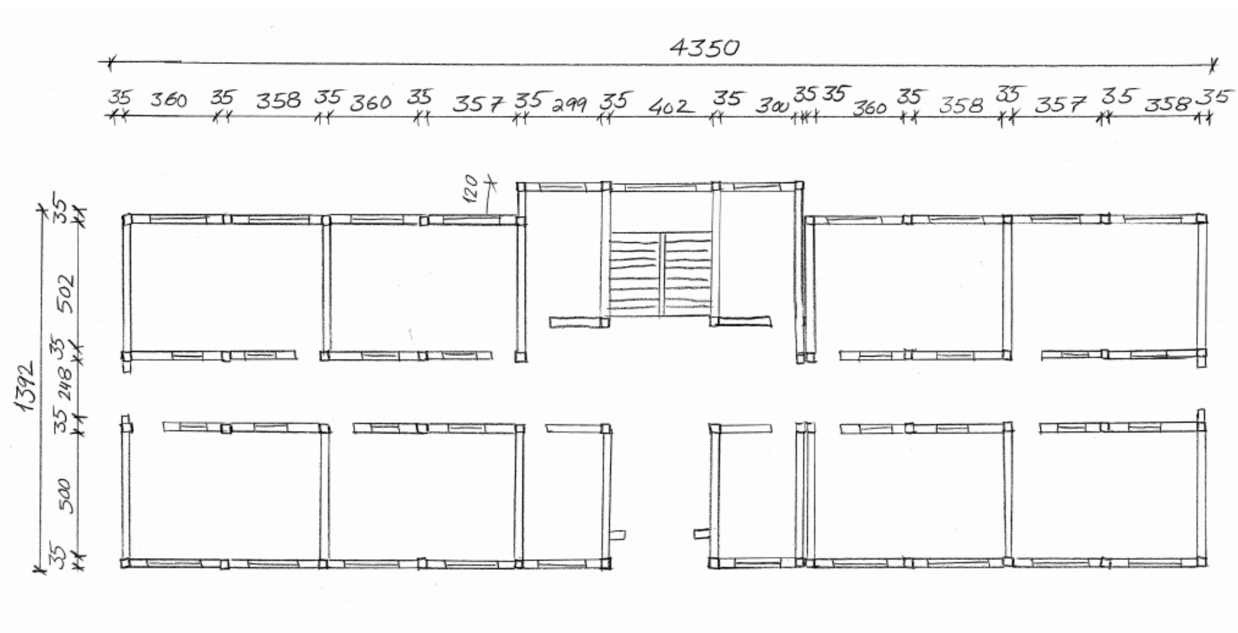

Figure A-74. Kabul School 37, typical floor plan

Figure A-75. Kabul School 38 (front view)

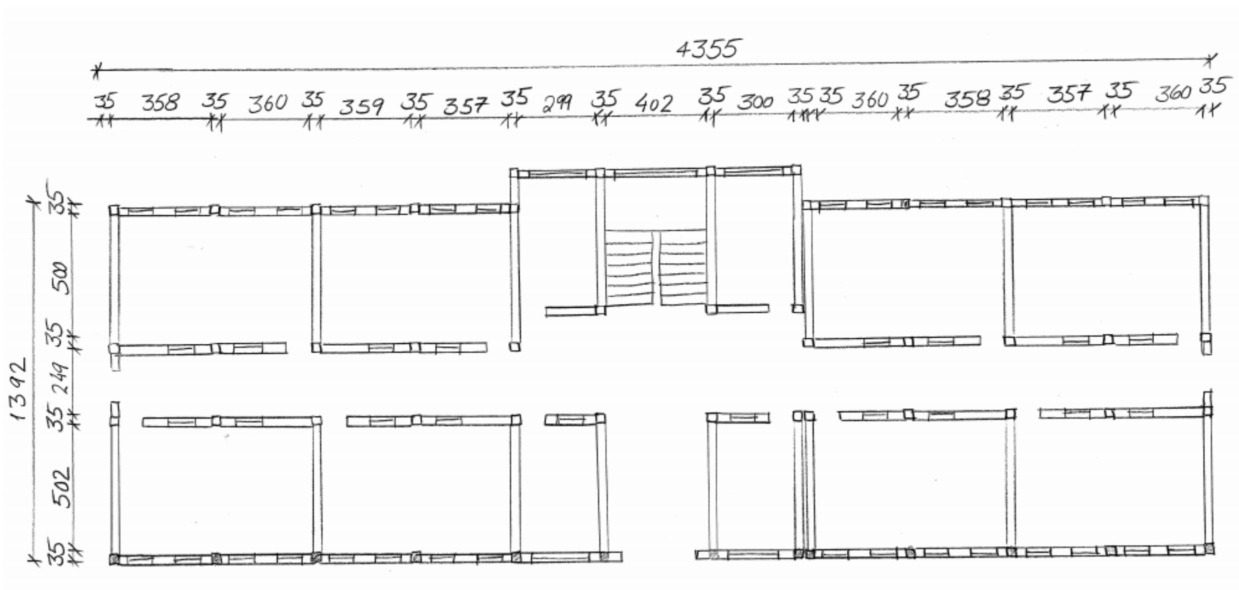

Figure A-76. Kabul School 38, typical floor plan

Figure 5 A-77. Kabul School 39 (front view)

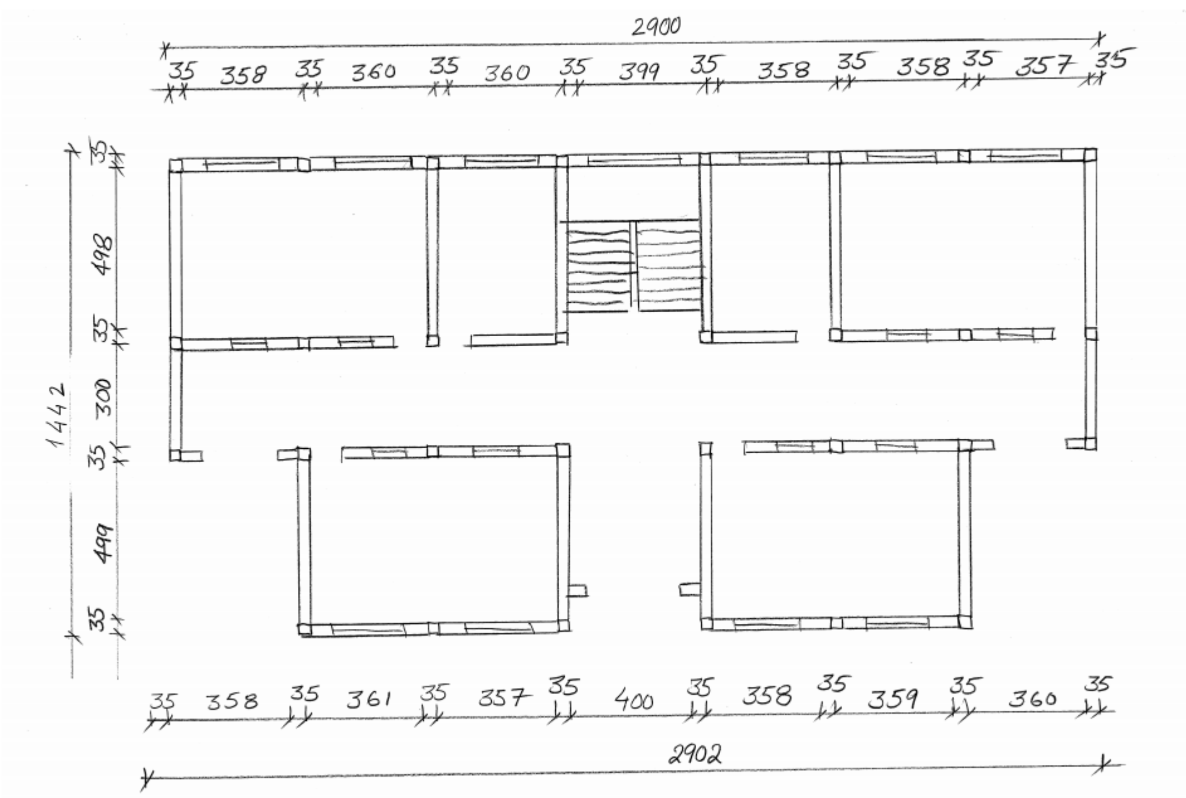

Figure A-78. Kabul School 39, typical floor plan

Figure 5A-79. Kabul School 40 (front view)

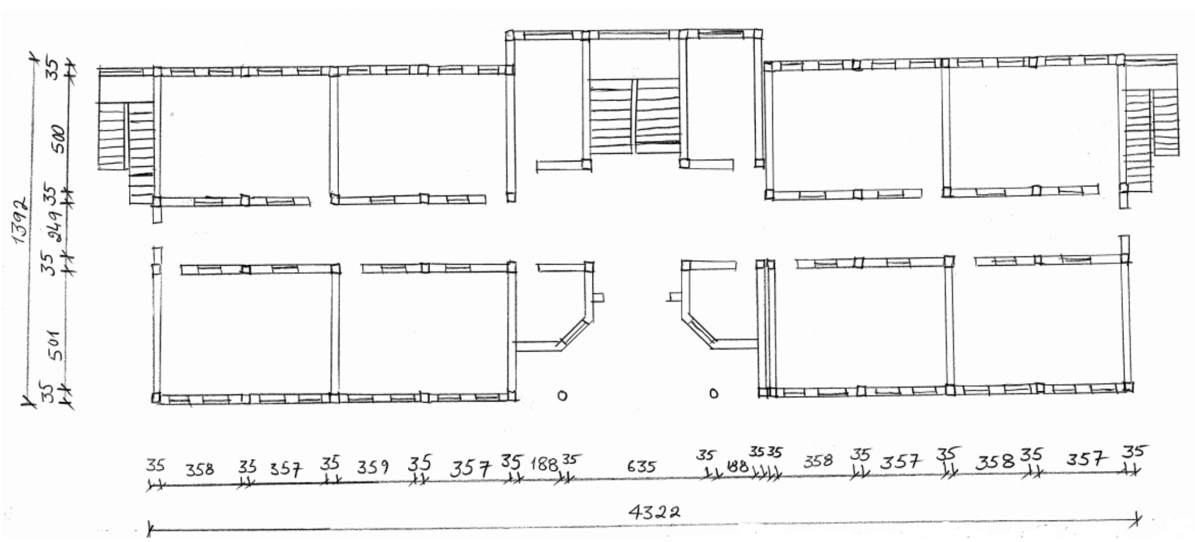

Figure A-80. Kabul School 40, typical floor plan

Figure A-81. Kabul School 41

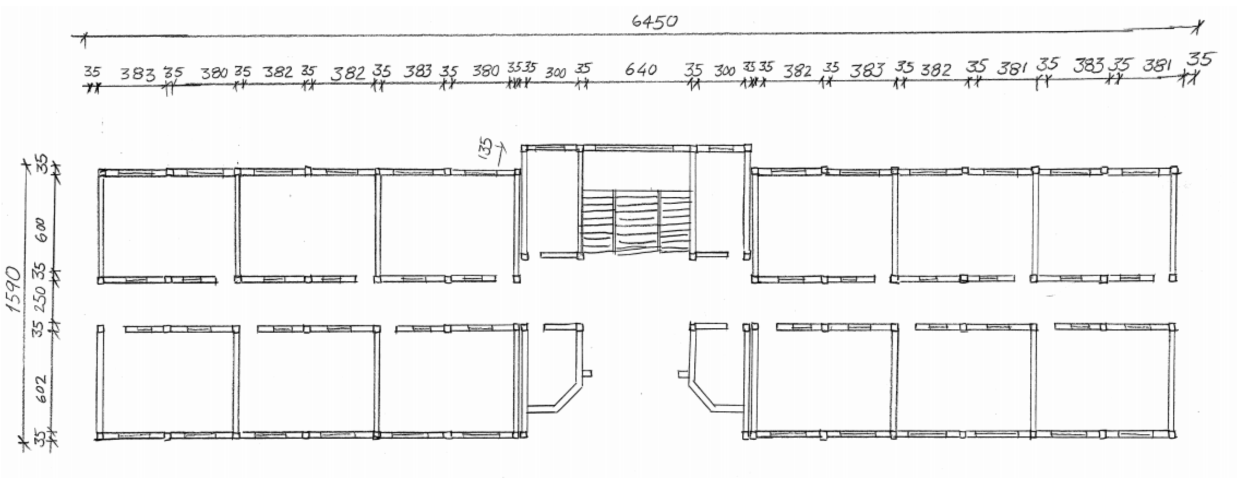

Figure 3A-82. Kabul School 41, typical floor plan

Figure A-83. Kabul School 42

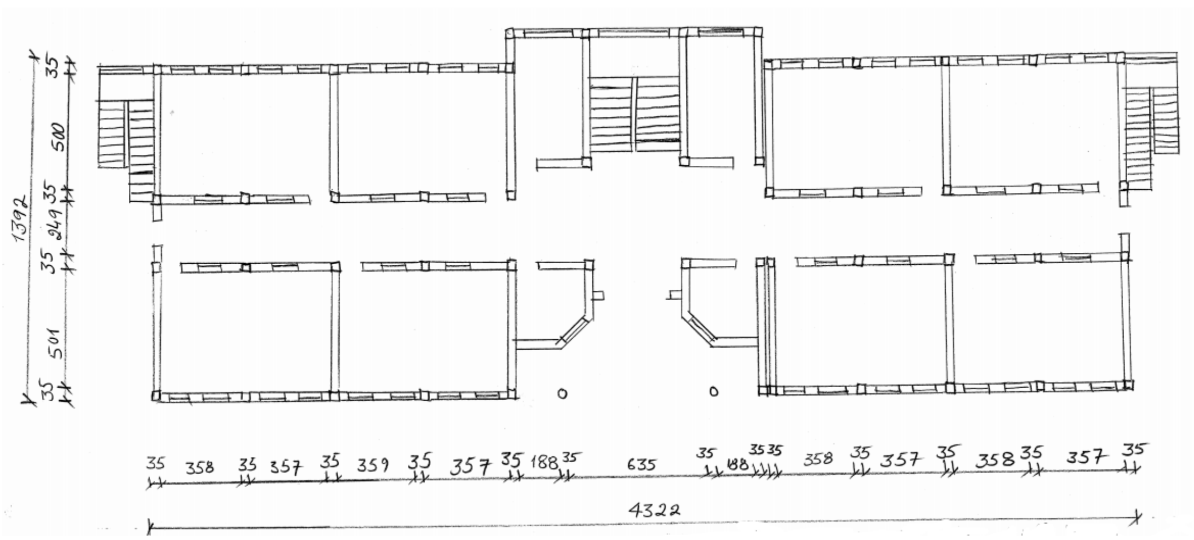

Figure A-84. Kabul School 42, typical floor plan

Figure A-85. Kabul School 43

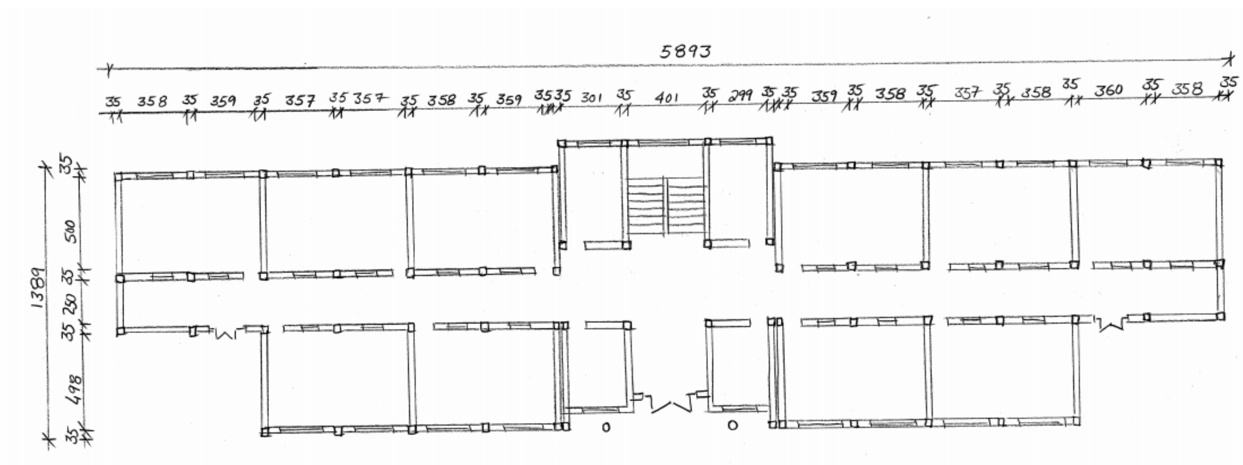

Figure A-86. Kabul School 43, typical floor plan

Figure A-87. Kabul School 44

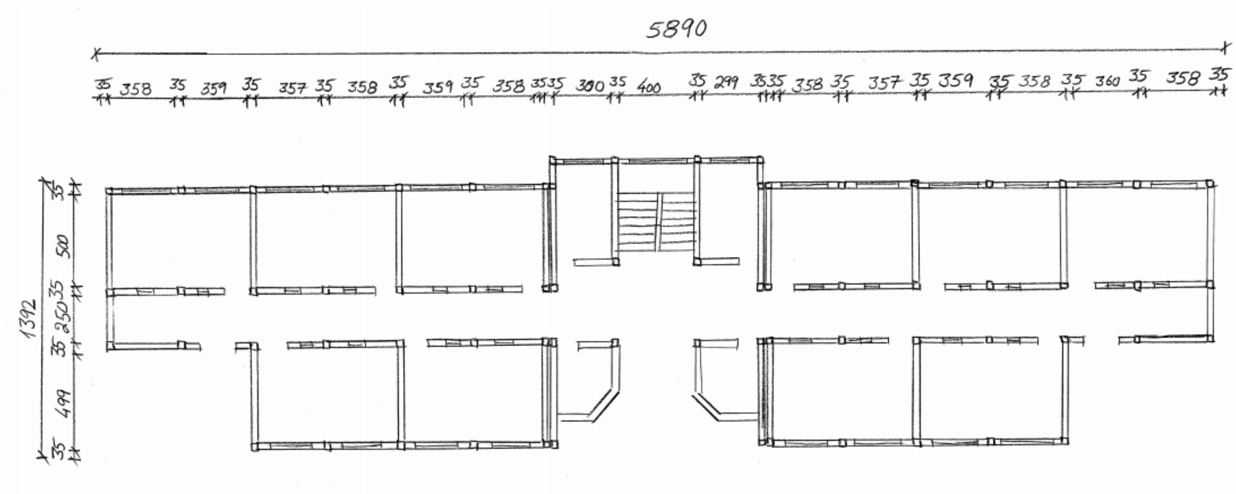

Figure A-88. Kabul School 44, typical floor plan

FigureA-89. Kabul School 45

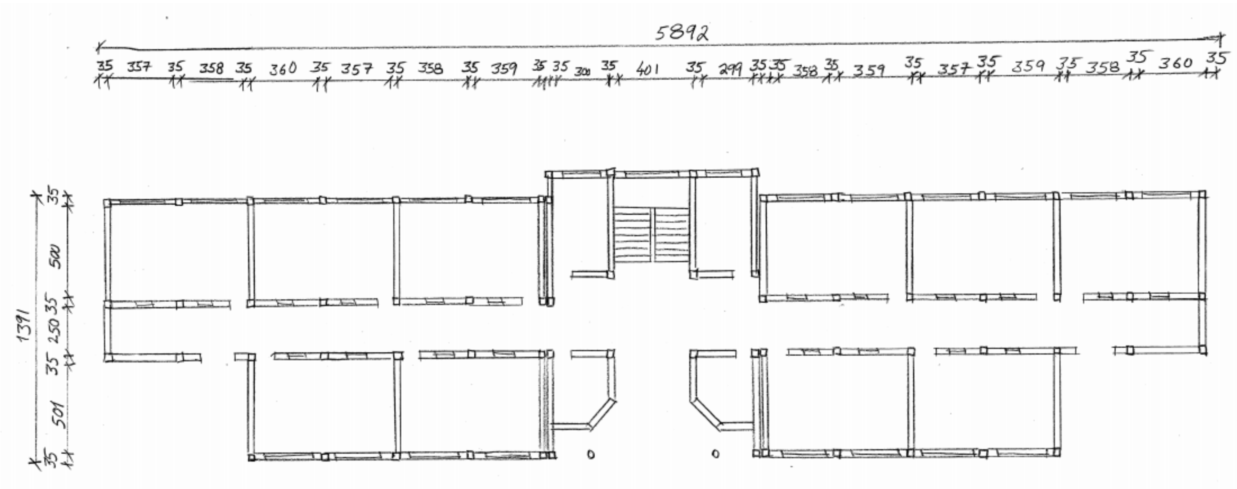

Figure A-90. Kabul School 45, typical floor plan

Figure A-91. Kabul School 46, typical floor plan

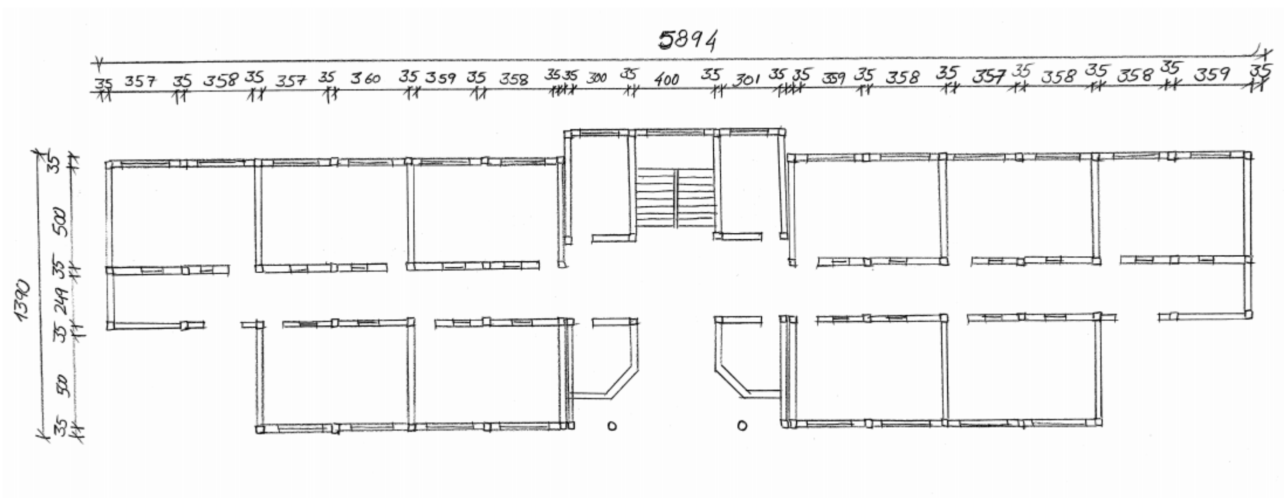

Figure A-92. Kabul School 46, typical floor plan

Figure A-93. Kabul School 47

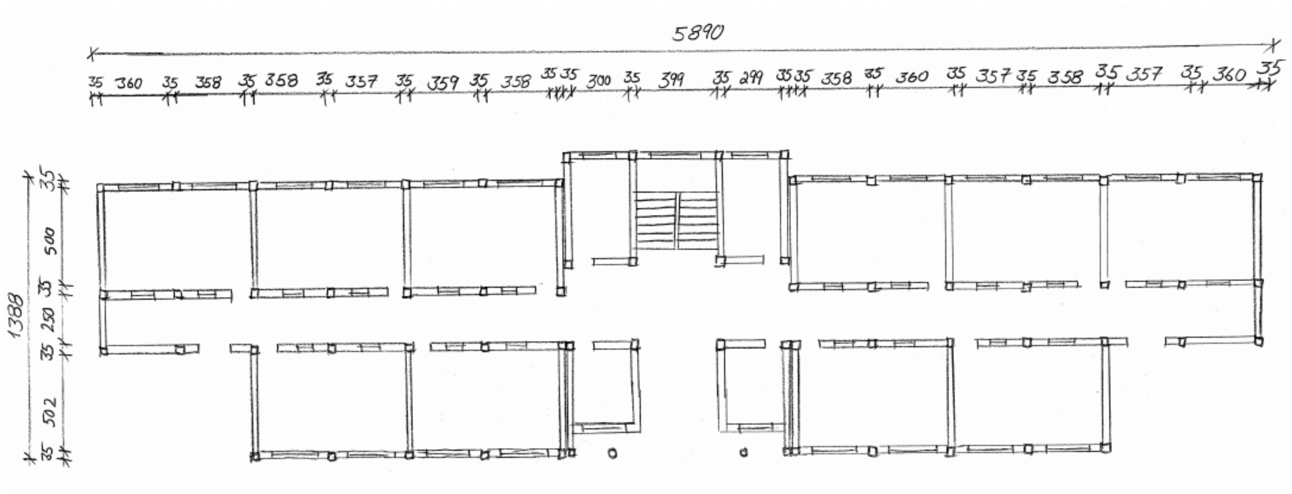

Figure A-94. Kabul School 47, typical floor plan

Figure A-95. Kabul School 48

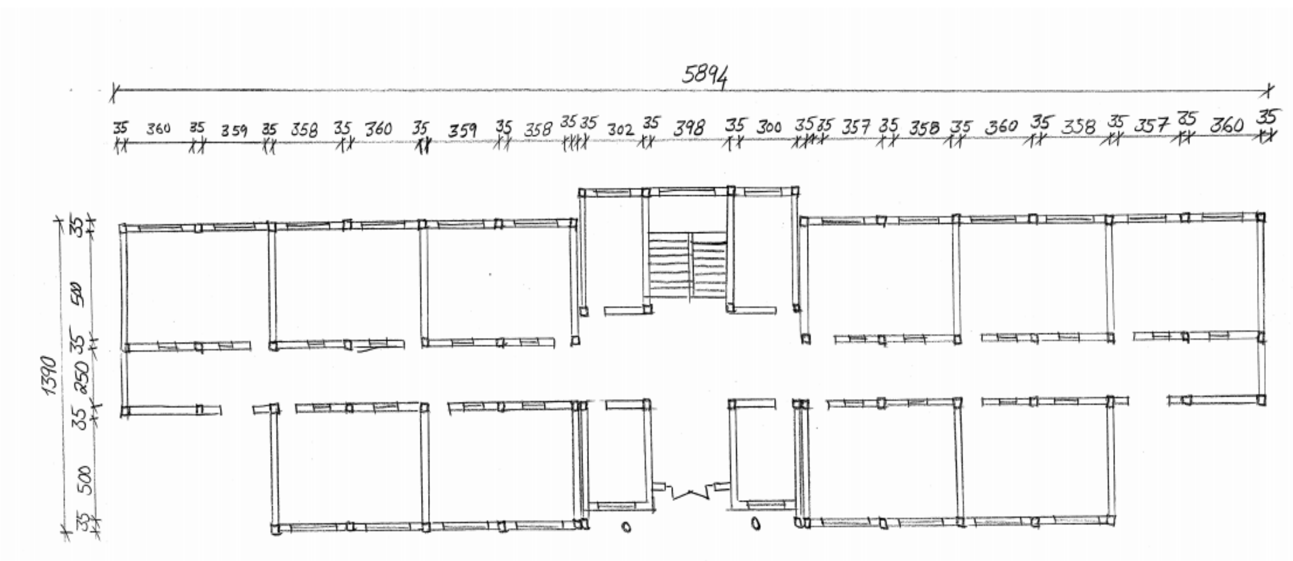

Figure A-96. Kabul School 48, typical floor plan

Figure A-97. Kabul School 49

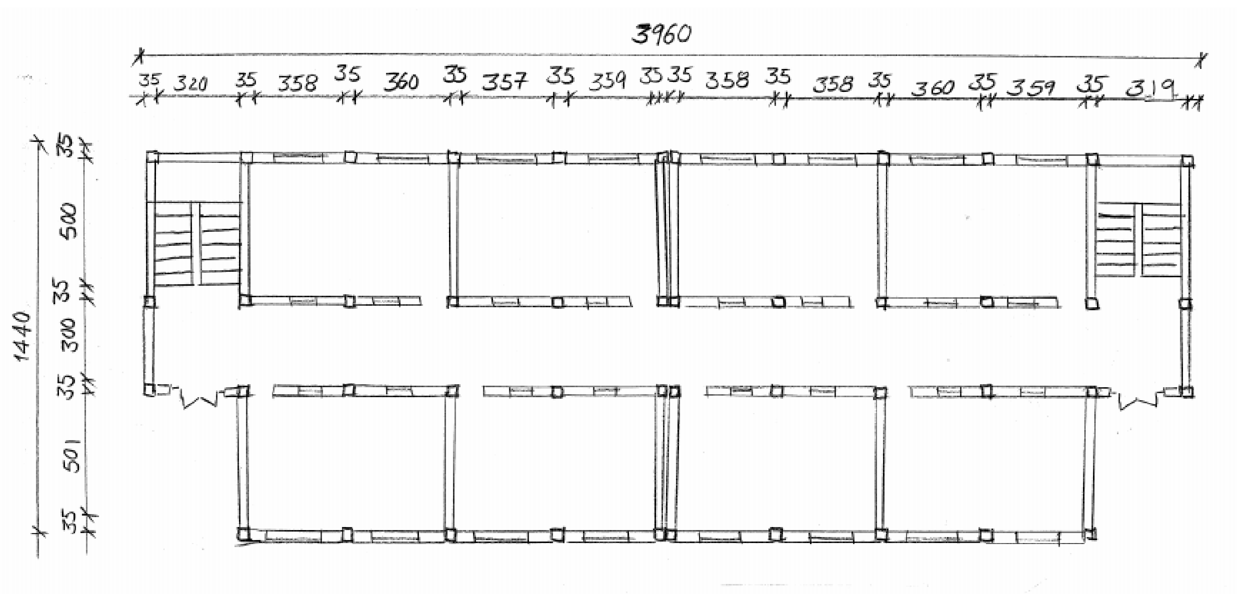

Figure A-98. Kabul School 49, typical floor plan

Figure A-99. Kabul School 50

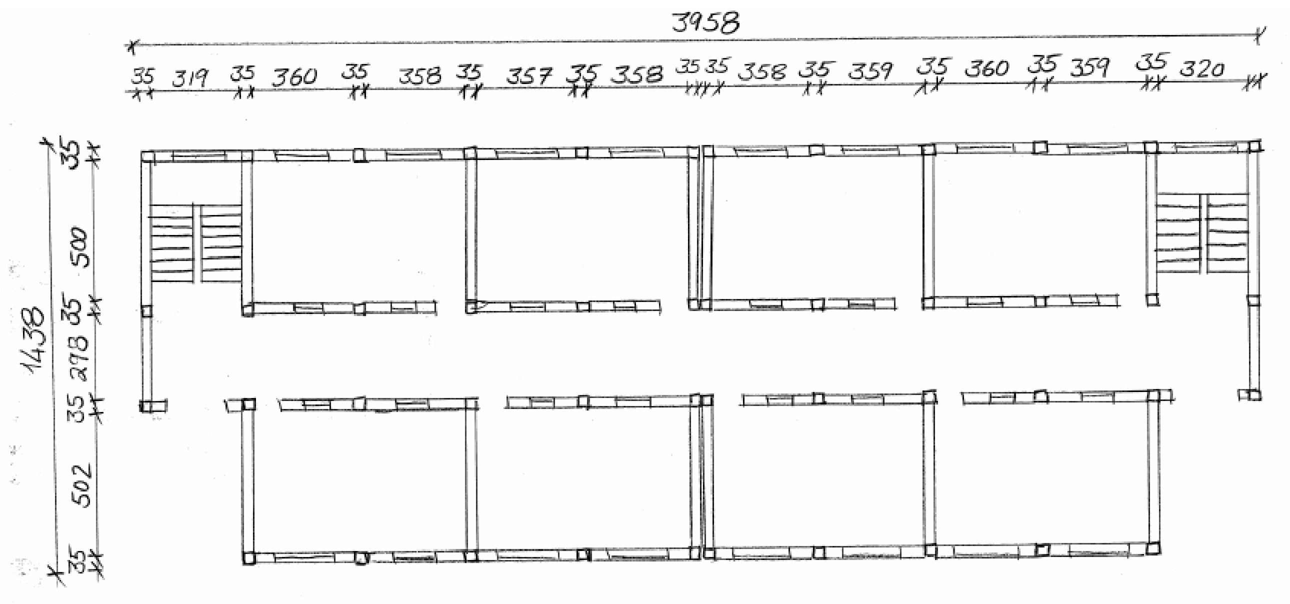

Figure A-100. Kabul School 50, typical floor plan

Figure A-101. Kabul School 51

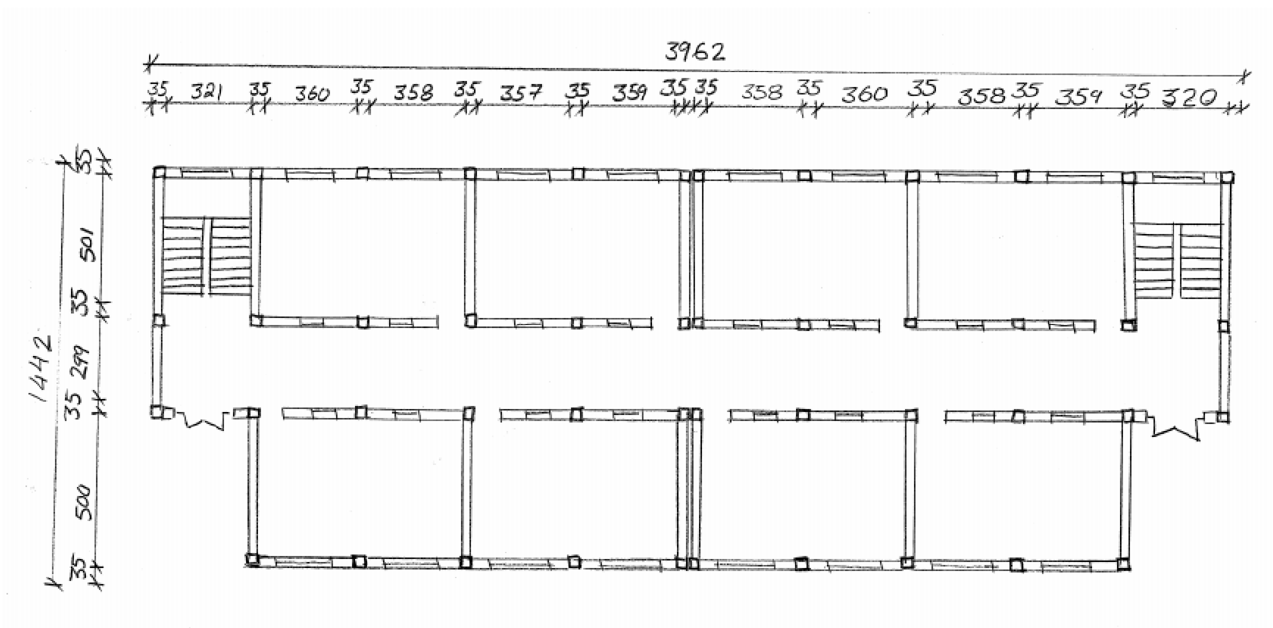

Figure A-102. Kabul School 51, typical floor plan

APPENDIX B – TAIWAN BUILDINGS DATA

Table B-1. Taiwan Buildings Data

Id	Distance to closest GM station (km)	No. Floors	First Floor Area [m^2]	Second Floor Area [m^2]	Total Floor Area [m^2]	First Floor Column Area [m^2]	First Floor Masonry Wall Area NS [m^2]	First Floor Masonry Wall Area EW [m^2]	structural Damage	PGA (g)	Column Index, CI [%] within 5km / PGA	Wall Index, WI [%] N-S	Wall Index, WI [%] E-W	Min Wall Index / PGA
94716	0.83	2	362	299	811	2.4	9.7	6.8	Severe	0.45	0.33	0.12	0.08	0.19
94668	1.98	3	479	434	1544	5.6	6.6	0.8	Severe	0.27	0.68	0.04	0.01	0.02
94687	0.74	3	321	321	1124	3.1	3	7.5	Severe	0.45	0.30	0.03	0.07	0.06
94784	0.81	2	480	480	1200	2.5	9.6	7.4	Severe	0.45	0.23	0.08	0.06	0.14
94740	0.73	3	352		1232	2.2	13	8.7	Severe	0.45	0.20	0.11	0.07	0.16
94688	0.23	3	820		2460	7.9	0	21	Severe	0.45	0.35	0.00	0.09	0.00

Table B-1. Continued

94694	94721	94671	94790	94768	94665	94693	94739	94783
2.01	1.98	1.69	4.84	0.55	0.25	2.05	0.81	0.77
3	3	2	1	3	2	3.5	2	3
700	400	297	930	345	416	580	297	143
700	415	339		345	416	580		143
2100	1127	636	930	850	833	2030	743	467
37	3.3	4.2	5.6	3	4	5.3	1.8	1
18.3	22.7	4.4	9.1	3.4	8.6	16	0.5	2.3
0	6.8	0	5.2	0	0	0	6	3.8
None	None	None	None	Severe	Severe	Severe	Severe	Severe
0.27	0.27	0.40	0.32	0.40	0.45	0.27	0.45	0.45
3.28	0.55	0.82	0.93	0.44	0.53	0.49	0.27	0.24
0.09	0.20	0.07	0.10	0.04	0.10	0.08	0.01	0.05
0.00	0.06	0.00	0.06	0.00	0.00	0.00	0.08	0.08
0.00	0.22	0.00	0.17	0.00	0.00	0.00	0.01	0.11

Table B-1. Continued

94758	94764	94669	94767	94699	94712	94723	94791	94766
2.41	0.41	2.17	0.59	0.30	4.11	0.87	4.85	1.47
2	2	2	2	4	3	2	1	1.2
686	63	788	371	1447	974	87	231	482
686		788	449		974	100		86
1715	158	1576	819	5400	2923	187	231	569
10.6	0.9	9.2	3.2	40	21.1	1.2	2.5	7.3
13.6	4	18.4	12	3.4	14.4	3.7	1.4	3.1
1.2	0.6	6.4	11.9	11	10.9	3.1	2.1	4.6
None	None	None	None	None	None	None	None	None
0.25	0.45	0.27	0.40	0.24	0.42	0.40	0.32	0.27
1.21	0.63	1.09	0.49	1.57	0.85	0.80	1.68	2.39
0.08	0.25	0.12	0.15	0.01	0.05	0.20	0.06	0.05
0.01	0.04	0.04	0.19	0.02	0.04	0.17	0.09	0.08
0.03	0.08	0.15	0.36	0.03	0.09	0.41	0.19	0.20

Table B-1. Continued

94724	94742	94765	94786	94757	94728	94749	94781	94780
1.11	0.57	0.57	2.18	2.14	4.93	4.92	0.78	0.96
2	2	4	2	4	2	2	3	2
560	165	410	560	404	246	180	207	81
550		410	560	404	246	180	170	81
1193	413	1435	1120	1616	616	390	632	201
5.2	2.4	5.1	4.2	6.8	2.2	1.3	2.5	1
23	7.7	8	9.6	0	11	6.4	2.8	5.1
5.1	2.5	12.8		11.5	2	2.6	10.7	0
None	None	None	None	None	None	None	None	None
0.40	0.45	0.45	0.27	0.15	0.17	0.17	0.20	0.20
0.54	0.64	0.39	0.70	1.43	1.06	0.99	1.01	1.27
0.19	0.19	0.06	0.09	0.00	0.18	0.16	0.04	0.25
0.04	0.06	0.09	0.00	0.07	0.03	0.07	0.17	0.00
0.11	0.13	0.12	0.00	0.00	0.19	0.40	0.23	0.00

Table B-1. Continued

94664	94777	94686	94695	94673	94743	94756	94700	94701
0.25	4.98	0.99	1.84	2.12	2.04	2.21	2.02	2.02
2	3	2.5	3	3	2	3	3	3
633	171	191	921	47	69	812	1300	1643
633	151		921	47	69	812	1300	1643
1265	492	525	2763	140	173	2437	3900	4929
5.5	2.5	3.2	8.7	0.4	0.7	7.2	15.8	21.2
14.6	3.4	4.1	21.1	0.7	1.9	15.2	16.8	18.5
6.5	1.9	0.1	0	2.6	4.1	3.7	4.3	10.9
Light	Light	Light	Moderate	Moderate	None	None	None	None
0.45	0.24	0.45	0.27	0.14	0.27	0.15	0.14	0.14
0.48	1.05	0.67	0.59	1.02	0.75	1.01	1.45	1.54
0.12	0.07	0.08	0.08	0.05	0.11	0.10	0.04	0.04
0.05	0.04	0.00	0.00	0.19	0.24	0.02	0.01	0.02
0.11	0.16	0.00	0.00	0.36	0.41	0.10	0.08	0.16

Table B-1. Continued

94690	94697	94682	94698	94785	94776	94763	94689
0.20	0.41	2.96	0.39	0.79	4.98	0.57	0.21
3	5	3	4	3	3	2	2
807	97	443	193	188	453	668	615
	97	565	193	122	416	550	
2421	534	1572	772	493	1444	1218	1230
8.6	3	6	3.6	1.5	6	7.4	5.2
0	0	6.1	5	5.6	0.8	8	14.8
18.5	10.5	1.5	0	2.3	5.8	3.7	3.5
Light	Light	Light	Light	Light	Light	Light	Light
0.45	0.24	0.25	0.24	0.45	0.24	0.45	0.45
0.39	1.19	0.75	0.99	0.34	0.87	0.68	0.47
0.00	0.00	0.04	0.06	0.11	0.01	0.07	0.12
0.08	0.20	0.01	0.00	0.05	0.04	0.03	0.03
0.00	0.00	0.04	0.00	0.10	0.02	0.07	0.06

APPENDIX C - EXAMPLE OF UPGRADING AN EXISTING BUILDING

As an example, consider "Kabul School 49" which is ranked as #7 in vulnerability (Fig. C-1). View of the front of the 3-story building is given in Fig.C-2. Typical floor plan showing the column axes, column locations, infill walls and openings are given in Fig. C-3.

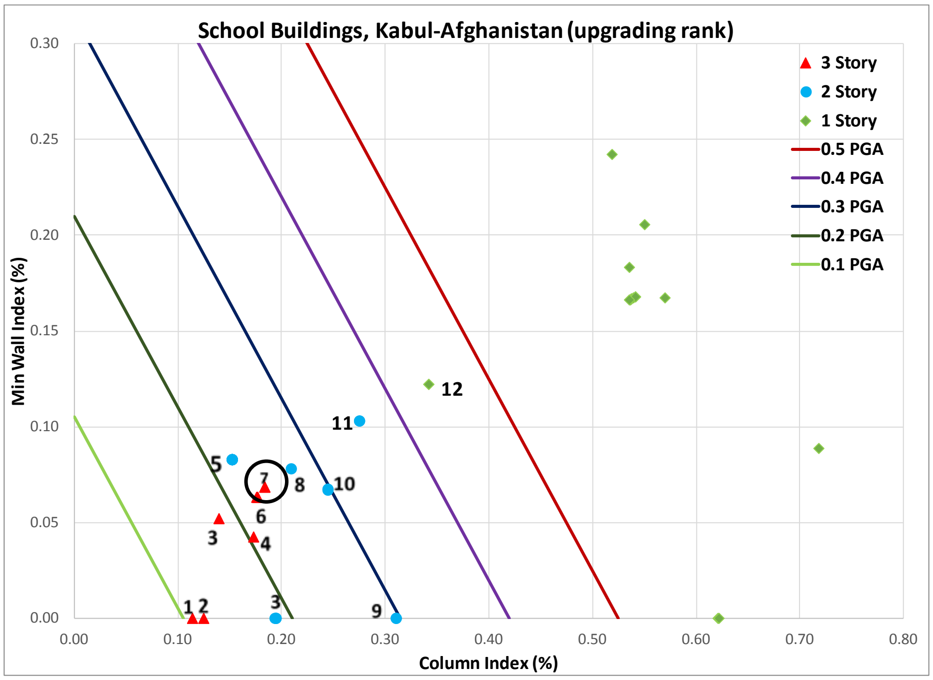

Figure C-1. Kabul school 49 ranked as #7 in vulnerability

Figure C-2. Kabul School 49 (Front View)

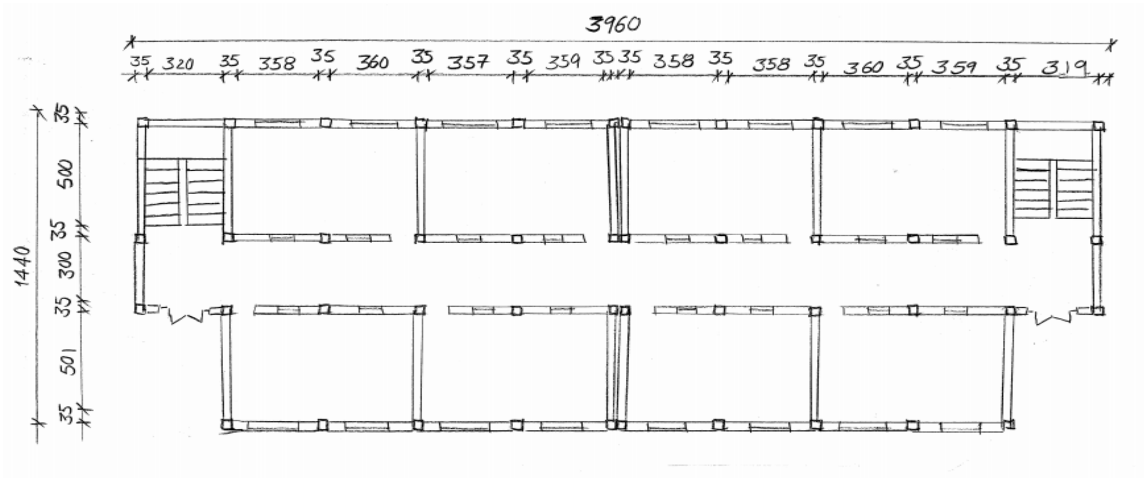

Figure C-3. Kabul School 49 (typical floor plan)

In its current form, this school building has the following Wall and Column Indices:

WI = 0.06% (weak direction)

WI = 0.15% (strong direction)

CI = 0.18%

PI = CI + WI (weak) = 0.18% + 0.06% = 0.24%

Based on Figure C-1, Kabul School 49 is currently between threshold levels for PGA 0.2g and 0.3g.

Following the recommendation in Chapter 4, the goal is to upgrade and bring this school building above the threshold level of 0.50, i.e.

One approach to achieve this can be to enlarge the columns to 0.35x0.80 cm and fill every other wall around the perimeter to achieve full bay (column-to-column, floor –to-ceiling and without any opening) solid masonry infill walls (see Figs. C-4 and C-5).

Figure C-4. Kabul School 49 (upgraded with solid masonry infill walls) (front view)

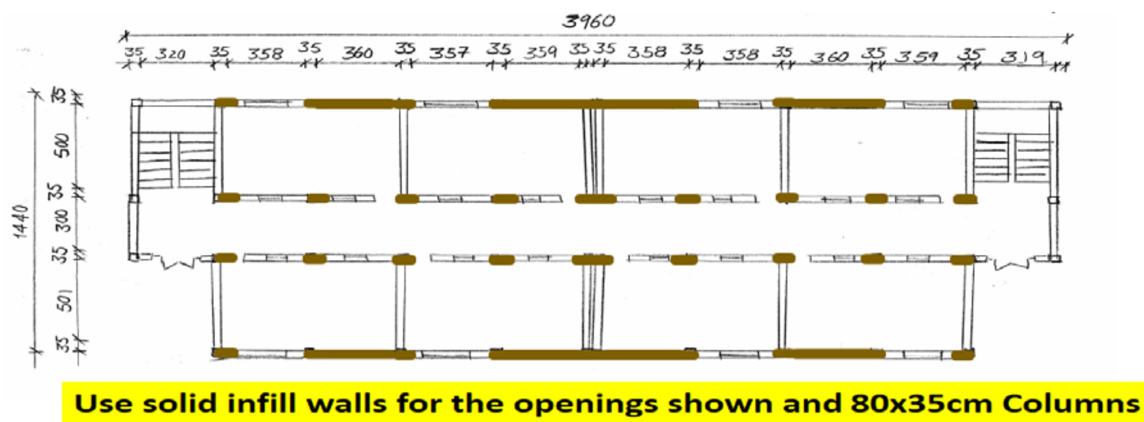

Figure C-5. Kabul School 49 (upgraded with larger columns and more walls)
(typical floor plan)

Use of larger columns and additional masonry solid infill walls increase Column Index to 0.38% and Wall Index in the weak direction to 0.13%:

WI = 0.13% (weak direction)

WI = 0.15% (strong direction)

CI = 0.38%

PI= 0.38% + 0.13% = 0.51% > 0.50%

The CI and WI for the upgraded building are shown in Figure C-10. Note that the building is still shown as “7” but only for identification purposes. The proposed upgrade would move Kabul school building 49 to outside the “more vulnerable to severe damage” zone.

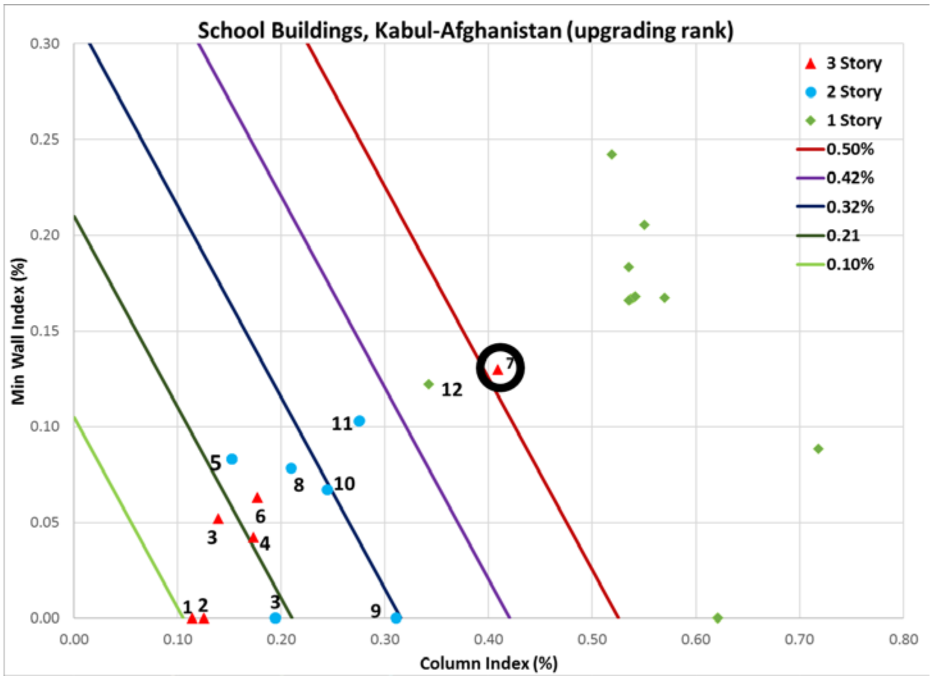

Figure C-6. Upgrading of Kabul School 49 (new location on the plot based on the use of larger columns and additional masonry solid infill walls)